

Stable Two-Coordinate, Open-Shell (d^1-d^9) Transition Metal Complexes

Philip P. Power*

Department of Chemistry, University of California, Davis, One Shields Avenue, Davis, California 95616, United States

CONTENTS

1. Introduction	3482
2. Some Historical Developments	3483
3. Bonding: General Considerations	3484
4. Unstable Two-Coordinate Transition Metal Complexes	3485
5. Synthesis, Structures, and Properties of Stable Two-Coordinate Transition Metal Complexes	3486
5.1. Chromium	3486
5.2. Manganese	3487
5.3. Iron	3488
5.4. Cobalt	3491
5.5. Nickel	3491
5.6. Structural Data Summary	3492
5.6.1. Geometries	3492
5.6.2. Bond Lengths	3493
5.6.3. Secondary Metal–Ligand Interactions	3494
5.6.4. Calculations	3494
5.7. Electronic Spectra	3495
5.8. Magnetism	3496
6. Reactions of Two-Coordinate Transition Metal Complexes	3497
6.1. Chromium Complexes	3497
6.2. Manganese Complexes	3498
6.3. Iron Complexes	3499
6.4. Cobalt Complexes	3502
6.5. Nickel Complexes	3502
7. Conclusions	3503
Author Information	3503
Corresponding Author	3503
Notes	3503
Biography	3503
Acknowledgments	3503
List of Abbreviations	3503
References	3504
Note Added after ASAP Publication	3507

1. INTRODUCTION

Stable, open-shell (d^1-d^9) transition metal complexes in which the metal is two-coordinate or quasi-two-coordinate are among the rarest and least investigated species in coordination chemistry.^{1–3} Their scarcity is due to several factors. Foremost among these is the difficulty in preventing association of monomeric coordinatively unsaturated two-coordinate species to give aggregates or extended ionic lattices in which the metal coordination number is increased to four or six. This is exemplified by the transition metal dihalides,⁴ which can be two-coordinate in the gas phase but form ionic lattices or layer

structures that have six-coordinate metals in the solid state. Similarly the simplest two-coordinate transition metal complexes, the dihydrides,⁵ which can be isolated in inert frozen matrices at low temperature and studied by submillimeter spectroscopy, decompose, or are transformed with disproportionation, to a variety of products upon warming.

The obvious way to prevent association and/or disproportionation is to use sterically large ligands to block such processes.⁶ Almost all currently known two-coordinate transition metal species rely on the steric effects of ligands to enable their isolation at room temperature, and it has proven possible to synthesize numerous examples using a variety of sterically encumbered alkyl, aryl, amido, alkoxo, or thiolato ligands. In general, the size of the ligands required to maintain two-coordination in the solid state is exceptionally large. At present, many of these large ligands require laborious syntheses, although some are commercially available.⁷

A further hindrance to the study of the two-coordinate complexes is that all currently known examples are extremely air and moisture sensitive despite the steric protection provided by the ligands.^{1–3} The reactivity studies that have been performed on the two coordinate complexes show that they often react readily with small molecules such as O₂, N₂O, and CO as well as forming complexes with Lewis bases such as THF, pyridine, phosphines, or various mono- or polyatomic anions.^{1–3,8}

Despite these difficulties, the two-coordinate complexes are attracting attention for several reasons. A major one is that the transition metal, which is complexed through just two atoms, has a very high degree of coordinative unsaturation with several open or singly occupied valence orbitals. This facilitates a rich coordination chemistry spanning a wide variety of substitution, addition, or oxidation reactions. In addition, the two-coordinate complexes, particularly those of iron, have been shown to be useful synthetic precursors for the synthesis of nanomaterials and well-defined catalytic sites.

Two-coordinate complexes are also of interest because of their magnetic properties.^{9–11} In complexes with linear coordination, the ligands are disposed along just one of the axes (by convention the *z*-axis), and where there is a degenerate ground electronic state, the first-order orbital magnetic moment arising from odd numbers of electrons in the $d_{x^2-y^2}$, d_{xy} , or the d_{xz} , d_{yz} orbital sets (vide infra) may be unquenched due to the absence of ligands that interact directly with these orbitals and hinder electron circulation. In certain cases, this permits essentially free ion magnetism to be observed. Also, the ligand field is highly anisotropic, and recent magnetic measurements

Received: December 7, 2011

Published: April 5, 2012

have indicated the presence of very high internal magnetic fields in such complexes.^{9–11} A high orbital angular momentum can be a major contributor to the extent of zero field splitting, which can affect the barriers to the reversal of magnetization in molecules.¹²

With the exception of the ternary salt K_2NiO_2 , which contains linear NiO_2^{2-} ions as part of an ionic lattice structure,¹³ all currently known two-coordinate transition metal compounds that are stable at or near room temperature are molecular species stabilized by large substituents. These compounds, their synthesis, properties, structures, and reaction chemistry form the main themes of this Review. Two-coordinate transition metal complexes characterized either in the gas phase or in frozen matrices, which are otherwise polymerized or unknown in the solid state (e.g., the above-mentioned halides or hydrides), are not discussed at length except where they provide important information relevant to spectroscopic or bonding discussions.

2. SOME HISTORICAL DEVELOPMENTS

Since the development of coordination theory by Werner over a century ago,¹⁴ the assumption that transition metal ions in complexes have characteristic coordination numbers and ligand sets that define the typical geometries, octahedral, tetrahedral, or square planar, has been central to coordination chemistry. The bonding theories developed for these so-called classical complexes have dealt overwhelmingly with species that had simple molecules or ions as ligands whose bonding atom(s) function as a source of negative charge density directed toward a metal cation.^{15–19} Examples of such ligands are typified by those often cited in various spectrochemical series,^{19–21} for example, CO , CN^- , PR_3 , H^- , CH_3^- , NO_2^- , ethylenediamine, NH_3 , pyridine, NCS^- , H_2O , O^{2-} , oxalate, OH^- , F^- , N_3^- , SCN^- , S^{2-} , Br^- , I^- , etc. The common aspect of these ligands is that generally they are not sterically large so that up to six donor atoms can be readily accommodated around a first row transition metal ion.

Systematic investigations of the effects of increasing the steric crowding of ligands on the structure and bonding of transition metal complexes stemmed from work by a number of groups in the late 1950s and 1960s on early transition metal alkoxides and amides, which showed that their coordination numbers could be limited to four or five by the use of substituents such as $-OBU^t$ or NMe_2 .^{22–24} However, in 1963, Bürger and Wannagat introduced the bulky silylamido group $-N(SiMe_3)_2$ to transition metal chemistry and published the preparation and (partial) characterization of the complexes $Cr\{N(SiMe_3)_2\}_3$,²⁵ $Mn\{N(SiMe_3)_2\}_2$,²⁵ $Fe\{N(SiMe_3)_2\}_3$,²⁶ $Co\{N(SiMe_3)_2\}_2$,²⁶ and $Ni\{N(SiMe_3)_2\}_2$.²⁵ The solubility of these complexes in hydrocarbons and their high volatility suggested that they might exist as unassociated molecules, which implied that they contained two-coordinate (Mn^{2+} , Co^{2+} or Ni^{2+}) or three-coordinate (Cr^{3+} and Fe^{3+}) metal ions. This suggestion was confirmed unambiguously by the publication of the X-ray crystal structure of $Fe\{N(SiMe_3)_2\}_3$ in 1969 by Hursthouse, Bradley, and Rodesiler, which showed that it had a monomeric, trigonal planar FeN_3 core having three-coordinate iron(III).²⁷ In addition, spectroscopic and magnetic studies of the related species $Cr\{NPr_2\}_3$ had shown in 1968²⁸ that it was monomeric and likely to contain three-coordinate Cr(III) (later confirmed by X-ray crystallography).²⁹ In 1971, Bradley and Fisher showed that the Co(II) species $Co\{N(SiMe_3)_2\}_2$ was a monomer in solution by cryoscopy and in the gas phase by

mass spectrometry. Furthermore, it was determined that it had a magnetic moment of $4.83 \mu_B$ in the solid state (Guoy balance), which was interpreted in terms of an orbitally nondegenerate ground state ($^4\Sigma_g^+$) of a linear $Co\{N(SiMe_3)_2\}_2$ monomer (also see later in this section).³⁰

Subsequently, in the 1970s and early 1980s, work on low coordinate, open-shell transition metal species was focused primarily on three-coordinate complexes.^{31–34} In particular, the $-N(SiMe_3)_2$ ligand was shown by Bradley and co-workers to be effective at stabilizing trigonal complexes in some first row transition metals and the lanthanides. In addition, the isoelectronic $-CH(SiMe_3)_2$ ligand was shown by Lappert and co-workers to yield related three-coordinate first row transition metal and lanthanide alkyls.³⁵ In the 1990s, work using a variety of sterically crowding ligands such as amides, aryloxides, triorganosiloxides, arylthiolates, as well as a new generation of “two sided” amido ligands,³⁶ developed by Cummins and co-workers, led to the synthesis of numerous new examples as well as extended the range of well-characterized three-coordinate complexes to heavier transition metals of groups 5 and 6 and groups 8 and 9.^{34,35} The three-coordinate heavier element derivatives of group 5 and 6 in particular were shown to have a very rich chemistry and were capable of activating numerous small molecules including N_2 and CO .

The synthesis and characterization of stable two-coordinate transition metal complexes was slower to develop.^{1–3} The first structural characterization of a two-coordinate molecular species in the solid state did not appear until 1985 when the synthesis and structure of the dialkyl $Mn\{C(SiMe_3)_3\}_2$, which had a strictly linear $C-Mn-C$ array ($Mn-C = 2.102(4) \text{ \AA}$), were published by Eaborn, Smith, and co-workers.³⁷ Essentially simultaneously, the linear, two-coordinate structure of the less crowded manganese dialkyl $Mn(CH_2Bu^t)_2$ (linear $C-Mn-C$; $Mn-C = 2.104(6) \text{ \AA}$) was determined at ca. $140 \text{ }^\circ\text{C}$ in the vapor phase by gas electron diffraction (ged) by Andersen, Haaland, and co-workers.³⁸ In 1987, the first X-ray crystal structures of two coordinate iron and cobalt molecules, the amido derivatives $M\{N(SiMePh_2)_2\}_2$ ($M = Fe$ or Co), which had bent geometries ($N-Fe-N = 169.0(1)^\circ$; $N-Co-N = 147.0(1)^\circ$) with further $M-C$ interactions in the range ca. $2.6-2.7 \text{ \AA}$, were described.³⁹ The synthesis and characterization of the iron(II) amide $Fe\{N(SiMe_3)_2\}_2$ were reported almost simultaneously.⁴⁰ This compound, along with its manganese(II) and cobalt(II) analogues, were shown by ged (gas electron diffraction) to have linear $N-M-N$ units and overall S_4 symmetry in the vapor phase at $130-150 \text{ }^\circ\text{C}$ with $M-N$ bond lengths of $1.95(2) \text{ \AA}$ (Mn), $1.84(2) \text{ \AA}$ (Fe), and $1.84(2) \text{ \AA}$ (Co).⁴⁰ The relatively large standard deviations of these distances were attributable to their closeness to, and hence strong correlation with, similar $Si-C$ bond distances within the molecule especially for the iron and cobalt derivatives. Structural studies of these three compounds in the crystalline phase showed that they formed dimers in which the three-coordinate metals are bound to two bridging and a terminal $-N(SiMe_3)_2$ ligand.^{41–43} The dimeric bridged structure reported for $(Me_3Si)_2NCo\{\mu-N(SiMe_3)_2\}_2CoN(SiMe_3)_2$ ⁴² was in disagreement with the proposed monomeric structure of $Co\{N(SiMe_3)_2\}_2$ in the solid state on the basis of magnetic data.³⁰ The gas-phase structure of $Mn\{CH(SiMe_3)_2\}_2$, which is isoelectronic to $Mn\{N(SiMe_3)_2\}_2$, was shown to be monomeric and linearly coordinated by ged.⁴⁴

These results were the subject of an early review/commentary in 1989, which also covered the hitherto

unpublished structures of borylamido derivatives of the formula $M\{(R)BR'_2\}_2$ ($M = \text{Cr, Mn, Fe, Co, or Ni}$; $R = \text{Ph or Mes}$, $R' = \text{Mes}$: the borylamido ligands were developed on the basis that they would be unlikely to bridge through nitrogen because of the delocalization of the nitrogen nonbonding pair onto boron; see section 5).¹ These species included the first characterizations of quasi-two-coordinate derivatives of chromium(II) and nickel(II). Thus, by about 1990, the structures of over a dozen transition metal complexes that were two coordinate, either in the solid state or in the gas phase, at moderate (<150 °C) temperatures were known. A review in 1994² added some further structures and surveyed the reactions of the two-coordinate species, which mainly concerned those of the amides $M\{N(\text{SiMe}_3)_2\}_2$ ($M = \text{Mn, Fe, or Co}$).² A more recent review by Kays (2010) featured coverage of transition metal diaryls, which included two-coordinate derivatives.³

3. BONDING: GENERAL CONSIDERATIONS

The metal coordination geometry in two-coordinate transition metal molecular complexes can be either linear or nonlinear. As will be seen (section 5), the majority of the currently known stable complexes have nonlinear coordination in the solid state. The splittings of the d-orbitals under linear ($D_{\infty h}$) or nonlinear (C_{2v}) simple ligand fields are shown in Figure 1.⁴⁵ For strictly

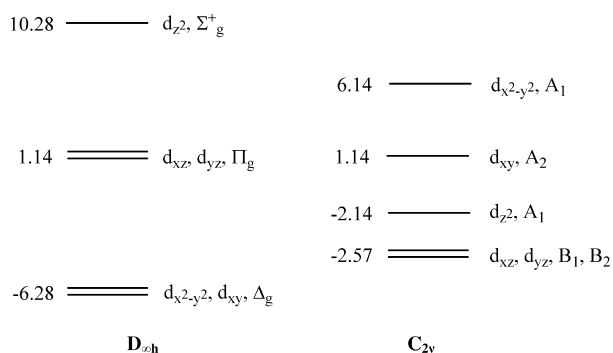


Figure 1. The d-orbital splittings in $D_{\infty h}$ and C_{2v} crystal fields adapted from reference 46. The numbers refer to the Dq values.

linear coordination with $D_{\infty h}$ point group symmetry, the crystal field splitting pattern, assuming no complicating effects such as π -bonding, or s-d hybridization which can affect the relative energies of the Σ_g^+ , Π_g , and Δ_g states, is shown in Figure 1. Upon bending the geometry, the originally degenerate Π_g (d_{xz} , d_{yz}) and Δ_g ($d_{x^2-y^2}$, d_{xy}) sets become further split, and the symmetries of the d-orbitals diverge. However, with a 90° bending angle, two of the d-orbitals become isoenergetic, although their symmetry designations differ, as shown in Figure 1. It should be borne in mind that the linear and nonlinear symmetries represent the local symmetry at the core of the molecule, in other words, the transition metal and the two atoms bonded directly to it. In reality, the ligands employed to stabilize linear coordination are more complex due to the presence of one or more substituents on the ligand atoms

bound to the metal. As a result, the original $D_{\infty h}$ symmetry of an idealized linear ML_2 molecule may become lowered. Thus, in the diakyl $Mn\{C(\text{SiMe}_3)_3\}_2$, the symmetry of the $Mn(\text{CSi}_3)_2$ moiety, which has a staggered configuration in the crystal phase, belongs to the point group D_{3d} .³⁷ The symmetry of the staggered $\text{Fe}\{\text{NSi}_2\}_2$ moiety in $\text{Fe}\{N(\text{SiMe}_3)_2\}_2$ ⁴⁰ is D_{2d} and that of the planar $\text{Fe}\{\text{NHC}(\text{ipso})\}_2$ core in $\text{Fe}\{N(\text{H})\text{Ar}^{\text{Pr}^i}\}_2$ ($\text{Ar}^{\text{Pr}^i} = \text{C}_6\text{H}_3\text{-2,6}(\text{C}_6\text{H}_2\text{-2,4,6-Pr}^i)_2$, see section 5) is C_{2h} . Reference to Table 1 shows that in D_{3d} symmetry the d_{xz} , d_{yz} and $d_{x^2-y^2}$, d_{xy} orbitals remain degenerate, whereas this is not so in D_{2d} point group symmetry where only the d_{xz} and d_{yz} orbitals remain degenerate. In C_{2h} symmetry, the d_{xz} , d_{yz} (B_g , B_g) and $d_{x^2-y^2}$, d_{xy} (A_g , A_g) are nondegenerate but have the same symmetry properties.

The d^1 – d^9 electron configurations predicted on the basis of a very simple ligand field approach (assuming M – L σ -interactions only) in linear coordination are shown in Figure 2 along with their ground states.^{45,46} A high spin configuration has been assumed in all cases, and as shall be seen this assumption has been borne out experimentally by magnetic measurements. The D and F ground states are split by a linear ligand field. The 2D (d^1) ground state is split into $^2\Sigma_g^+$, $^2\Pi_g$, and $^2\Delta_g$ component states with $^2\Delta_g$ lying lowest. For the 3F (d^2) state, the splitting pattern is $^3\Sigma_g^+$, $^3\Pi_g$ and $^3\Delta_g$ and $^3\Phi_g$ with $^3\Sigma_g^+$ lying lowest. There is also an excited 3P state of the same multiplicity, which will be split further into Σ_g^+ and Π_g components. For the 4F (d^3) state in a linear field, the $^4\Phi_g$ state is lowest and the Σ_g^+ state is highest with an excited 4P state being split into Σ_g^+ and Π_g levels. For 5D (d^4), the ground state is $^5\Sigma_g^+$. The states for electron configurations d^6 – d^9 can be obtained in a similar way.⁴ It can be seen that degenerate ground states are expected for configurations d^1 ($^2\Delta_g$), d^3 ($^4\Phi_g$), d^6 ($^5\Delta_g$), and d^8 ($^3\Phi_g$) with the remaining configurations having nondegenerate ground states for the d^2 , d^4 , d^7 , and d^9 electron configurations.

As was seen for the d-orbital splitting, lowering the point group symmetry of a molecule does not always lead to further splitting of the states. For example, when $D_{\infty h}$ symmetry is lowered to D_{3d} symmetry, the coordination of the metal remains linear, and the splitting of an F ground state into Σ_g^+ , Π_g , Δ_g or Φ_g component states in $D_{\infty h}$ symmetry correlates to A_{1g} or E_g states in D_{3d} symmetry. In D_{2d} (or in S_4) symmetry, however, the degeneracy of the original Δ_g state is lowered to B_1 , B_2 (B, B in S_4), although the degeneracy of the Π_g state is maintained as an E state. In D_{2h} symmetry, the original degeneracy of the Φ_g and Δ_g states correlates to nondegenerate A and B states. The point groups C_{2h} , C_{2v} and C_2 contain no degenerate symmetry representations. The splitting of the ground state of the various d^1 – d^9 configurations leads to the expectation that, with linear or near linear coordination, two absorption bands should be observed for the D ground states (that is to say, the D states that correspond to the electron configurations d^1 , d^4 , d^6 , and d^9) because these states are split into three component states (Σ_g^+ , Π_g , and Δ_g) by the linear

Table 1. Symmetries of the d-Orbitals in Various Two-Coordinate Crystal Fields

d-orbital	$D_{\infty h}$	$C_{\infty v}$	D_{3d}	D_{2h}	D_{2d}	S_4	C_{2h}	C_{2v}	C_2
z^2	Σ_g^+	$\Sigma^+(A_1)$	A_{1g}	A_g	A_1	A	A_g	A_1	A
xz, yz	Π_g	$\Pi(E_1)$	E_g	B_{2g}, B_{3g}	E	E	B_g, B_g	B_1, B_2	B, B
x^2-y^2, xy	Δ_g	$\Delta(E_2)$	E_g	A_g, B_{1g}	B_1, B_2	B, B	A_g, A_g	A_1, A_2	A, A

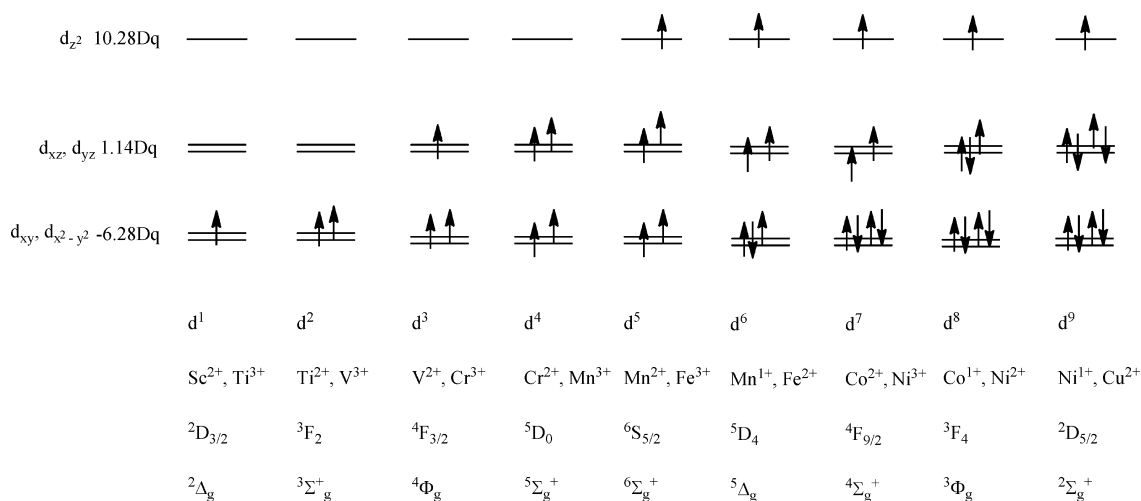


Figure 2. d^1 – d^9 d-orbital splitting and ground states in a simple linear crystal field. (Note: A D state is predicted to split as Σ_g^+ , Π_g , and Δ_g and an F state as Σ_g^+ , Π_g , and Δ_g and Φ_g in $D_{\infty h}$ symmetry.)

crystal field. For the F ground states (corresponding to the d^2 , d^3 , d^7 , and d^8 configurations), three absorptions may be expected because of the splitting into four components (Σ_g^+ , Π_g , Δ_g , and Φ_g) by the linear crystal fields, and two further absorptions are also possible as a result of transitions to an excited P state of the same multiplicity, which is split into the two components Σ_g^+ and Π_g in a linear ligand field.

4. UNSTABLE TWO-COORDINATE TRANSITION METAL COMPLEXES

Two-coordinate transition metal hydrides and halides do not have a stable existence under ambient conditions and as a result fall outside the coverage of this Review. Yet, their study has provided important insights that are applicable to stable two-coordinate complexes.^{4,5} The hydrides are the simplest two-coordinate transition metal species, and, although they are unstable at room temperature, they can be generated and trapped in frozen matrices at low temperature and studied by submillimeter spectroscopy.⁵ Analyses of the IR spectra of the trapped MH_2 species were consistent with bent geometries, although in these cases the matrix environment can also affect the structures.⁵ The MH_2 species are the simplest molecules available for computational study, and the results of early work^{47–49} on the first row MH_2 species suggested that they had a linear structure like their halide counterparts. Later, increasingly sophisticated calculations^{50–54} with larger basis sets have indicated that most geometries are bent with the exception of MnH_2 ^{49,52d} and FeH_2 ,^{52e,53} which may be linear, or near linear,^{48–50} and have high spin ground-state configurations.^{5,50–53} The structure of NiH_2 , which has an acute H–Ni–H angle and a low spin ground state, appears to be unique.^{51,52g} In general, the lowest lying spin states of lower multiplicity were calculated to lie at significantly higher energies than the ground states.^{54,55} For the ground-state structures, it was found that the bond angles are quite sensitive to the basis set used and the potential energies for bending are relatively flat.^{47,53,54} This suggested that for species isolable under ambient conditions, whose structures will be discussed below, the coordination geometry can be affected by relatively weak interactions such as secondary metal–ligand or ligand–ligand interactions or packing forces. However, an explanation of the calculated bent structures of the MH_2 molecules cannot involve

these considerations obviously because such effects must be absent in the gas phase. The underlying reasons for the bent geometries must therefore lie in their electronic structure. An example is provided by the structure and bonding of CrH_2 ,⁵⁴ which was calculated to have a v-shaped arrangement with C_{2v} symmetry and a H–Cr–H angle of 114.4° (cf., 110° calculated in ref 52c) with a 5B ground state. However, this state lies just $4.2 \text{ kcal mol}^{-1}$ lower in energy than that of a linear $D_{\infty h}$ ground state. The bent structure is consistent with some d–s hybridization (the optimal angle for sd hybrids is 90° in contrast to 180° in sp and 60° for d–d hybridizations). Also, it will be recalled that the ground state of a chromium atom is 7S ($3d^5 4s^1$) whose energy is considerably (ca. 1 eV)⁵⁵ lower than the 5D ($3d^4 4s^2$) state. Although each hybridization scenario is a possibility with an 7S or 5D chromium ground state, the 5D state would probably favor 4s–4p hybrid orbitals to prevent the loss of exchange energy upon bond formation with unpaired electrons. It seems likely that orbital hybridization changes across the 3d series as the relative energies of the 4s, 3d, and 4p electrons change. The variation in orbital mixing can result in a variety of nonlinear interligand angles at the metal. Calculations and spectroscopic data for second and third row transition metal dihydrides in the gas phase have also afforded bent geometries.⁵ Further evidence of the generally bent geometry of transition metal dihydrides has come from electron-spin resonance spectroscopy.^{56,57} Theoretical studies on the related transition metal dimethyls⁵⁸ and their positive ions indicated bent geometries for the neutral molecules except for the later first row metal dimethyls, which were calculated to have linear structures. In addition to these calculations, there have been a few computational studies of model complexes for real molecules. Most of these have concerned complexes of amido or related ligands, and these will be discussed individually in later sections when their structures are considered in the next section.

Two-coordinate transition metal halides have been studied for more than half a century by various approaches that include ged, IR, and electronic spectroscopy as well as computational methods.⁴ Their examination continues to interest both experimentalists and theoreticians. These seemingly simple triatomic molecules were originally believed to be linear mainly on the basis of ged and IR data.^{4,59} However, it is now

Table 2. Selected Structural and Magnetic Data for Two-Coordinate Chromium Complexes

complex	M–L (Å)	M–L (Å)	L–M–L (deg)	μ_{eff} (μ_{B})	ref
Cr{N(Ph)BMes ₂ } ₂	1.98(2)	2.328(2), 2.406(2)	110.8(1)	4.91	66
Cr{N(Mes)BMes ₂ } ₂	1.980(7), 1.987(7)	2.38(2), 2.39(2)	112.3(3)	4.92	67
Cr{N(H)Ar ^{Me₆} } ₂	1.943(4), 1.977(4)	2.337(4), 2.488(5)	120.9(5)	4.35	69
Cr{N(H)Ar ^{Pr₄} } ₂	1.9764(14)	2.630–2.948	180	4.26	69
Cr{N(H)Ar ^{Pr₄} } ₂	1.9966(14)	2.48	180	4.22	69
Cr(SAr ^{Pr₆}) ₂	2.3505(5)	2.502(3)	180	4.93	73
Ar ^{Pr₄} Cr(μ : η^3 : η^6 -CH ₂ Ph)Cr(η^6 -HAr ^{Pr₄})	2.051(3)(Ar)	2.474(3)	111.9(1)	4.9	75
	2.098(3)Bz				
	2.279(3)Bz				
	2.407(3)Bz				
Cr(THF)Ar ^{Pr₄}	2.087(3) (C), 2.062(5) (O)	>3.0	173.7(2)	5.95	75,80
Cr(PMe ₃)Ar ^{Pr₄}	2.116(2) (C), 2.464(5) (P)	>3.0	167.39(4)	6.17	75,80
Ar ^{Pr₄} CrCrAr ^{Pr₄}	2.131(1) (C), 1.8351(4) (Cr)	2.294(1)	102.78(1)		74,75
Me ₃ Si-4-Ar ^{Pr₄} CrCrAr ^{Pr₄} -4-SiMe ₃	2.136(1) (C), 1.8077(7) (Cr)	2.322(2)	101.65(6)		75
MeO-4-Ar ^{Pr₄} CrCrAr ^{Pr₄} -4-OMe	2.131(2) (C), 1.8160(5) (Cr)	2.311(2)	102.25(4)		75
F-4-Ar ^{Pr₄} CrCrAr ^{Pr₄} -4-F	2.135(3) (avg C), 1.831(2) (Cr)	2.301(6) (avg)	102.5(3) (avg)		75
Ar ^{Pr₄} CrFe(η^5 -C ₅ H ₅)(CO) ₂	2.06(2) (C), 2.488(7) (Fe)	2.365(2)	141.31(6)	4.3	81

recognized that the original experimental data that were obtained were often complicated by monomer–dimer and higher aggregate equilibria as well as the presence of impurities from decomposition due to the high temperatures necessary for data collection. Electron diffraction data for most of the first row dihalides have been reported.^{2,60} However, the most recent work, which includes reevaluation of earlier data, suggests that in several cases electron diffraction data alone are not capable of giving unambiguous solutions to their structures.^{60–62} This is exemplified by a study of VCl₂ by a combination of ged and computational work, which indicated that it has a linear structure but with a ⁴Σ_g⁺ ground state in contrast to a simple crystal field prediction of ⁴Φ_g in Figure 2.⁶⁰ This is probably a result of V–Cl π-bonding. In contrast, monomeric CrCl₂ was recently calculated to have a bent geometry with a ⁵B₂ ground state and Cl–Cr–Cl bond angle of 149(10)°.⁶¹ From consideration of the linear structure, it was calculated that ⁵Π_g had the lowest energy of the three high spin states ⁵Σ_g⁺, ⁵Π_g, and ⁵Δ_g. However, ⁵Π_g is not a minimum on the potential energy surface but is a transition state undergoing a Renner–Teller distortion to split into a ⁵B and an ⁵A state of a bent structure.⁶¹ Both the vanadium and the chromium structures possess shallow potential wells for bending in the 120–180° angle range. Other calculations at various levels for CrCl₂^{63–65} indicated that the ⁵Π_g state lies at lower energy than ⁵Σ_g⁺ in contrast to the ⁵Σ_g⁺ ground state predicted in Figure 2. However, the energy difference between the ⁵Π_g and ⁵Σ_g⁺ states is not large.⁶¹ The calculations for VCl₂⁶⁰ and CrCl₂⁶⁴ indicated that the π-interactions that occur between the halogens and the metals are the likely cause of the changes in the ordering of the Σ, Π, and Δ states. In very recent work on the iron dihalides, ged data for FeBr₂ and FeI₂ indicated nonlinear structures with bending angles of 155.9(29)° and 157(3)°, although computations predicted linear structures for all of the iron dihalides FeX₂ (X = F, Cl, Br, I).⁶² The apparently conflicting data are a consequence of the low energy barriers to deformation of the X–Fe–X angle, which again underlines the difficulties in assigning structures on the basis of one physical method alone.

5. SYNTHESIS, STRUCTURES, AND PROPERTIES OF STABLE TWO-COORDINATE TRANSITION METAL COMPLEXES

At present, well-characterized, stable, two-coordinate, open-shell transition metal complexes concern derivatives of the elements chromium, manganese, iron, cobalt, and nickel. They have been synthesized by a relatively small number of routes with salt metathesis and amine elimination being the most prominent. A few other routes involve reduction of organic metal halide precursors, insertion into metal–ligand bonds, or elimination reactions. The currently known complexes will be discussed group by group.

5.1. Chromium

Structurally characterized, stable two-coordinate chromium derivatives are listed in Table 2. The first compounds to be reported were the Cr(II) borylamido complexes Cr{N(Ph)BMes₂}₂⁶⁶ and Cr{N(Mes)BMes₂}₂⁶⁷ (Mes = C₆H₂-2,4,6-Me₃), which were synthesized by salt metathesis reactions between the respective lithium borylamide salts and CrCl₂(THF)₂.⁶⁸ The structural data for these compounds show that they have Cr–N bond lengths near 1.98 Å and a very strongly bent coordination with N–Cr–N angles of 110.8(1)° and 112.3(3)°, respectively. There are also relatively short intramolecular Cr---C interactions in the range ca. 2.33–2.41 Å to two ipso carbons from separate boron mesityl groups of the borylamide ligands. A relatively narrow N–Cr–N angle of 120.9(5)° was also observed in the primary amido species Cr{N(H)Ar^{Me₆}}₂,⁶⁹ which is stabilized by the primary amido ligand –N(H)Ar^{Me₆} (Ar^{Me₆} = C₆H₃-2,6(C₆H₂-2,4,6-Me₃)₂).⁷⁰ It has Cr–N bond lengths similar to those of the borylamides and also displays Cr---C (2.2337(4) and 2.485(5) Å) interactions to ipso carbons of the flanking mesityls of the terphenyl substituent. Increasing the size of the terphenyl amido group to N(H)Ar^{Pr₄}⁷¹ or Ar^{Pr₄}⁷² (Ar^{Pr₄} = C₆H₃-2,6(C₆H₃-2,6-Prⁱ)₂, Ar^{Pr₆} = C₆H₃-2,6(C₆H₂-2,4,6-Prⁱ)₃)₂ allows linear metal coordination to be observed in the orange complexes Cr{N(H)Ar^{Pr₄}}₂ and Cr{N(H)Ar^{Pr₆}}₂.⁶⁹ Similarly, the bis thiolato complex Cr(SAr^{Pr₆})₂,⁷³ which was also synthesized by salt metathesis, has a linear S–Cr–S unit. The three linear species all feature a

weaker Cr---C(ipso) interaction with a flanking ring of the terphenyl ligands of ca. 2.5 Å.

Included in Table 2 are data for the dark red quintuple bonded species $\text{ArCr}\equiv\text{CrAr}$ ($\text{Ar} = \text{Ar}^{\text{Pr}^i}$, $\text{Ar}^{\text{Pr}^i-4-X}$, $X = \text{SiMe}_3$, OMe , or F).^{74,75} They are all Cr(I) derivatives in which the quintuple bond is formed by electron pairing of the five d-electrons from each of the two ArCr(I) fragments. They were synthesized by reduction of ArCrCl precursors with KC_8 . It can be seen that they feature strongly bent chromium coordination ($\text{Cr}-\text{Cr}-\text{C} = \text{ca. } 102^\circ$), which is believed to be due in part to metal sd hybridization (Figure 3).⁷⁶ The Cr-C σ -bonds are in

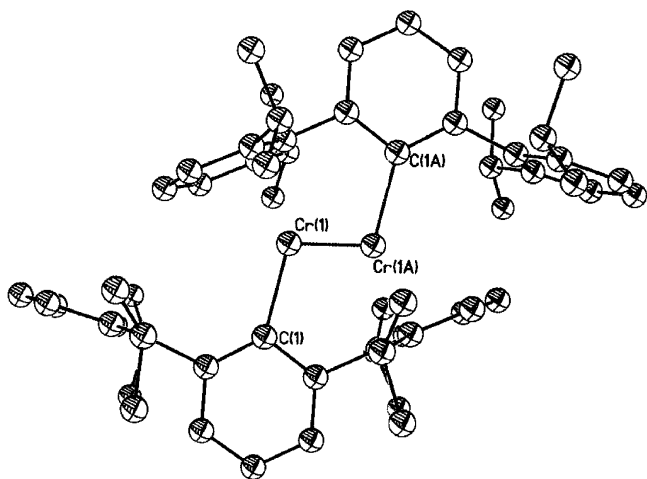


Figure 3. Thermal ellipsoid (30%) drawing of the quintuple bonded $\text{Ar}^{\text{Pr}^i}_2\text{CrCrAr}^{\text{Pr}^i}$. H atoms are not shown. Some structural details are given in Table 2.⁷⁴

the narrow range 2.131(1)–2.136 (Å), and there are also relatively short Cr---C approaches to the ipso-carbon of the flanking ring of the terphenyl substituent in the range 2.29–2.32 Å. These interactions have been calculated to have energies of only ca. 2 kcal mol⁻¹ and have little effect on the CrCr bond distance.⁷⁷ The Cr–Cr bond lengths in these compounds lie in the range 1.8077(7)–1.8351(4) Å consistent with quintuple bonding. The shortness of these bonds has been exceeded only by dichromium species featuring ligands that bridge the chromiums⁷⁸ and cause shortening of the Cr–Cr bond.⁷⁹ The multiple bonded complexes in Table 2 display weak temperature independent paramagnetism.

If the terphenyl ligand employed in the ArCrCl precursor is the extremely crowding Ar^{Pr^i} ($\text{Ar}^{\text{Pr}^i} = \text{C}_6\text{H}-2,6(\text{C}_6\text{H}_2-2,4,6-\text{Pr}^i_3)_2-3,5-\text{Pr}^i_2$), Cr–Cr bond formation upon reduction with KC_8 is prevented by steric hindrance, and a two-coordinate mononuclear Cr(I) species can be isolated.^{75,80} If the reduction is carried out in THF, the two-coordinate Cr(I), d⁵ complex $\text{Ar}^{\text{Pr}^i}\text{Cr}(\text{THF})$, which has a wide C(ipso)–Cr–O angle of 173.7(2)°, is obtained. When the reduction is performed in the same solvent in the presence of PMe_3 , the corresponding two-coordinate complex $\text{Ar}^{\text{Pr}^i}\text{Cr}(\text{PMe}_3)$ (C(ipso)–Cr–P = 167.39(4)°, Figure 4) can be crystallized from the reaction mixture.⁸⁰ Both complexes had magnetic properties consistent with a high spin d⁵ electron configuration.

Reduction of $\text{Ar}^{\text{Pr}^i}\text{CrCl}$ in toluene in the absence of the Lewis bases THF or PMe_3 with the intention of forming the Cr(I) η^6 -arene half-sandwich complex $\text{Ar}^{\text{Pr}^i}\text{Cr}(\eta^6\text{-PhMe})$

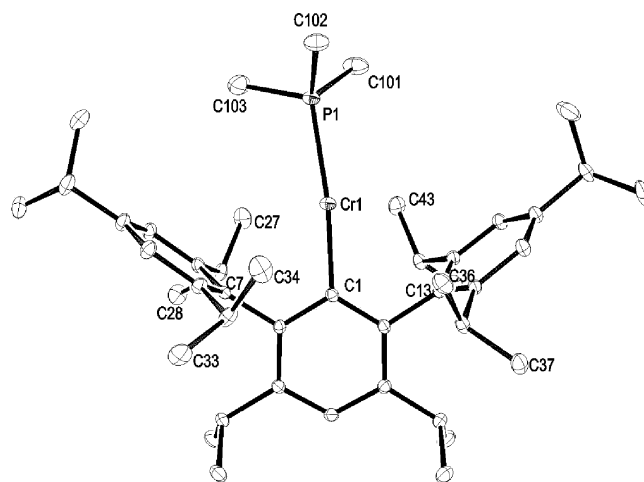


Figure 4. Thermal ellipsoid drawing (30%) of $\text{Ar}^{\text{Pr}^i}\text{Cr}(\text{PMe}_3)$. H atoms are not shown. Some structural details are given in Table 2.⁷⁵

resulted in disproportionation to form the Cr(II)/Cr(0) species $\text{Ar}^{\text{Pr}^i}\text{Cr}(\mu_2\text{-}\eta^2\text{-}\eta^6\text{-CH}_2\text{Ph})\text{Cr}(\text{Ar}^{\text{Pr}^i}\text{H})$ (see Scheme 2 in section 6.1).⁷⁵ The Cr(II) ion is η^1 - σ -bonded to an Ar^{Pr^i} ligand via the C(ipso) of the central aryl ring and is also bound to a benzyl ligand derived from toluene, most strongly to the methylene carbon and less strongly to the ipso (2.279(3) Å) and ortho (2.407(3) Å) carbons from the phenyl group of the benzyl ligand. The Cr(II) ion also displays an approach of 2.474(3) Å to an ipso carbon of one of the flanking rings of the σ -bonded terphenyl ligand. In contrast, the Cr(0) atom is sandwiched between the aryl ring of the benzyl group and a flanking aryl ring of an uncharged protonated terphenyl ligand ($\text{Ar}^{\text{Pr}^i}\text{H}$) with Cr–centroid distances of 1.626 and 1.664 Å.

The Cr–Fe bonded complex $\text{Ar}^{\text{Pr}^i}\text{CrFe}(\eta^5\text{-C}_5\text{H}_5)(\text{CO})_2$ ⁸¹ was synthesized by the reaction of $\text{Ar}^{\text{Pr}^i}\text{CrCl}$ with $\text{KFe}(\eta^5\text{-C}_5\text{H}_5)(\text{CO})_2$.⁸² It features a Cr–Fe bond length of 2.488(7) Å. However, the coordination at chromium is nonlinear (C(ipso)–Cr–Fe = 141.31(6)°), and there is a relatively short Cr---C distance of 2.365 (2) Å to the ipso carbons of the flanking ring of the terphenyl ligand. The Cr–Fe bond is believed to be of a dative type in which the anion $[\text{Fe}(\eta^5\text{-C}_5\text{H}_5)(\text{CO})_2]^-$ behaves as an electron donor to a $[\text{Ar}^{\text{Pr}^i}\text{Cr}]^+$ moiety.

5.2. Manganese

The currently known structurally characterized two-coordinate manganese derivatives are listed in Table 3. Two-coordination in stable manganese complexes was first verified via almost simultaneous reports describing the structures of $\text{Mn}\{\text{C}(\text{SiMe}_3)_3\}_2$ ³⁷ (Figure 5) in the solid state (X-ray crystallography) and of $\text{Mn}(\text{CH}_2\text{Bu}^t)_2$ ³⁸ in the gas phase (ged) in 1985. The isolation of the latter species had originally been reported in 1976 by Wilkinson and co-workers.^{83a} The compounds were obtained in good yield by the reaction of MnCl_2 with $\text{Mg}(\text{Cl})\text{CH}_2\text{Bu}^t$, $\text{Mg}(\text{CH}_2\text{Bu}^t)_2$, or $\text{LiC}(\text{SiMe}_3)_3$. The two structurally characterized dialkyls possess strictly linear coordination with almost identical Mn–C bond distances near 2.1 Å. In the solid state, $\text{Mn}(\text{CH}_2\text{Bu}^t)_2$ was reported to have a tetrameric structure with a linear array of four manganese atoms with bridging alkyl groups with the two end manganese atoms having three coordination.^{83a} The related

Table 3. Selected Structural and Magnetic Data for Two-Coordinate Manganese Complexes

complex	M–L (Å)	M---L (Å)	L–M–L (deg)	μ_{eff} (μ_{B})	ref
Mn(CH ₂ Bu ^t) ₂ (ged)	2.104(6)		180		38,83a
Mn{CH(SiMe ₃) ₂ } ₂ (ged)	2.01(3)		180	5.49	44
Mn{C(SiMe ₃) ₃ } ₂	2.102(4)		180	5.1	37
MnMes* ₂	2.108(2)	2.78	159.7(1)	5.9	84
Mn(Ar ^{Me₆}) ₂	2.095(3) avg	2.774(3)	166.4(1), 173.0(1)	5.89	85
Mn(Ar ^{Prⁱ}) ₂	2.113(2)		160.19(9)		86
MnAr ^{Prⁱ} {N(H)Ar ^{Me₆} }	2.095(1)(C), 1.981(1)(N)	2.595(1)	132.58(5)	5.92	87
Mn{N(H)Ar ^{Me₆} } ₂	1.976(2), 1.982(3)	2.675(2), 2.600(2)	138.19(9)	5.73	89
Mn{N(H)Ar ^{Prⁱ} } ₂	1.952(2)	2.733(4)	176.09(12)	5.91	89
Mn{N(SiMe ₃) ₂ } ₂ (ged)	1.95(2)		180		40
Mn{N(SiMePh ₂) ₂ } ₂	1.989(3), 1.988(3)	2.774(5)	170.7(1)	5.72	90
Mn{N(Mes)BMes ₂ } ₂	2.046(4)	2.536(5)	160.4(2)	5.98	91
Mn(NC ₁₂ H ₂₄ -3,6-Me ₂ -1,8-Ph ₂) ₂	2.044(2), 2.041(2)	2.683(1)-2.705(2)	178.58(6)	5.81	92
Mn(SeAr ^{Me₆}) ₂	2.498(1)	2.696, 2.716	119.9(1)		93
Mn(SAr ^{Prⁱ}) ₂	2.3041(7)	2.951(2)	180	6.01(2)	83
Ar ^{Prⁱ} MnFe(η^5 -C ₅ H ₅)(CO) ₂	2.081(2) (C), 2.451(2) (Fe)		166.82(6)	5.2	81

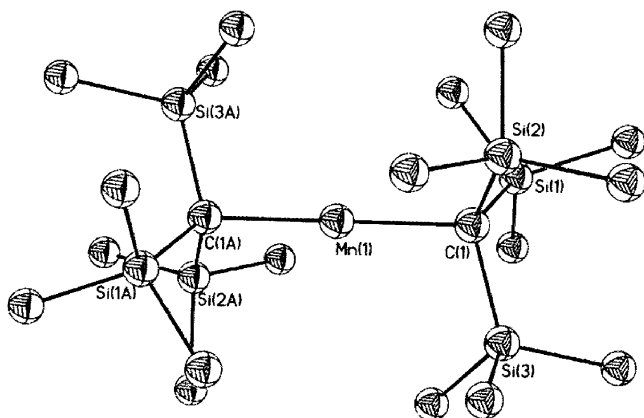


Figure 5. Thermal ellipsoid drawing (30%) of Mn{C(SiMe₃)₃}₂. H atoms are not shown. Some structural details are given in Table 3.³⁷

{Mn(CH₂SiMe₃)₂}_n species^{83a} was shown to have an infinite chain structure in the solid state in which the manganese atoms are tetrahedrally coordinated by four bridging –CH₂SiMe₃ groups. The details of its structure together with its TMEDA (*N,N,N',N'*-tetramethylethylenediamine), pyridine, or 1,4-dioxane complexes were described recently.^{83b} The more crowded dialkyl Mn{CH(SiMe₃)₂}₂ was also shown to have linear metal coordination in the vapor phase by ged.⁴⁴ The manganese diaryls MnMes*₂ (Mes* = C₆H₂-2,4,6-Bu^t₃),⁸⁴ Mn(Ar^{Me₆})₂,⁸⁵ and Mn(Ar^{Prⁱ})₂⁸⁶ were obtained in good yield from MnCl₂ and the respective lithium aryls. X-ray crystallography showed that they had Mn–C bond lengths similar to those of the dialkyls. However, the coordination was bent in each case with C–Mn–C angles between 159.7(1)° and 173.0(1)°, and there were also rather long Mn---C secondary interactions.

The mixed aryl/amido complex Ar^{Prⁱ}Mn{N(H)Ar^{Me₆}}₂,⁸⁷ synthesized from [Li(THF)Ar^{Prⁱ}MnI₂]⁸⁸ and LiN(H)Ar^{Me₆}, displayed a much greater bending angle of 132.58(5)°. Apparently, the interposition of the nitrogen atom between the terphenyl ligand and the metal facilitates geometrically a stronger dipolar interaction (Mn---C = 2.595(1) Å) between the metal and ipso carbon of a flanking mesityl ring. A similar bending angle (138.19(9)°) is observed in the bisamido species

Mn{N(H)Ar^{Me₆}}₂,⁸⁹ which also displays two somewhat longer Mn–C interactions.

Increasing the size of the terphenyl substituents produces almost linear coordination in Mn{N(H)Ar^{Prⁱ}}₂ (N–Fe–N = 176.09(12)°)⁸⁹ and linear coordination in the thiolato derivative Mn{SAr^{Prⁱ}}₂, which has the same terphenyl substituent on the ligating atom.⁷³ Secondary metal–ligand contacts in these complexes are lengthened to over 2.7 and 2.9 Å, respectively. The other amido derivatives in Table 3, which include the silylamide Mn{N(SiMePh₂)₂}₂,⁹⁰ the borylamide Mn{N(Mes)BMes₂}₂,⁹¹ and the carbazolidine derivative Mn(NC₁₂H₂₄-3,6-Me₂-1,8-Ph₂)₂, display bending angles in the range 160.4(2)–178.58(6)°. The previously mentioned Mn{N(SiMe₃)₂}₂ has a linear N–Mn–N unit in the vapor phase by ged,⁴⁰ but it is dimerized via amido bridging in the solid state.^{41,42} The selenolate derivative Mn(SeAr^{Me₆})₂⁹³ has a strongly bent (Se–Mn–Se = 119.9(1)°) core. However, the secondary Mn---C interactions near 2.7 Å are not particularly short. The list of stable two-coordinate manganese species is completed by metal–metal bonded species Ar^{Prⁱ}MnFe(η^5 -C₅H₅)(CO)₂⁸¹ with an Mn–Fe distance of 2.451(2) Å. There are no Mn---C approaches shorter than 3.0 Å, although there is a C(ipso)–Mn–Fe bending angle of 166.82(6)°.

5.3. Iron

Iron derivatives are the most numerous and intensely studied two-coordinate species (Table 4). This is because of the preeminent importance of iron and the fact that the two-coordinate iron(II) species, particularly Fe{N(SiMe₃)₂}₂, have proven to be very useful synthetically. In addition, their magnetic properties have attracted considerable interest (see below) because in some cases their magnetic moments approach free ion values.^{9–11} The first stable, two-coordinate, structurally authenticated iron species were Fe{N(SiMePh₂)₂}₂ (by X-ray crystallography)³⁹ and Fe{N(SiMe₃)₂}₂ (by ged),⁴⁰ which were reported almost simultaneously. They were synthesized by a straightforward salt metathesis route by the addition of 2 equiv of the lithium silylamide to FeBr₂ or FeBr₂(THF)₂ in diethyl ether. The Fe{N(SiMe₃)₂}₂ derivative is monomeric with a linear N–Fe–N unit in the vapor phase by ged, but it dimerizes to {(Me₃Si)₂N}Fe{ μ -N(SiMe₃)₂}₂Fe{N(SiMe₃)₂} in the solid state.⁴³ The more sterically crowded

Table 4. Selected Structural and Magnetic Data for Two-Coordinate Iron Complexes

complex	Fe–L (Å)	Fe...L (Å)	L–Fe–L (Å)	μ_{eff} (μ_{B})	ref
FeMes* ₂	2.058(4), 2.051(5)	2.822(8) 2.744(6)	157.9(2) 158.9(3)	5.18(0.1) 4.77	84,96
Fe{C(SiMe ₃) ₃ } ₂	2.045(4)		180	6.6–7.0	9,97,98
Fe(Ar ^{Me_e}) ₂	2.040(3) avg	2.751(3)–2.915(3)	164.4(1) 171.1(1)	4.90	85
Fe(Ar ^{Prⁱ}) ₂	2.059(1)	3.114(4) 3.068(C)	150.34(6)	4.82	99
FeAr ^{Prⁱ} {N(H)Ar ^{Me_e} } ₂	2.046(1)(C) 1.932(1)(N)	2.457(1)	134.97(5)	5.36(15)	87
{CH ₂ C ₆ H ₂ -2(C ₆ H ₃ -2-N(H)FeAr ^{Prⁱ}) ₂ }	2.045(2) 1.909(2)	2.866(2)	139.91(8)	5.29	100
Fe{N(SiMe ₃) ₂ } ₂ (ged)	1.84(2)		180		40
Fe{N(SiMe ₂ Ph) ₂ } ₂	1.896(2), 1.909(2)	2.633	172.1(1)		90
Fe{N(SiMePh ₂) ₂ } ₂	1.916(2) 1.918(2)	2.695(5)	169.0(1)	5.07	39,90
Fe{N(SiMe ₃)Dipp} ₂	1.851(4)		180	5.51	95
Fe{N(H)Ar ^{Me_e} } ₂	1.909(3)	2.690	140.9(2)	5.25–5.80	11
Fe{N(H)Ar ^{Prⁱ} } ₂	1.901(14)	2.792	180	7.0–7.8	11
Fe(NBu ^t) ₂	1.880(2) avg		179.45(8)	5.55	10
Fe{N(Mes)BMes ₂ } ₂	1.938(2)	2.521	166.6(1)	4.92	66
Fe{N(CH ₂ Bu ^t)(Dipp)} ₂	1.842(2)	2.728	168.8(2)		94
Fe(NC ₁₂ H ₂₄ -3,5-Me ₂ -1,8-Ph ₂) ₂	1.972(2) 1.976(2)	2.697(2)–2.713(3)	177.92(9)	4.73	92
Fe{N(SiMe ₃) ₂ } ₂ SAr ^{Me_e}	1.913(6)(N) 1.923(5)(N) 2.308(2)(S) 2.314(2)(S)	2.423 2.457	118.9(2) 120.8(2)	4.5	101
Fe(OAr ^{Prⁱ}) ₂	1.8472(9)	2.765(3)	180	5.28	99
Fe(OAr ^{AdⁱMe}) ₂	1.775(4), 1.838(3)		175.43(15)	5.1	104b
Fe(Ar ^{AdⁱPrⁱ}) ₂	1.774(2), 1.773(2)		171.15(11)		104b
Fe(SAr ^{Me_e}) ₂	2.275(2) 2.277(2)	2.470 2.535	121.8(1)	4.3	101
Fe(SAr ^{Prⁱ}) ₂	2.1867(6) 2.3517(6)	2.427(1)	151.48(2)	4.88(3)	73
Fe(SAr ^{Me_e})(SC ₆ H ₃ -2,6(SiMe ₃) ₂)	2.2782(7) 2.2697(6)	2.389(2)	128.84(3)	5.1	102
Fe(SAr ^{Me_e}) ₂	2.2417(9) 2.2905(13)	2.437(4)	116.58(3)	5.3	102
Fe(SMPhInd) ₂	2.29		161.4		103
Ar ^{Prⁱ} FeFe(η^5 -C ₅ H ₅)(CO) ₂	2.022(4) (C)–2.3931(8) (Fe)		163.94(12)	5.0 (300 K)	81

Fe{N(SiMePh₂)₂}₂ (Figure 6) displays a monomeric, bent structure (N–Fe–N = 169.0(1)°) in the solid state with a long Fe...C contact to an ipso carbon from one of the ligand phenyl groups.³⁹ The related species Fe{N(SiMe₂Ph)₂}₂⁹⁰ has a very similar structure with a bending angle of 172.1(1)°. Several other examples of bis(amido) iron complexes have been structurally characterized including the borylamide Fe{N(Mes)BMes₂}₂,⁶⁶ Fe{N(CH₂Bu^t)Dipp}₂,⁹⁴ the carbazolato salt Fe{NC₁₂H₂₄-3,5-Me-1,8-Ph₂}₂,⁹² which were synthesized by salt metathesis, and Fe{N(H)Ar^{Me_e}}₂,¹¹ which was synthesized by reaction of Fe{N(SiMe₃)₂}₂ with H₂NAr^{Me_e}. All of these complexes display varying degrees of bending of the iron coordination. In contrast, Fe(NBu^t)₂,¹⁰ and Fe{N(SiMe₃)Dipp}₂⁹⁵ (both synthesized by salt metathesis) and Fe{N(H)Ar^{Prⁱ}}₂¹¹ (synthesized by the reaction of Fe{N(SiMe₃)₂}₂ and 2 equiv of H₂NAr^{Prⁱ} with amine elimination), have N–Fe–N angles of 179.45(8)°, 180°, and 180°, respectively. Their putatively degenerate ground states confer

high magnetic moments because of unquenched orbital first-order angular momentum (see below).

The first two-coordinate diorganoiron complex to be reported was FeMes₂*.^{84,96} It has nonlinear iron coordination with a C–Fe–C angle near 158° and Fe–C distances in the range 2.05–2.06 Å. The first stable iron(II) dialkyl, the linear coordinated Fe{C(SiMe₃)₂}₂, was synthesized in good yield via salt metathesis by Weidlein⁹⁷ and LaPointe.⁹⁸ Its linear coordination prompted a detailed investigation of its magnetic properties by Reiff and co-workers who showed that the orbital angular momentum was virtually unquenched, and its magnetic moment was close to the free ion value. Two iron(II) diaryl complexes, Fe(Ar^{Me_e})₂⁸⁵ and Fe(Ar^{Prⁱ})₂,⁹⁹ both of which have bent geometries, were also synthesized by salt metathesis. The structure of Fe(Ar^{Me_e})₂ is noteworthy because the two crystallographically independent molecules have C–Fe–C angles of 164.4(1)° and 171.1(1)°, suggesting that is a shallow potential energy well for bending the coordination, implying

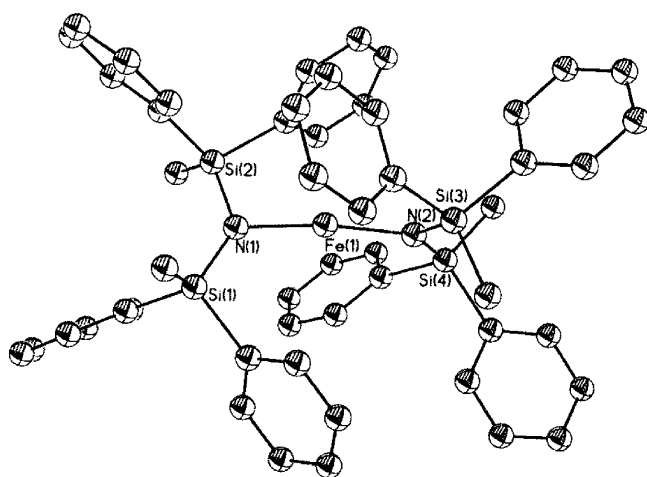


Figure 6. Thermal ellipsoid drawing (30%) of the iron(II) amide $\text{Fe}\{\text{N}(\text{SiMePh}_2)_2\}_2$. H atoms are not shown. Some structural details are given in Table 4.³⁹

that it is susceptible to deformation by packing forces within the crystal.⁸⁵

The heteroleptic aryl/amido complexes $\text{Ar}^{\text{Pr}^i}\text{Fe}\{\text{N}(\text{H})\text{Ar}^{\text{Me}_e}\}$ ($\text{C}-\text{Fe}-\text{N} = 134.97(5)^\circ$)⁸⁷ and $\{\text{CH}_2\text{C}_6\text{H}_2-2(\text{C}_6\text{H}_3-2-\text{N}(\text{H})-\text{FeAr}^{\text{Pr}^i})_2$ ($\text{C}-\text{Fe}-\text{N} = 139.91(8)^\circ$) displayed strongly bent geometries.¹⁰⁰ The structures also featured relatively short $\text{Fe}\cdots\text{C}$ secondary interactions, and, as argued earlier, the presence of an atom (i.e., nitrogen) between the metal and aryl groups facilitates the $\text{M}\cdots\text{C}$ interaction geometrically (cf., $\text{N}-\text{Fe}-\text{N} = 140.9(2)^\circ$ in $\text{Fe}\{\text{N}(\text{H})\text{Ar}^{\text{Me}_e}\}_2$).¹¹ Other structures where iron is complexed by terphenyl substituted thiolato ligands also display strong bending or other structural distortions. Thus, the bithiolato complexes $\text{Fe}(\text{SAr}^{\text{Me}_e})_2$,¹⁰¹ $\text{Fe}(\text{SAr}^{\text{Me}_e})_2$,¹⁰² $\text{Fe}(\text{SAr}^{\text{Me}_e})\{\text{SC}_6\text{H}_3-2,6(\text{SiMe}_3)_2\}$,¹⁰² and $\text{Fe}(\text{SMPHnd})_2$ (MPHnd , see list of abbreviations)¹⁰³ have the $\text{S}-\text{Fe}-\text{S}$ angles of $121.8(1)^\circ$, $116.58(3)^\circ$, $128.84(3)^\circ$, and 161.4° , respectively, and the heteroleptic amido/thiolato complex $\text{Fe}(\text{SAr}^{\text{Me}_e})\{\text{N}(\text{SiMe}_3)_2\}$ ¹⁰¹ has a bending angle near 120° . The more crowded dithiolate $\text{Fe}\{\text{SAr}^{\text{Pr}^i}\}_2$ ⁷³ is part of a series of $\text{M}\{\text{SAr}^{\text{Pr}^i}\}_2$ ($\text{M} = \text{Cr}, \text{Mn}, \text{Fe}, \text{Co}, \text{and Ni}$) complexes.⁷³ The

$\text{Cr}, \text{Mn}, \text{Co}, \text{and Ni}$ derivatives are linearly, or almost linearly, coordinated. The iron species, however, displays greater bending and has an $\text{S}-\text{Fe}-\text{S}$ angle of $151.48(2)^\circ$. Moreover, there is a short $\text{Fe}\cdots\text{C}$ interaction of $2.427(1) \text{ \AA}$ to a flanking aryl ring of one of the SAr^{Pr^i} ligands, and the $\text{Fe}-\text{S}-\text{C}(\text{ipso})$ angle for this ligand is a relatively narrow $100.05(5)^\circ$, whereas the $\text{Fe}-\text{S}-\text{C}(\text{ipso})$ angle for the other SAr^{Pr^i} ligand is $128.17(5)^\circ$. In addition, the $\text{Fe}-\text{S}$ bond length ($2.3517(6) \text{ \AA}$) to the SAr^{Pr^i} thiolato group having the narrower $\text{Fe}-\text{S}-\text{C}(\text{ipso})$ angle is considerably longer than the other $\text{Fe}-\text{S}$ distance ($2.1807(6) \text{ \AA}$). Thus, the coordination of the iron is far from symmetrical, and the data suggest an incipient tendency for rearrangement of the structure to a species that involves a $\text{Fe}-\eta^6\text{-arene}$ interaction and a weakened $\text{Fe}-\text{S}$ bond. In contrast to the thiolato derivative, the bis(aryloxo) complex $\text{Fe}\{\text{OAr}^{\text{Pr}^i}\}_2$ ⁹⁹ displays a crystallographically required linear $\text{O}-\text{Fe}-\text{O}$ coordination. This compound was first synthesized by the unusual route involving the reaction of oxygen with the diaryl $\text{Fe}(\text{Ar}^{\text{Pr}^i})_2$, which inserts into the $\text{Fe}-\text{C}$ bonds to yield the diaryloxo $\text{Fe}(\text{OAr}^{\text{Pr}^i})_2$. The compound can also be synthesized in higher yield by the reaction of $\text{Fe}\{\text{N}(\text{SiMe}_3)_2\}_2$ with 2 equiv of the phenol $\text{HOAr}^{\text{Pr}^i}$.^{104a} The $\text{Fe}-\text{O}$ distance is $1.8472(9) \text{ \AA}$, and there are long contacts ($\text{Fe}\cdots\text{C} = 2.765(3) \text{ \AA}$) to the ipso-carbons from two of the flanking aryl rings of the terphenyl ligands. Treatment of $\text{Fe}\{\text{N}(\text{SiMe}_3)_2\}_2$ with 2 equiv of the phenols $\text{HOAr}^{\text{Ad}_2\text{Me}}$ ($\text{HO}(\text{C}_6\text{H}_2-2,6(1-\text{Ad})_2-4-\text{Me})$) or $\text{HOAr}^{\text{Ad}_2\text{Pr}^i}$ ($\text{HO}(\text{C}_6\text{H}_2-2,6(1-\text{Ad})_2-4-\text{Pr}^i)$) afforded the two coordinate Fe^{2+} species $\text{Fe}(\text{OAr}^{\text{Ad}_2\text{Me}})_2$ or $\text{Fe}(\text{OAr}^{\text{Ad}_2\text{Pr}^i})_2$ with amine elimination.^{104b} The former species has an $\text{O}-\text{Fe}-\text{O}$ angle of $175.43(15)^\circ$ and two different $\text{Fe}-\text{O}$ bond lengths of $1.775(4)$ and $1.838(3) \text{ \AA}$, which correspond to different $\text{Fe}-\text{O}-\text{C}(\text{ipso})$ angles of $163.2(3)^\circ$ and $99.7(3)^\circ$. The latter has two similar $\text{Fe}-\text{O}$ distances of $1.774(3)$ and $1.773(2) \text{ \AA}$ as well as close $\text{Fe}-\text{O}-\text{C}(\text{ipso})$ angles of $153.6(3)^\circ$ and $152.2(3)^\circ$ and an $\text{O}-\text{Fe}-\text{O}$ angle of $171.15(11)^\circ$. The compound $\text{Ar}^{\text{Pr}^i}_2\text{FeFe}(\eta^5\text{-C}_5\text{H}_5)(\text{CO})_2$ features an iron-iron bond ($2.3931(8) \text{ \AA}$) between the differently substituted iron atoms. It has a bent $\text{C}-\text{Fe}-\text{Fe}$ angle of $163.94(12)^\circ$ at the two-coordinate iron. It was synthesized in a manner analogous to that described earlier for

Table 5. Selected Structural and Magnetic Data for Two-Coordinate Cobalt Complexes

complex	M-L (Å)	M-L (Å)	L-M-L (deg)	μ_{eff} (μ_{B})	ref
$\text{Co}(\text{Ar}^{\text{Me}_e})_2$	2.001(3)	2.679(2)	162.84(10), 172.17(11)		85
$\text{Co}(\text{Ar}^{\text{Pr}^i})_2$	2.014(2)	2.878(8)	159.34(8)	4.38	106
$\text{CoAr}^{\text{Pr}^i}\{\text{N}(\text{SiMe}_3)_2\}$	1.9732(16) (C), 1.8747(14) (N)		179.02(11)	5.82	106
$\text{CoAr}^{\text{Pr}^i}\{\text{N}(\text{H})\text{Ar}^{\text{Me}_e}\}$	90 K: 1.977(1) (C) 1.875(3) (N)	2.077(3)	101.75(11)	1.77	87
	240 K: 1.992(2) (C) 1.880(2) (N)	2.393(2)	133.90(6)	4.70	87
$\text{Co}\{\text{N}(\text{SiMe}_3)_2\}_2(\text{ged})$	1.84(2)		180		40
$\text{Co}\{\text{N}(\text{SiMePh}_2)_2\}_2$	1.901(3)	2.584(7), 2.588(7)	147.0(1)	4.42	39
$\text{Co}\{\text{N}(\text{SiMe}_3)\text{Dipp}\}_2$	1.8196(11)		180	4.90	95
$\text{Co}\{\text{N}(\text{Ph})\text{BMes}_2\}_2$	1.909(5)	2.388(6), 2.387(5)	127.1(2)	4.11	66
$\text{Co}\{\text{N}(\text{Mes})\text{BMes}_2\}_2$	1.910(3)	2.629(5), 2.734(5)	168.4(1)	4.36	60
$\text{Co}(\text{SAr}^{\text{Pr}^i})_2$	2.1912(6) 2.1939(5)	2.660(3), 2.665(3)	179.52(2)	5.75(2)	73
$\text{Co}\{\text{N}(\text{H})\text{Ar}^{\text{Me}_e}\}_2$	1.827(8), 1.845(8)	2.56	144.1(2)	4.7	105
$\text{Co}\{\text{N}(\text{H})\text{Ar}^{\text{Pr}^i}\}_2$	1.8645(19)	2.61	180	6.3	105

its chromium and manganese congeners.⁸¹ Its Mössbauer spectrum displays absorptions for its two distinct iron atoms.

5.4. Cobalt

A list of structurally characterized two-coordinate cobalt complexes is provided in Table 5. The synthesis, by salt metathesis, and partial characterization of the silylamide $\text{Co}\{\text{N}(\text{SiMe}_3)_2\}_2$ was first described by Burger and Wannagat in 1963.²⁶ In 1971, it was shown to be monomeric in the vapor phase by mass spectrometry and by cryoscopy and in cyclohexane solution.³⁰ In 1988, it was shown by X-ray diffraction to have a linear N–Co–N geometry with a Co–N distance of 1.84(2) Å in the vapor phase,⁴⁰ like its iron and manganese analogues, it is dimerized via bridging of the amido ligands to give three-coordinate cobalt atoms.⁴² The crystal structure of the more crowded $\text{Co}\{\text{N}(\text{SiMePh}_2)\}_2$ (also obtained by salt metathesis) showed it to be a monomer with a bent metal coordination (N–Co–N = 147.0(1)°), a Co–N bond length of 1.901(3) Å, and two Co···C interactions involving the phenyl substituents at ca. 2.59 Å.³⁹ Subsequently, several other homoleptic Co(II) amido complexes were synthesized and structurally characterized. All have bent geometries except $\text{Co}\{\text{N}(\text{H})\text{Ar}^{\text{Pr}^i}\}_2$ ¹⁰⁵ and $\text{Co}\{\text{N}(\text{SiMe}_3)_2\text{Dipp}\}_2$,⁹⁵ which have strictly linear N–Co–N units.

The heteroleptic mixed aryl/amido derivatives $\text{Ar}^{\text{Pr}^i}\text{Co}\{\text{N}(\text{SiMe}_3)_2\}_2$ ¹⁰⁶ and $\text{Ar}^{\text{Pr}^i}\text{Co}\{\text{N}(\text{H})\text{Ar}^{\text{Me}_e}\}_2$ ⁸⁷ were synthesized by the reaction of $(\text{Ar}^{\text{Pr}^i}\text{CoCl})_2$ with the appropriate lithium amide. The former species has an almost linear C–Co–N geometry. In contrast, $\text{Ar}^{\text{Pr}^i}\text{Co}\{\text{N}(\text{H})\text{Ar}^{\text{Me}_e}\}_2$ adopts two different temperature-dependent structures. At 90 K, it has a very strongly bent coordination (C–Co–N = 101.75(11)°) with further very close 2.077(3) Å Co···C interactions as well as a low spin, $S = 1/2$, electron configuration. At 240 K, the structure displays a much wider C–Co–N angle of 133.90(6)° and a weaker Co···C interaction of 2.393(2) Å. These changes are a consequence of a spin state crossover transition to a high spin configuration, $S = 3/2$, which occurs at 229 K.⁸⁷

The diaryls $\text{Co}(\text{Ar}^{\text{Me}_e})_2$ ⁸⁵ (Figure 7) and $\text{Co}(\text{Ar}^{\text{Pr}^i})_2$ ¹⁰⁶ are the only known stable, homoleptic diorganocobalt(II) compounds. Both complexes were synthesized by salt metathesis and have Co–C bond lengths near 2.0 Å. The first stable example of a two-coordinate diorganocobalt species, $\text{Co}(\text{Ar}^{\text{Me}_e})_2$, was reported by Kays and co-workers and features two crystallographically independent molecules like its iron counterpart $\text{Fe}(\text{Ar}^{\text{Me}_e})_2$. These molecules have different bending angles (C–Co–C = 162.84(10)° or 172.17(11)°), suggesting a soft, easily deformed C–Co–C core unit. The list of cobalt species is completed by the thiolato complex $\text{Co}(\text{SAr}^{\text{Pr}^i})_2$,⁷³ which has an almost linear S–Co–S coordination.⁷³

5.5. Nickel

The bisamido species $\text{Ni}\{\text{N}(\text{SiMe}_3)_2\}_2$, which was reported by Bürger and Wannagat in 1964, was obtained as a red oil from a salt metathesis reaction.²⁵ However, unlike its Mn, Fe, and Co analogues, it decomposes to a black substance upon standing at room temperature.¹⁰⁷ Its structure is unknown but presumably it is monomeric in the vapor phase like its manganese, iron, and cobalt congeners.⁴⁰ Stable, structurally characterized, two-coordinate nickel complexes are listed in Table 6. The red borylamido complexes $\text{Ni}\{\text{N}(\text{Ar})\text{BMe}_2\}_2$ (Ar = Ph or Mes,

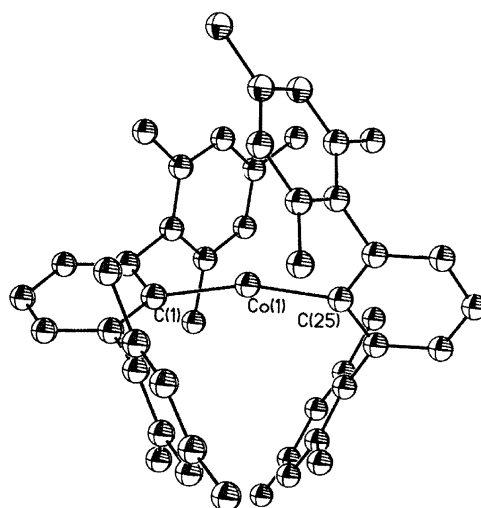


Figure 7. Thermal ellipsoid drawing (30%) of the cobalt diaryl $\text{Co}(\text{Ar}^{\text{Me}_e})_2$. H atoms are not shown. Some structural details are given in Table 5.⁸⁵

Figure 8)^{66,67} were the first, formally two-coordinate, Ni(II) complexes to be structurally characterized and were synthesized by salt metathesis. The Ph-substituted species has a very bent geometry with an N–Ni–N angle of 135.7(1)° and Ni–N bond length of 1.885(4) Å with further Ni···C approaches of 2.370(3) and 2.402(4) Å. The corresponding mesityl substituted derivative has a much wider N–Ni–N angle of 167.1(9)° and longer Ni···C interactions of 2.611(3) and 2.703(3) Å. The blue primary amido derivatives $\text{Ni}\{\text{N}(\text{H})\text{Ar}^{\text{Me}_e}\}_2$,¹⁰⁵ $\text{Ni}\{\text{N}(\text{H})\text{Ar}^{\text{Pr}^i}\}_2$,¹⁰⁸ and $\text{Ni}\{\text{N}(\text{H})\text{Ar}^{\text{Pr}^i}\}_2$ ¹⁰⁵ were reported more recently. The latter two complexes have linear nickel coordination, whereas $\text{Ni}\{\text{N}(\text{H})\text{Ar}^{\text{Me}_e}\}_2$ has a bent geometry with an N–Ni–N angle of 154.60(14)°. The Ni–N range of bond lengths in these three complexes, ca. 1.81–1.83 Å, is noticeably shorter than the 1.86–1.88 Å range in the borylamido derivatives. The list of two-coordinate Ni(II) species is completed by the thiolato complex $\text{Ni}(\text{SAr}^{\text{Pr}^i})_2$,⁷³ which has almost linear nickel coordination with an S–Ni–S angle of 174.22(6)° and Ni–S bond length near 2.17 Å.

The remaining two-coordinate nickel complexes are, with one important exception, derivatives of Ni(I) and are complexed by neutral carbene or phosphine donor ligands in combination with anionic amido or thiolato coligands. The first to be characterized were the heteroleptic amido/carbene complexes $[\{\text{CHN}(\text{Dipp})\}_2\text{C}]\text{Ni}\{\text{N}(\text{SiMe}_3)_2\}_2$ ¹⁰⁹ and $[\{\text{CHN}(\text{Dipp})\}_2\text{C}]\text{Ni}\{\text{N}(\text{H})\text{Dipp}\}_2$,¹⁰⁹ which were synthesized as yellow crystals by the reaction of the dimeric carbene nickel chloride precursor with 2 equiv of $\text{NaN}(\text{SiMe}_3)_2$ or $\text{LiN}(\text{H})\text{Dipp}$. The $-\text{N}(\text{SiMe}_3)_2$ derivative has an almost linear geometry with C–Ni–N = 178.7(8)°, whereas its $-\text{N}(\text{H})\text{Dipp}$ analogue is more strongly bent with C–Ni–N angles of 163.2(2)° or 167.4(2)°. The more recently reported species $\{\text{CHN}(\text{Dipp})\}_2\text{C}]\text{NiN}(\text{H})\text{Ar}^{\text{Me}_e}$ ¹⁰⁹ also has a wide C–Ni–N angle of 174.2(13)°. The orange, heteroleptic carbene/thiolato derivative $[\{\text{CHN}(\text{Mes})\}_2\text{C}]\text{NiSAr}^{\text{Me}_e}$ and the related phosphine/thiolato species $(\text{Ph}_3\text{P})\text{NiSAr}^{\text{Me}_e}$ were synthesized in a similar manner.¹¹¹ The less crowding PPh_3 ligand permits bending of the nickel coordination to 107.30(3)°, which is accompanied by apparently strong Ni···C interactions of 2.129(3) and 2.147(3) Å. The geometry in the corresponding

Table 6. Selected Structural and Magnetic Data for Two-Coordinate Nickel Complexes

complex	M–L (Å)	M···L (Å)	L–M–L (deg)	μ_{eff} (μ_{B})	ref
$\{[\text{CHN}(\text{Dipp})]_2\text{C}\}[\text{Ni}(\text{N}(\text{SiMe}_3)_2)]$	1.865(2) (N)		178.7(8)	1.9	109
	1.879(2) (C)				
$\{[\text{CHN}(\text{Dipp})]_2\text{C}\}[\text{NiN}(\text{H})\text{Dipp}]$	1.831(4) (N)		163.2(2)	2.3	109
	1.806(4)		167.4(2)		
	1.878(5) (C)				
	1.860(5)				
$\{[\text{CHN}(\text{Mes})]_2\text{C}\}[\text{NiSAr}^{\text{Me}_6}]$	2.2424(7) (S)	2.090(5)	163.27(16)		111
		2.098(5)			
$(\text{Ph}_3\text{P})\text{NiSAr}^{\text{Me}_6}$	1.935(2) (C)				
	2.2378(7) (S)	2.129(3)	107.30(3)	1.93	111
		2.147(3)			
	2.2034(9) (P)				
$\{[\text{CHNC}_6\text{H}_2-2,6(\text{C}_6\text{H}_2-2,6(\text{CHPh}_2)_2-4\text{Me})_2]_2\text{C}\}[\text{NiNAr}^{\text{Me}_6}]$	1.663(3) (N)		174.2(13)	2.77	110
	1.917(3) (C)				
$\text{Ni}\{\text{N}(\text{H})\text{Ar}^{\text{Pr}^i}_2\}_2$	1.818(3)	2.680	180.0(2)	2.79	108
$\text{Ni}\{\text{N}(\text{H})\text{Ar}^{\text{Me}_6}_2\}_2$	1.819(3)	2.56	154.60(14)	3.12	105
	1.812(3)				
$\text{Ni}\{\text{N}(\text{H})\text{Ar}^{\text{Pr}^i}_2\}_2$	1.8284(15)	2.58	180	2.92	105
$\text{Ni}\{\text{N}(\text{SiMe}_3)\text{Dipp}\}_2$	1.8029(9)		180	3.15	95
$\text{Ni}\{\text{N}(\text{Ph})\text{BMes}_2\}_2$	1.885(4)	2.370(3)	135.7(1)	2.91	66
		2.402(4)			
$\text{Ni}\{\text{N}(\text{Mes})\text{BMes}_2\}_2$	1.865(2)	2.611(3)	167.9(1)	2.9	67
	1.867(2)	2.703(3)			
$\text{Ni}(\text{SAr}^{\text{Pr}^i}_2)_2$	2.172(2)	2.640(5)	174.22(6)	2.58(3)	73
	2.175(2)	2.657(5)			

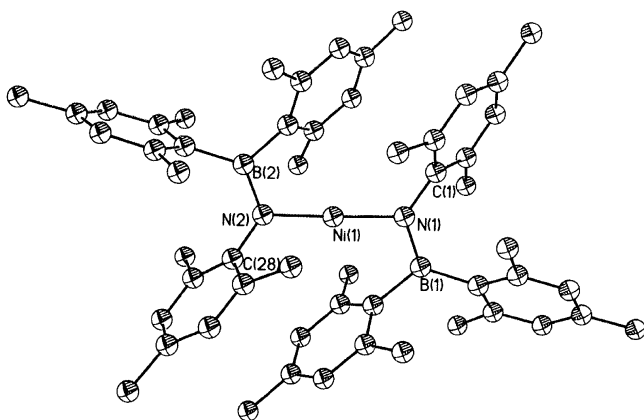


Figure 8. Thermal ellipsoid drawing (30%) of the nickel borylamide $\text{Ni}\{\text{N}(\text{Mes})\text{BMes}_2\}_2$. H atoms are not shown. Some structural details are given in Table 6.⁶⁷

carbene derivative is much less distorted with a C–Ni–S angle of $163.27(16)^\circ$, although there remain strong Ni···C interactions near 2.1 Å.

The reaction of $\text{N}_3\text{Ar}^{\text{Me}_6}$ with the complex $[\{\text{CN}(\text{Ar}^*)\}_2\text{C}]\text{Ni}(\eta^6\text{-PhMe})$ ($\text{Ar}^* = \text{C}_6\text{H}_2-2,6(\text{CHPh}_2)_2-4\text{Me}$) produced the unique two-coordinate nickel imido species $[\{\text{CN}(\text{Ar}^*)\}_2\text{C}]\text{NiNAr}^{\text{Me}_6}$ (Figure 9) with N_2 elimination. It featured almost linear nickel coordination C–Ni–N = $174.24(13)^\circ$ and a short, formally double Ni–N bond with Ni–N = $1.663(3)$ Å.¹¹⁰

5.6. Structural Data Summary

5.6.1. Geometries. Tables 2–6 list the structures of 80 two-coordinate complexes. Inspection of the structural data shows that just 18 of these have strictly linear coordination, of which five are gas-phase structures determined by ged. In effect, out of 73 solid-state structures, only 13 have strictly linear

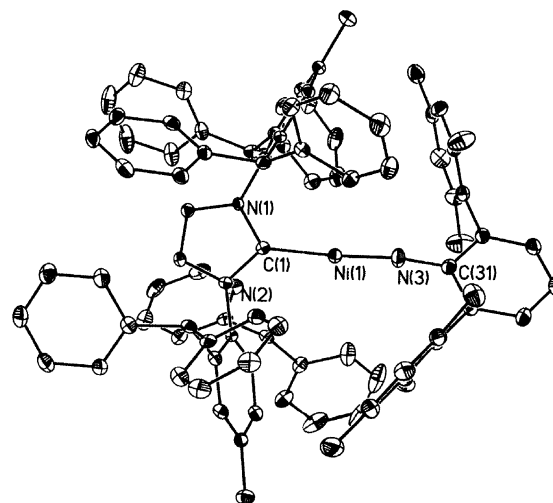


Figure 9. Thermal ellipsoid drawing (30%) of a two-coordinate nickel(II) imide. H atoms are not shown. Some structural details are given in Table 6.¹¹⁰

coordination. The remaining 60 display varying deviation from linearity. The bending of the geometries ranges from minor in 18 quasi-linear (interligand angle $>170^\circ$) complexes to very severe as in the N–Cr–N angle of $110.8(1)^\circ$ observed in $\text{Cr}\{\text{N}(\text{Ph})\text{BMes}_2\}_2$ or the ca. $101\text{--}103^\circ$ range of C–Cr–Cr angles in the quintuple bonded ArCrCrAr species.

Bearing in mind that calculations have indicated shallow potential wells for bending in two-coordinate transition metal dihydride^{47,53,54} and dihalide^{60–65} complexes, the interligand angle in the two-coordinate complexes isolated in the solid state may be influenced by several effects: (1) interactions between the metal and electron-rich parts of the ligand that are facilitated by bending the geometry, (2) packing effects, (3)

Table 7. Selected Electronic Absorption Spectral Data for Two-Coordinate Cobalt Complexes^a

complex		absorptions (cm ⁻¹)			ref
CoCl ₂ (gas)	19 000	14 500	10 300	4000	118,119
Co{N(SiMe ₃) ₂ } ₂	24 400	17 100	14 500	6500	30
Co{N(SiMePh ₂) ₂ } ₂	19 010	15 770	12 470		39
Co{N(Ph)BMes ₂ } ₂	24 290	20 010	16 400	12 470	66
Co{N(Mes)BMes ₂ } ₂		16 000	12 820	12 580	60
Co(NC ₁₂ H ₈ -3,6-Me ₂ -1,8-Ph ₂) ₂	25 120	17 280	10 600		92
Co{N(H)Ar ^{Pr_i4} } ₂	29 240	17 670			69
Co{N(H)Ar ^{Me₆} } ₂		19 010			69
Co(Ar ^{Pr_i4}){N(SiMe ₃) ₂ }	26 300	20 620			106
Co(Ar ^{Pr_i4}){N(H)Ar ^{Me₆} }	18 250	14 370			87
Co(Ar ^{Me₆}) ₂	25 970	19 200			85
CoAr ^{Pr_i4}	27 800	20 800			106
Co(SAr ^{Pr_i4}) ₂	22 620	16 050			73

^aOnly bands at lower energy than ca. 33,000 cm⁻¹ or 300 nm are listed. Several complexes feature intense bands at higher energies which probably arise from charge transfer or π - π^* transitions in ligands containing aryl groups.

ligand field or hybridization effects, and (4) Renner–Teller distortions involving vibronic coupling of the ground and an excited state, which can lead to a stabilization of a bent configuration.^{53b,61} If the ligands are extremely large, however, steric repulsion between them across the metal can override (1)–(4) and impose a linear geometry. For example, it seems likely that large Renner–Teller distortions are unlikely to occur in cases of extreme steric crowding because of the increased steric pressure that would result from bending, although small distortions can occur because of the vibration of the metal ion perpendicular to the N–M–N axis. The large transmetallic steric effects of the larger terphenyl substituted amido and thiolato ligands impose linear geometries in almost all complexes of formula M{N(H)Ar^{Pr_i4}}₂,^{69,108} M{N(H)-Ar^{Pr_i4}}₂,^{11,69,89,105} and M(SAr^{Pr_i4})₂. When the size of the terphenyl substituent is decreased to Ar^{Me₆}, however, the steric repulsion is apparently no longer sufficient, and variably bent geometries, which display interligand angles in the range of ca. 121–155°, are observed in all complexes of formula M{N(H)-Ar^{Me₆}}₂. Most likely, the bending in these complexes is driven by electrostatic interactions between the metal ion and one or more of the electron-rich flanking aromatic rings of the terphenyl ligand. It is noteworthy that such interactions are also observed in the d⁵, Mn²⁺ complex Mn{N(H)Ar^{Me₆}}₂ (N–Mn–N = 138.19(9)°) where there are no ligand field effects because of the half-filled d⁵-electron valence shell. Further inspection of the data in Table 3 shows that bending of the coordination in the manganese complexes is the rule rather than the exception.

Deviations from linear geometry may in some cases be correlated with the size of the metal ion. For example, the complexes M{N(H)Ar^{Me₆}}₂ have N–M–N angles of 120.9(5)° (Cr),⁶⁹ 138.19(9)° (Mn),⁸⁹ 140.9(2)° (Fe),¹¹ 144.1(2)° (Co),¹⁰⁵ and 154.60(14)° (Ni).¹⁰⁵ Thus, for the larger metal (Cr in this case) with the less crowded environment, a greater deviation from linearity is observed. However, steric effects form only part of the explanation. The structures of the pairs of metal diaryls M(Ar^{Me₆})₂⁸⁵ and M(Ar^{Pr_i4})₂ (M = Mn,⁸⁶ Fe,⁹⁹ and Co¹⁰⁶) show that the more crowded Ar^{Pr_i4} derivatives have C–M–C angles that are up to ca. 10° narrower than those of the less bulky Ar^{Me₆} substituted complexes, which is contrary to what is expected on the basis of steric considerations. Oddly the C–M–C angles in the M(Ar^{Pr_i4})₂ species, which are 160.19(4)°

(Mn), 150.34(6)° (Fe), and 159.34(8)° (Co), do not correlate with metal size and are also narrower than those in the generally linear amido derivatives M{N(H)Ar^{Pr_i4}}₂, which carry the same terphenyl substituent but are less crowded because the terphenyl group is separated from the metal by the amido nitrogen atom. Also, the diaryls M(Ar^{Me₆})₂ (M = Mn, Fe, or Co)⁸⁵ each crystallize as two crystallographically distinct molecules that display C–M–C angles that differ by up to ca. 9° (e.g., C–Co–C = 162.8(1)° and 172.2(1)° in Co(Ar^{Me₆})₂), which suggests a shallow potential well for bending and that packing effects^{53b,61} may play a significant role in determining the interligand angle at the metal. Depending on the ground state, Renner–Teller effects¹¹² may also be a factor in bending the geometries. However, there have been few calculations on model species that would provide useful information on this aspect of the structures.

5.6.2. Bond Lengths. The remaining structural parameter of primary interest in these complexes is the metal–ligand distance. Unsurprisingly, Shannon–Prewitt radii^{113a} are unavailable for two-coordinate, transition metal ions. However, it is possible to use single bond covalent radii^{113b} for the metal (Cr, 1.22 Å; Mn, 1.19 Å; Fe, 1.16 Å; Co, 1.11 Å; and Ni, 1.10 Å) and ligating atoms to estimate bond lengths. Over one-half of the two-coordinate compounds in Tables 2–5 are amido derivatives and, as a result, may be used as illustrative examples. Thus, the addition of the single bond covalent radius for nitrogen (0.73 Å) to the metal radii above yields the bond lengths Cr–N 1.95 Å, Mn–N 1.92 Å, Fe–N 1.89 Å, Co–N 1.84 Å, and Ni–N 1.83 Å. The data in Tables 2–5 have metal–nitrogen ranges of Cr–N 1.94–2.0 Å, Mn–N 1.99–2.05 Å, Fe–N 1.84–1.98 Å, Co–N 1.87–1.91 Å, and Ni–N 1.82–1.89 Å (the metal–nitrogen distances in the M{N(SiMe₃)₂}₂ compounds are not included in the comparison due to strong correlation of the M–N scattering with that of silicon–nitrogen).⁴⁰ It can be seen that the experimental Mn–N and Co–N bond distances lie above the predicted bond length, and most of the measured Cr–N, Fe–N, and Ni–N bond lengths lie at the upper end of the ranges given above so that it is fair to say that the predicted covalent radii tend to underestimate the M–N bond lengths in the two-coordinate amides. Similarly, in the diorgano Mn, Fe, or Co complexes, the predicted M–C bond lengths for Mn (1.94 Å), Fe (1.91 Å), and Co (1.86 Å) are shorter than the measured M–C bond lengths, which are near 2.1 Å for Mn–C, 2.05 Å for Fe–C, and 2.0 Å for Co–C.

The experimentally determined M–S bond lengths in the homoleptic bisthiolato derivatives⁷³ are also about 0.05–0.1 Å longer than predicted. The longer than expected bond lengths in the two-coordinate complexes may be a consequence of the large sizes of the ligands used to stabilize them. For example, the data for the closely related pairs of complexes $M\{N(H)Ar^{Me_6}\}_2$ and $M\{N(H)Ar^{Pr^i}\}_2$ tend to support this view with longer bond lengths observed (except in the case of manganese where they are about equal) for the bulkier amido ligand. The lengthening of the metal ligand bonds by steric effects of the large ligands also receives support from data on related amido complexes with less bulky substituents. For example, the Cr(II) dimers $R_2NCr(\mu-NR_2)_2CrNR_2$,^{114,115} which feature three-coordinate chromium, have terminal Cr–N distances of 1.927(3) Å (R = Prⁱ) and 1.942(7) Å (R = Cy), which, despite the higher metal coordination number, are shorter than those in Table 2 and are more in line with the predicted distance. Similarly, the terminal M–N distances in the iron⁴³ and nickel dimers $Ph_2NM(\mu-NPh_2)_2MNPPh_2$,¹⁰⁷ which also feature three-coordinate metals, are 1.895(3) and 1.828(9) Å and essentially identical to the bond lengths predicted by the sum of the respective covalent radii.

5.6.3. Secondary Metal–Ligand Interactions. The structural data in Tables 2–7 also list distances for secondary interactions between the ligands and metals in many cases. These distances vary from being only 0.1 Å longer than the corresponding single σ -bond as seen in the low temperature structure of $CoAr^{Pr^i}\{N(H)Ar^{Me_6}\}$ ⁸⁷ (Co---C = 2.077(3) vs 1.977(1) Å for the Co–C σ -bond) to greater than 3.0 Å in numerous others where secondary interactions are very weak. Calculations on some of the complexes (e.g., the $Ar^{Pr^i}CrCrAr^{Pr^i}$ ⁷⁴ quintuple bonded dimer, where the relatively short secondary Cr---C interaction (2.294(1) Å) exceeds the Cr–C σ -bond (2.131(1) Å) by only 0.16 Å) have indicated that despite the short distance the secondary interactions are weak (ca. 2 kcal mol⁻¹). In contrast, others have argued,¹¹⁶ on the basis of Mössbauer spectroscopy of low coordinate iron complexes such as the two-coordinate $Fe(SAr^{Me_6})\{N(SiMe_3)_2\}$,¹⁰¹ that the secondary interactions effectively raise the coordination number and that this nominally two-coordinate complex should be regarded as a three-coordinate species on the basis of its isomer shift ($\delta = 0.66$ mm s⁻¹) and quadrupole splitting ($\Delta E = 0.79$ mm s⁻¹), which resemble the values observed for three coordinate iron species such as $[Fe(SMe_s^*)_3]^-$ ($\delta = 0.57$, $\Delta E = 0.81$ mm s⁻¹) and $Fe\{N(SiMe_3)_2\}_2THF$ ($\delta = 0.57$, $\Delta E = 0.97$ mm s⁻¹). Mössbauer studies of the two-coordinate iron species $Fe\{C(SiMe_3)_3\}_2$,⁹ $Fe\{N(H)Ar^{Pr^i}\}_2$,¹¹ and $Ar^{Pr^i}FeFe(\eta^5-C_5H_5)(CO)_3$ ⁸¹ showed that their relatively uniform δ values of 0.4, 0.38, and 0.42 mm s⁻¹ are significantly lower than the 0.53–0.66 mm s⁻¹ range reported for three-coordinate iron complexes and are consistent with their two-coordinate character (ΔE values are 1.3, 0.68, and 0.96 mm s⁻¹, respectively). On the other hand, the bent complex $Fe\{N(H)Ar^{Me_6}\}_2$ ¹¹ has $\delta = 0.76$ mm s⁻¹ and $\Delta E = 0.87$ mm s⁻¹, which is seemingly consistent with the coordination number of three or more for iron. However, examination of the structural data for both the bent $Fe\{N(H)Ar^{Me_6}\}_2$ and linear $Fe\{N(H)Ar^{Pr^i}\}_2$ shows that they both have Fe---C approaches involving carbons from the flanking rings from the terphenyl nitrogen substituents that do not differ greatly. For the linear $Fe\{N(H)Ar^{Pr^i}\}_2$, the

closest Fe---C approaches to two different flanking $C_6H_2-2,4,6-Pr^i_3$ rings are near 2.792 Å, whereas for the bent complex $Fe\{N(H)Ar^{Me_6}\}_2$ (N–Fe–N = 140.9(2)°), the Fe---C distances are 2.690 and 2.588 Å.¹¹ Given that both sets of Fe---C distances greatly exceed that of an Fe–C single bond (ca. 2.05 Å, cf., Table 4), the data suggest that the Mössbauer parameters are extraordinarily sensitive to relatively small changes in the iron coordination sphere. However, whether such differences warrant changing the description of the coordination of the number of the complex remains an open question. Clearly, the secondary interactions are significantly weaker than the primary ligation. Unfortunately, there appears to be no detailed computational work on a broad range of complexes that might afford a clearer picture of the strength of these interactions.

5.6.4. Calculations. Few calculations have been carried out on the bonding in the stable two-coordinate complexes. Early SCF calculations on $Mn(NH_2)_2$ as a model species for $Mn\{N(SiMe_3)_2\}_2$ suggested that the Mn–N bond was very polar and that $p\pi-d\pi$ bonding was negligible.⁴⁰ Photoelectron spectroscopy of the $M\{N(SiMe_3)_2\}_2$ (M = Mn, Fe, or Co) complexes identified ionization energies near 8.0 eV for the highest energy valence d-electrons, the nitrogen lone pairs (ca. 8.5 eV), and the M–N σ bonds (9.1–9.6 eV).⁴⁰ Ab initio molecular orbital calculations within a Hartree–Fock approximation on the high spin ⁶A₁ ground state of $MnMe_2$ with Gaussian type basis sets afforded an Mn–C distance of 2.13 Å and a polarized Mn–C bond. Unrestricted DFT (6-311+G* basis set) calculations for $Fe(NR_2)_2$ (R = H, Me, or Bu^t) were also undertaken.¹⁰ The calculated structure for the high spin (i.e., S = 2), two-coordinate amide $Fe(NBu^t)_2$ featured an Fe–N bond length of 1.90 Å close to the 1.88 Å experimental value and a dihedral angle of 77° (cf., experimental 80.5°) between the two NC₂ planes. In the rigid orbital spin restricted approximation, the high spin Fe²⁺ (d⁶ ion) in D_{2d} symmetry has the electron configuration $(xy, x^2-y^2)^3(z^2)^1(xz, yz)^2$. The xz and yz levels are π^* orbitals, whereas z^2 is a σ^* orbital. The iron d_{z²} orbital is strongly hybridized with the 4s orbital, which reduces its antibonding level and lowers its energy. DFT calculations for $Fe\{N(H)Ph\}_2$ and $Fe\{N(H)C_6H_3-2,6-Ph_2\}_2$ as models for $Fe\{N(H)Ar^{Pr^i}\}_2$ and $Fe\{N(H)Ar^{Me_6}\}_2$ reproduced the experimental structures accurately and showed that the triplet states are more than 30 kcal mol⁻¹ higher in energy.¹¹ Similar Fe–N bonding to that in the $Fe(NBu^t)_2$ species was also calculated and featured hybridization of the 3d_{z²} and 4s, which produces a stabilization and lowers energy.¹⁰ Calculations for a high spin d⁶ ion in a two-coordinate site under the effects of crystal-field and spin orbit coupling as a model system for $Fe\{C(SiMe_3)_3\}_2$ confirmed its unusual properties and its high g₁₁ value (g = 12) for the ground states,^{9,117a} as well as the high internal magnetic fields as measured by Mössbauer spectroscopy.^{117b} EPR data for the $Fe(NBu^t)_2$,¹⁰ $Fe\{N(H)Ar^{Me_6}\}_2$,¹¹ and $Fe\{N(H)Ar^{Pr^i}\}_2$ ¹¹ also afforded high g₁₁ values >10. DFT calculations of the two-coordinate nickel(II) imido species $[\{CHNC_6H_2-2,6(C_6H_2-2,6(CHPh_2)_2-4-Me)\}_2]CNiNAr^{Me_6}$ confirmed the presence of a strongly stabilized 3d_{z²}–4s, essentially nonbonding, doubly occupied orbital and unpaired electrons in the almost degenerate d_{xz} and d_{yz} π^* -orbitals at higher energy. The d⁸ configuration is completed by two electron pairs and the more stable d_{xy} and d_{x²-y²} nonbonding orbitals. The short Ni–N distance is caused by Ni–N π bonding in addition to σ bonding to both the imido and the carbene ligand. Despite the

Table 8. Selected Electronic Absorption Spectral Data for Homoleptic Two-Coordinate Iron Complexes

complex	absorptions (cm ⁻¹)				ref
Fe(Ar ^{Me₆}) ₂	28 330	27 320	26 180	24 330	85
Fe(Ar ^{Prⁱ}) ₂	27 030			24 000	99
Fe[N(H)Ar ^{Me₆}] ₂	31 060			23 040	11
Fe{N(H)Ar ^{Prⁱ} } ₂	32 260	31 250		22 220	11
Fe(NC ₁₂ H ₈ -3,6-Me ₂ -1,8-Ph ₂) ₂	32 570	31 450	26 180	20 960	92
Fe{N(CH ₂ Bu ^t)Dipp} ₂	29 590		25 710	18 520	94
Fe(OAr ^{Prⁱ}) ₂	27 030			23 980	99
Fe(SAr ^{Me₆}) ₂	25 320			22 120	102
Fe(SAr ^{Prⁱ}) ₂	25 970				73
Fe(SAr ^{Me₆}){SC ₆ H ₅ -2,6-(SiMe ₃) ₂ }	25 970				102

paucity of computational work on the isolated two-coordinate species, it is clear the calculations will play a key role in the future development of the area. Such work will be essential for a rational interpretation of their spectra (e.g., electronic) and magnetic properties.

5.7. Electronic Spectra

The electronic spectra of the stable open-shell two-coordinate transition metal complexes have usually been included in reports describing their preparation, X-ray crystal structures, and magnetic properties. However, attempts at detailed interpretations and spectral assignments have been rare. Beginning in the 1960s, there have been several studies of the electronic spectra of gaseous transition metal dihalides and their d–d transitions.⁴ The absorptions generally appear in the range of 4000–22 000 cm⁻¹ (2500–455 nm) and with extinction coefficients that vary from tens to hundreds of mol⁻¹ L cm⁻¹ absorption units (except where they are superimposed on more intense symmetry allowed absorptions, e.g., charge transfer or π – π^* transitions that extend into the visible region). The spectra have been interpreted in terms of ligand field parameters appropriate for $D_{\infty h}$ point group symmetry.^{118–120} However, a number of reports^{60,65} have indicated that, in contrast to ligand field predictions of Figures 1 and 2, the standard energetic order of the 3d orbitals $\sigma > \pi > \delta$ is not reproduced by DFT studies on the dihalides. This is thought to be due to σ -donor ligand induced s–d hybridization and destabilization of the 3d π -levels by the π -donating halide ligands.⁶⁵

The ligand field interpretations published for the metal halide spectra in the gas phase can assist in the assignment of the UV–vis spectra of two-coordinate transition metal species in solution. This approach was used in 1971 for the amido complex Co{N(SiMe₃)₂}₂, which has a d⁷, ⁴F ground state.³⁰ It had already been recognized from previous work on higher coordinate transition metal amides that the amido ligand field strength was significantly larger than that of chloride.^{121,122} This permitted assignments for the four bands observed for Co{N(SiMe₃)₂}₂ as follows: ⁴ $\Sigma_g^+ \rightarrow \Pi_g(P)$ (24 400 cm⁻¹), ⁴ $\Sigma_g^+ \rightarrow \Sigma_g^+(P)$ (17 100 cm⁻¹), ⁴ $\Sigma_g^+ \rightarrow \Delta_g(F)$ (14 500 cm⁻¹), and ⁴ $\Sigma_g^+ \rightarrow \Pi_g(F)$ (6500 cm⁻¹). However, it may also be that the two lower energy absorptions are due to ⁴ $\Sigma_g^+ \rightarrow \Phi_g(F)$ (14 500 cm⁻¹) and ⁴ $\Sigma_g^+ \rightarrow \Delta_g(F)$ (6500 cm⁻¹) with a third, lowest energy ⁴ $\Sigma_g^+ \rightarrow \Pi_g(F)$ absorption lying outside the range of the instrument. The corresponding bands for CoCl₂ (gas) appeared at 19 000, 14 500, 10 300, and 4000 cm⁻¹ (see Table 7), which are considerably lower in energy. Three absorption bands were observed for Co{N(SiMePh₂)₂}₂ at 19 010, 17 100, and 12 470 cm⁻¹, but these correspond more closely with those of CoCl₂

(gas) (a fourth, lower energy band was not observed presumably because it lay beyond the frequency range of the UV–vis spectrometer in the near-infrared region). These data suggest that the ligand field produced by the –N(SiMePh₂)₂ ligand is weaker than that of –N(SiMe₃)₂. The energies of the absorption bands for the borylamide Co{N(Ph)BMes₂}₂ correspond more to those of Co{N(SiMe₃)₂}₂ with the lower energy absorption again unobserved. There are two bands relatively close in energy at 16 400 and 15 240 cm⁻¹, suggesting that the very bent solid-state geometry, which may lift the degeneracy of the ⁴ Π_g , ⁴ Δ_g , and ⁴ Φ_g levels, is retained in solution. The spectrum reported for Co(NC₁₂H₈-3,6-Me₂-1,8-Ph₂)₂⁹² also features three bands at similar energies. For several complexes, however, only two bands were observed at higher energies. This is exemplified by the series of compounds Co(Ar^{Prⁱ})₂{N(SiMe₃)₂}, Co(Ar^{Me₆})₂, Co(Ar^{Prⁱ})₂, and Co(SAr^{Prⁱ})₂. It is unclear at present why the remaining bands are not observed. However, a comparison of the two high energy bands in Ar^{Prⁱ}Co{N(SiMe₃)₂}₂ with those of Co{N(SiMe₃)₂}₂ (cf., Table 7) suggests that replacement of one of the –N(SiMe₃)₂ ligands with the aryl ligand Ar^{Prⁱ} leads to a shift to higher absorption energies. This is reinforced by the spectrum of Co(Ar^{Prⁱ})₂, which has two bands displaying a further shift to higher energy that leads to the view that the aryl ligand produces a stronger ligand field than that of the amido ligand.

For two-coordinate iron(II) complexes, the ground state is ⁵D, which in principle can be split by a linear field into three components ⁵ Δ_g , ⁵ Π_g , and ⁵ Σ_g^+ in order of increasing energy. Thus, two absorption bands are expected on this basis. Yet electronic spectra for many of the known iron(II) compounds were reported to be featureless but with an increasing absorption toward higher frequencies as exemplified by Fe{N(SiMe₂Ph)}₂, Fe{N(SiMePh₂)₂}, Fe{N(Mes)BMes₂}, FeMes₂^{*}, and Fe{C(SiMe₃)₃}. The spectra of several other complexes, for example, Fe{N(SiMe₃)₂}, Fe(NBu^t)₂, Fe{N(SiMe₃)₂}SAr^{Me₆}, and Fe(SAr^{Me₆})₂, have not been published. A list of spectral maxima for some homoleptic iron(II) complexes is presented in Table 8. Broadly speaking, most of the compounds display two absorptions, one in the range 27 000–32 000 cm⁻¹ and a lower energy band in the range 23 000–26 000 cm⁻¹. Some of these bands were split further into two or more absorptions possibly as a result of bending the coordination geometry of the metal. However, the overall pattern suggests that these bands could fit ⁵ $\Delta_g \rightarrow \Sigma_g^+$ and ⁵ $\Delta_g \rightarrow \Pi_g$ transitions. Nonetheless, the energies of these transitions are quite high, which seems inconsistent with the

relatively low overall ligand field strength expected for a two-coordinate complex. Thus, the possibility that they are charge transfer bands cannot be excluded.

Fewer data are available for two-coordinate Cr(II) complexes. In this case, the ground state is also 5D , which splits into $^5\Sigma_g^+$, $^5\Pi_g$, and $^5\Delta_g$ states (i.e., the inverse of the Fe(II)) in a linear field. In the linear coordinated $\text{Cr}\{\text{N}(\text{H})\text{Ar}\}_2$ ($\text{Ar} = \text{Ar}^{\text{Pr}^4}$ and Ar^{Pr^6}) and the bent $\text{Cr}\{\text{N}(\text{H})\text{Ar}^{\text{Me}_6}\}_2$, two absorptions in the ranges 29 000–30 000 and 24 000–25 000 cm^{-1} were observed. These energies are similar to those measured for the corresponding two-coordinate iron complexes. The spectrum of $\text{Cr}(\text{NC}_{12}\text{H}_4\text{-3,6-Me}_2\text{-1,8-Ph}_2)_2$ also features a number of bands in the 28 000–32 000 cm^{-1} region in addition to an absorption of 25 575 cm^{-1} , which are broadly similar to those of the terphenyl substituted amides, and there is also a weaker absorption at lower energy. In contrast, the borylamido complexes $\text{Cr}\{\text{N}(\text{Ar})\text{BMe}_2\}_2$ ($\text{Ar} = \text{Ph}$ or Mes) display two absorptions: one at around 12 500 cm^{-1} , while the other appears at higher energies, 14 880 cm^{-1} (Ph) or 16 030 cm^{-1} (Mes). These frequencies are ca. 50% lower than those observed for the linear amides. The extremely bent geometries observed for these borylamides and the apparently strong secondary Cr–C interactions confer a distorted pseudotetrahedral ligand field with a lower crystal field splitting at the chromiums, which may account for the change in frequencies observed.

Only a handful of two-coordinate Ni(II) species have been characterized. The ground state is 3F , which is further split in a linear ligand field into four component levels and there is also a higher energy 3P state that is also split so that up to five absorptions are predicted. However, only single absorptions at ca. 13 000 cm^{-1} have been reported for $\text{Ni}\{\text{N}(\text{H})\text{Ar}^{\text{Me}_6}\}_2$, $\text{Ni}\{\text{N}(\text{H})\text{Ar}^{\text{Pr}^4}\}_2$, and $\text{Ni}\{\text{N}(\text{H})\text{Ar}^{\text{Pr}^6}\}_2$. No UV–vis absorption spectra for most of the Ni(I), d^9 (2D ground state) heteroleptic complexes have been published, although $[\{\text{CHN}(\text{Mes})\}_2\text{C}]\text{-NiSAr}^{\text{Me}_6}$ was reported to have an absorption band at 31 850 cm^{-1} .

The interpretation of the electronic spectra of the two coordinate complexes has, until now, been mainly grounded in the ligand field approach. This takes little account of possible complicating effects such as π -bonding. However, it may also be that only computational methods involving high level calculations will provide the advances necessary for a deeper understanding of the molecular energy levels and bonding.

5.8. Magnetism

Tables 2–6 include room temperature μ_{eff} data for the two-coordinate complexes. These data were collected mainly by one of two methods (or combination thereof), which involved their measurement in solution either by the Evans' method¹²³ or, more commonly, by using a SQUID magnetometer. Generally speaking, the data from the Evans' method measurements were obtained at room temperature and provide no information on their temperature dependence or the purity of the complex. Virtually all of the recent data have been obtained using SQUID magnetometers, however. With the exception of the quintuple bonded dichromium(I) species ArCrCrAr ($\text{Ar} = \text{Ar}^{\text{Pr}^4}$, $\text{Ar}^{\text{Pr}^4}\text{-4-SiMe}_3$, $\text{Ar}^{\text{Pr}^4}\text{-4-OMe}$, $\text{Ar}^{\text{Pr}^4}\text{-4-F}$), which display weak temperature independent paramagnetism, all of the open-shell two-coordinate complexes exhibit paramagnetic behavior consistent with the Curie–Weiss law. In addition, a high spin electron configuration is observed in all cases except

$\text{CoAr}^{\text{Pr}^4}\{\text{N}(\text{H})\text{Ar}^{\text{Me}_6}\}$, which undergoes a spin state crossover to become low spin below 229 K.⁸⁷ The magnetic moments of the d^5 manganese(II) and chromium(I) derivatives correspond (usually closely) to the spin-only value expected (5.92 μ_B) for their d^5 electron configuration. As mentioned in the Introduction, the remaining d^1 – d^4 and d^6 – d^9 two-coordinate complexes may exhibit highly anisotropic internal magnetic fields as well as high orbital angular momenta and zero field splittings. These may lead to high barriers to spin flipping necessary for single molecular magnetism.^{124–127}

Aside from the above-mentioned d^5 species, there exist stable two-coordinate complexes only for the d^4 , d^6 , d^7 , d^8 , and d^9 configurations. These species may exhibit more complex paramagnetic behavior that may arise from several effects, principally from unquenched first order orbital angular magnetism and spin orbit coupling. For a stable complex with idealized $D_{\infty h}$ symmetry, the first-order orbital angular momentum has been interpreted to be due to the motion of an electron around the z -axis via its continuous transfer between two degenerate orbitals related to each other by a rotation about the z -axis.^{9–11,128} A further requirement is that there must be no electron in the second orbital with the same spin as that in the first. In other words, the spin multiplicity should not change as a result of such motion. Reference to the simple model in Figure 2 shows that the above criteria are met only for the d^1 , d^3 , d^6 , and d^8 configurations which are predicted to have degenerate ground state in $D_{\infty h}$ symmetry. Of these, only d^6 and d^8 complexes have been investigated so far because stable two-coordinate complexes with d^1 and d^3 configurations have not been reported. The d^6 dialkyl $\text{Fe}\{\text{C}(\text{SiMe}_3)_3\}_2$, which was synthesized independently by Weidlein⁹⁷ and LaPointe,⁹⁸ was investigated by Reiff and co-workers.⁹ As previously mentioned, its structure is rigorously linear with Fe–C distances near 2.05 Å and local $D_{\infty h}$ symmetry at iron and overall D_{3d} symmetry for $\text{Fe}(\text{CSi}_3)_2$. In either point group, the $d_{x^2-y^2}$, d_{xy} and d_{xz} , d_{yz} orbital pairs are degenerate (cf., Table 1), and it is apparent from Figure 1 that an electron may transfer between the $d_{x^2-y^2}$, d_{xy} orbitals under the conditions described above without change of spin. Mössbauer spectroscopy at room temperature afforded isomer shift and quadrupole splittings consistent with a two-coordinate iron(II) center. At low temperature, a fully resolved hyperfine splitting pattern was observed from which a very high internal orbital field of ca. +200 T was estimated. DC SQUID magnetization measurements afforded $M_{\text{saturation}} = \text{ca. } 32\,500 \text{ emu mol}^{-1}$ in comparison to the calculated saturation values for spin-only behavior for $S = 2$ and $S = 3$ of 22 339 and 33 495 emu mol^{-1} . In effect, the inclusion of the orbital contribution almost matches the $S = 3$ value and is equivalent to adding two full spins relative to the spin-only behavior. The calculated moment for the ground-state 5D_4 free-ion term $\mu_J = \{g_J^2(J + 1)\}^{1/2}$, $L = S = 2$, $J = 4$, $g = 3/2$ is 6.71 μ_B and corresponds to the experimentally observed moment of 6.6–7 μ_B for the complex. It is thus apparent that the two linearly disposed alkyl groups have a negligible orbital angular momentum quenching effect.

Investigations of three other two-coordinate Fe(II) complexes confirmed and further illuminated the above findings. The almost linear, N–Fe–N = 179.45(8)°, coordinated complex¹⁰ $\text{Fe}(\text{NBU}^t)_2$ had a relatively high effective magnetic moment of 5.55 μ_B and a large internal magnetic field estimated to be +155 T. The linear $\text{Fe}\{\text{N}(\text{H})\text{Ar}^{\text{Pr}^6}\}_2$ was found to have a effective magnetic moment in the range 7.0–7.50 μ_B and an

estimated internal field of ca. +170 T.¹¹ In contrast, the closely related complex $\text{Fe}\{\text{N}(\text{H})\text{Ar}^{\text{Me}_6}\}_2$ displays very different magnetic behavior. Because of the smaller size of the ligands, this complex has a strongly bent $\text{N}-\text{Fe}-\text{N} = 140.9(2)^\circ$ geometry as well as significant $\text{Fe}-\text{C}$ secondary interactions that may raise the effective coordination number of the metal.¹¹⁶ It displays a significantly reduced μ_{eff} value of 5.25–5.80 μ_{B} and a much lower orbital field of ca. +116 T. The data for the two amido complexes demonstrate a large quenching of the first-order orbital angular momentum upon bending the linear geometry and a strong correlation of the orbital field with symmetry is also apparent. The presence of significant orbital moments in both complexes was confirmed by EPR spectroscopy.

The remaining electron configuration for which a first-order orbital magnetic moment may be present is d^8 , for example, in a linear Ni^{2+} complex. In this case, the two degenerate orbitals related by a rotation are the d_{xz} and d_{yz} orbitals between which the electron may circulate. Investigations of the magnetic properties of the linear complexes $\text{Ni}\{\text{N}(\text{H})\text{Ar}^{\text{Pr}^i}\}_2$ and $\text{Ni}\{\text{N}(\text{H})\text{Ar}^{\text{Pr}^i}\}_2$ and the bent complex $\text{Ni}\{\text{N}(\text{H})\text{Ar}^{\text{Me}_6}\}_2$ showed that they had magnetic moments in the range 2.8–3.1 μ_{B} , which are very similar to the spin-only value of 2.83 μ_{B} (cf. free ion value = 5.59 μ_{B}). Inspection of the μ_{B} data for the other Ni(II) species in Table 6 shows that none of them displays magnetic moments much above the spin-only value. An explanation of their apparent lack of orbital moments may lie in the fact that the four linear or near linear Ni(II) complexes in the table employ either amido or thiolato ligands. In the structures observed in the solid state, a lone pair orbital from each of the amido or thiolato ligand may interact in a π -fashion with one but not both of the d_{xz} or d_{yz} orbitals on the metal. In this way, their degeneracy is lifted, and the orbital angular momentum is quenched, leading to the observed spin-only values. Unfortunately, at present, no stable nickel dialkyls, for example, similar to the iron species $\text{Fe}\{\text{C}(\text{SiMe}_3)_2\}_2$, are known. Because π -bonding to a simple alkyl ligand is negligible, such a complex is therefore expected to have pure metal–ligand σ -bonding, which should not lift the degeneracy of the d_{xz} and d_{yz} orbitals and permit first-order orbital angular momentum to be observed. The μ_{eff} values for the Ni(I), d^9 complexes lie slightly above the spin-only value of 1.73 μ_{B} .

The magnetism of the linear coordinated d^4 and d^7 complexes of Cr(II) and Co(II) derivatives in Tables 2 and 5 has also been investigated. For these, no first-order orbital angular momentum is predicted. For Cr(II), the borylamide complexes $\text{Cr}\{\text{N}(\text{Ph})\text{BMes}_2\}_2$ and $\text{Cr}\{\text{N}(\text{Mes})\text{BMes}_2\}_2$, which were measured by the Evans' method, afforded μ_{B} values that were close to the spin-only value of 4.90 μ_{B} . However, more recent measurements of the newly synthesized $\text{Cr}\{\text{N}(\text{H})\text{Ar}^{\text{Me}_6}\}_2$, $\text{Cr}\{\text{N}(\text{H})\text{Ar}^{\text{Pr}^i}\}_2$, and $\text{Cr}\{\text{N}(\text{H})\text{Ar}^{\text{Pr}^i}\}_2$ have afforded μ_{B} values in the range 4.22–4.35 μ_{B} , which lie significantly below the spin-only value of 4.90 μ_{B} .⁶⁹ It may be speculated that the origin of this reduction lies in spin orbit coupling, which, because of the sign of the coupling constant in the less than half-filled shells, leads to a reduction of the magnetic moment below the spin-only value.^{124,128} However, much more data on a greater number of two-coordinate Cr(II) complexes will be needed to confirm these observed reductions of the effective magnetic moments in the amido derivatives.

Inspection of the magnetic data in Table 5 shows that all of the μ_{B} values for the cobalt complexes are higher than the spin-

only value of 3.87 μ_{B} with the exception of $\text{CoAr}^{\text{Pr}^i}\{\text{N}(\text{H})\text{Ar}^{\text{Me}_6}\}$, which becomes low-spin, $S = 1/2$, by a spin state transition at low temperature to afford $\mu_{\text{eff}} = 1.77 \mu_{\text{B}}$. At room temperature, $\mu = 4.70 \mu_{\text{B}}$ for the $S = 3/2$ configuration. A bent geometry is observed for both spin states, but the secondary $\text{Co}-\text{C}(\text{ligand})$ interactions are observed to become much stronger (the $\text{Co}-\text{C}$ distance decreases from 2.693(2) to 2.077(3) Å) in the low spin case so that at this temperature the complex is quasi three-coordinate. It is remarkable that μ values exceeding 5.5 μ_{B} can be observed in the four linear or near-linear Co(II) complexes and that the highest value of ca. 6.2 μ_{B} , which is observed for $\text{Co}\{\text{N}(\text{H})\text{Ar}^{\text{Pr}^i}\}_2$,¹⁰⁵ approaches the free ion value of 6.63 μ_{B} . The data suggest that there is a very strongly enhanced out of state spin orbit coupling that can induce moments close to the free ion moment. Obviously, data for a greater range of two-coordinate cobalt complexes will be required to check the generality of these very high μ_{B} values. Most likely, this is caused by the relatively large negative value of the spin orbit coupling constant for Co^{2+} , which when combined with the relatively weak ligand field leads to the enhancement of the observed magnetic moment.^{105,128}

In summary, the data obtained thus far shows that two-coordinate complexes can exhibit large effects on orbital angular momenta. This opens the prospect of inducing particularly high zero field splittings and high barriers to the reversal of molecular magnetism.

6. REACTIONS OF TWO-COORDINATE TRANSITION METAL COMPLEXES

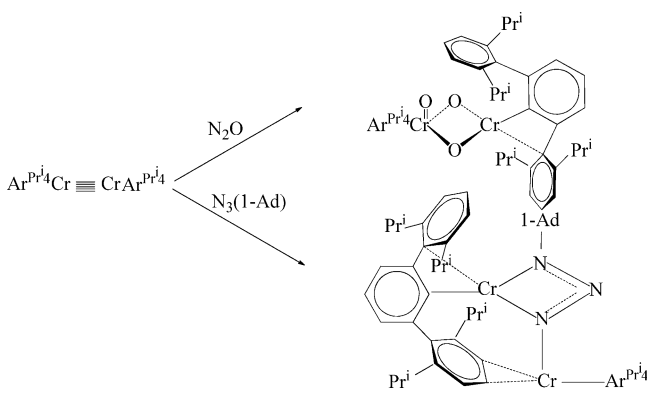
6.1. Chromium Complexes

The chemistry of two-coordinate chromium complexes has not been investigated extensively. For example, the reaction chemistry of the chromium(II) amido derivatives listed in Table 2 remains essentially unexamined. However, there are several reactions of related associated chromium(II) amides and alkyls that suggest that they should have a rich redox chemistry involving reactions with small molecules. For example, the reaction of dimeric $\{\text{Cr}(\text{NCy}_2)_2\}_2$ or $\text{Cr}\{\text{N}(\text{1-Ad})(\text{C}_6\text{H}_3\text{-3,5-Me}_2)\}_2$ with oxygen afforded $\text{Cr}(\text{O})_2(\text{NCy}_2)_2$ or $\text{Cr}(\text{O})_2\{\text{N}(\text{1-Ad})(\text{C}_6\text{H}_3\text{-3,5-Me}_2)\}_2$.¹²⁹ In addition, the intermediates $[\text{Cr}\{\text{N}(\text{1-Ad})(\text{C}_6\text{H}_3\text{-3,5-Me}_2)\}_2(\mu\text{-O})]_2$ and $[\text{Cr}\{\text{N}(\text{1-Ad})(\text{C}_6\text{H}_3\text{-3,5-Me}_2)\}_2(\mu\text{-O})]$ were spectroscopically and structurally characterized.¹²⁹ It seems likely that the recently reported two-coordinate amides $\text{Cr}\{\text{N}(\text{H})\text{Ar}\}_2$ ($\text{Ar} = \text{Ar}^{\text{Me}_6}, \text{Ar}^{\text{Pr}^i}$, and Ar^{Pr^i})⁶⁹ will also give oxidized species when reacted with O_2 but may have different aggregation due to the larger substituents. Also, the unusual and unique tetrameric Cr(II) dialkyl $\{\text{Cr}(\mu\text{-CH}_2\text{SiMe}_3)_2\}_4$ suggests that with suitable ligands a monomeric two-coordinate diorgano chromium(II) species is feasible with larger ligands.¹³⁰

The quintuple bonded two-coordinate Cr(I) complex $\text{Ar}^{\text{Pr}^i}\text{CrCrAr}^{\text{Pr}^i}$ was reacted with several substrates including CO , O_2 , Bu^tNC , N_2O , and several organoazides. However, crystalline products were obtained only from the reactions with N_2O or $\text{N}_3(\text{1-Ad})$.¹³¹ Treatment of $\text{Ar}^{\text{Pr}^i}\text{CrCrAr}^{\text{Pr}^i}$ with excess N_2O afforded the oxidized Cr(III)/Cr(V) product $\text{Ar}^{\text{Pr}^i}\text{Cr}(\mu\text{-O})\text{Cr}(\text{Ar}^{\text{Pr}^i})\text{O}$ as shown in Scheme 1.

One Cr is bound to an Ar^{Pr^i} ligand and two oxygens, which bridge to the second chromium. The latter is also bound to an

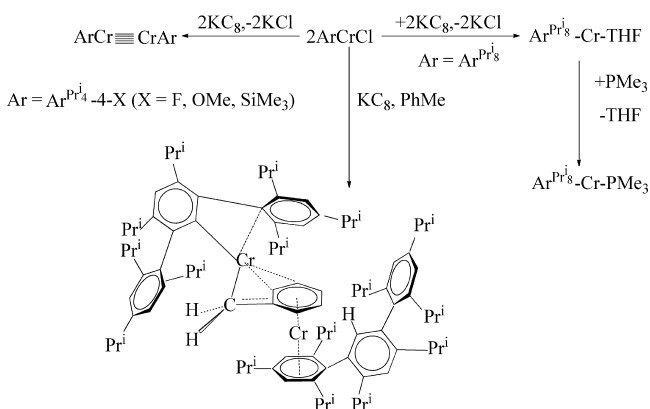
Scheme 1. Reactions of $\text{Ar}^{\text{Pr}^i}\text{Cr}\equiv\text{CrAr}^{\text{Pr}^i}$ with N_2O and $\text{N}_3(1\text{-Ad})$, in $\text{Ar}^{\text{Pr}^i}\text{Cr}(\mu_2\text{-O})\text{CrAr}^{\text{Pr}^i}(\text{O})$ ¹³¹



$\text{Ar}^{\text{Pr}^i}\text{Cr}$ ligand and a terminal oxygen. The $\text{Cr}(\text{III})(\mu_2\text{-O})_2\text{Cr}(\text{V})$ core features shorter $\text{Cr}(\text{V})\text{-O}$ bond distances to $\text{Cr}(\text{V})$ (1.764(3) Å) than to $\text{Cr}(\text{III})$ (1.809(4) Å). The terminal $\text{Cr}\text{-O}$ bond length is much shorter at 1.575(3) Å. The $\text{Cr}\text{-C}$ ipso distances are also slightly different, and there is a close approach (2.385(4) Å) of a flanking ring ipso-carbon atom to $\text{Cr}(\text{III})$ so that $\text{Cr}(\text{III})$ is quasi four-coordinate. Magnetic studies indicate little or no coupling between the unpaired electron on each chromium. The metal–metal bond in $\text{Ar}^{\text{Pr}^i}\text{Cr}\equiv\text{CrAr}^{\text{Pr}^i}$ is also completely cleaved by reaction with 1-adamantanyl azide. The two $\text{CrAr}^{\text{Pr}^i}$ units are bridged by the organoazide ligand so that its three nitrogen atoms chelate one of the chromiums. The second chromium is σ -bonded to the unsubstituted end-nitrogen of the azide moiety and to an Ar^{Pr^i} group as well as interacting with a flanking ring attached to the first chromium (Scheme 1). Magnetic studies indicated that the two Cr^{2+} ions had the unusual configuration $S = 1$, which exhibited little coupling.

When $\text{Ar}^{\text{Pr}^i}\text{CrCl}$ or related aryl chromium monohalide derivatives with modified $\text{Ar}^{\text{Pr}^i}\text{-4-X}$ substituents ($X = \text{F}, \text{O}, \text{Me}$, or SiMe_3) are reduced with KC_8 in THF, molecules with $\text{Cr}\equiv\text{Cr}$ quintuple bonds are isolated. However, if the size of the terphenyl substituent is increased to Ar^{Pr^i} , $\text{Cr}\text{-Cr}$ bond formation is prevented and mononuclear $\text{Cr}(\text{I})\text{-THF}$ adduct is isolated as shown in Scheme 2.

Scheme 2. Reduction Products of Various ArCrCl Species with KC_8 in the Presence of THF, PMe_3 , or Toluene



The coordinated THF can be replaced if the reduction is performed in the presence of PMe_3 . This affords the two-coordinate complex $\text{Ar}^{\text{Pr}^i}\text{-Cr-PMe}_3$ with a slightly bent structure (Figure 4). As already mentioned in section 5.1, when the reduction is carried out in toluene, the anticipated half-sandwich $\text{Ar}^{\text{Pr}^i}\text{Cr}(\eta^6\text{-PhMe})$ is not formed. Instead, a disproportionation was observed, which afforded the $\text{Cr}(\text{II})/\text{Cr}(\text{0})$ species illustrated in Scheme 2. Apparently, this disproportionation arises from the inherently lower stability of $\text{RCr}(\eta^6\text{-arene})$ half sandwich complexes and related species in comparison to their later transition metal counterparts.^{132,133}

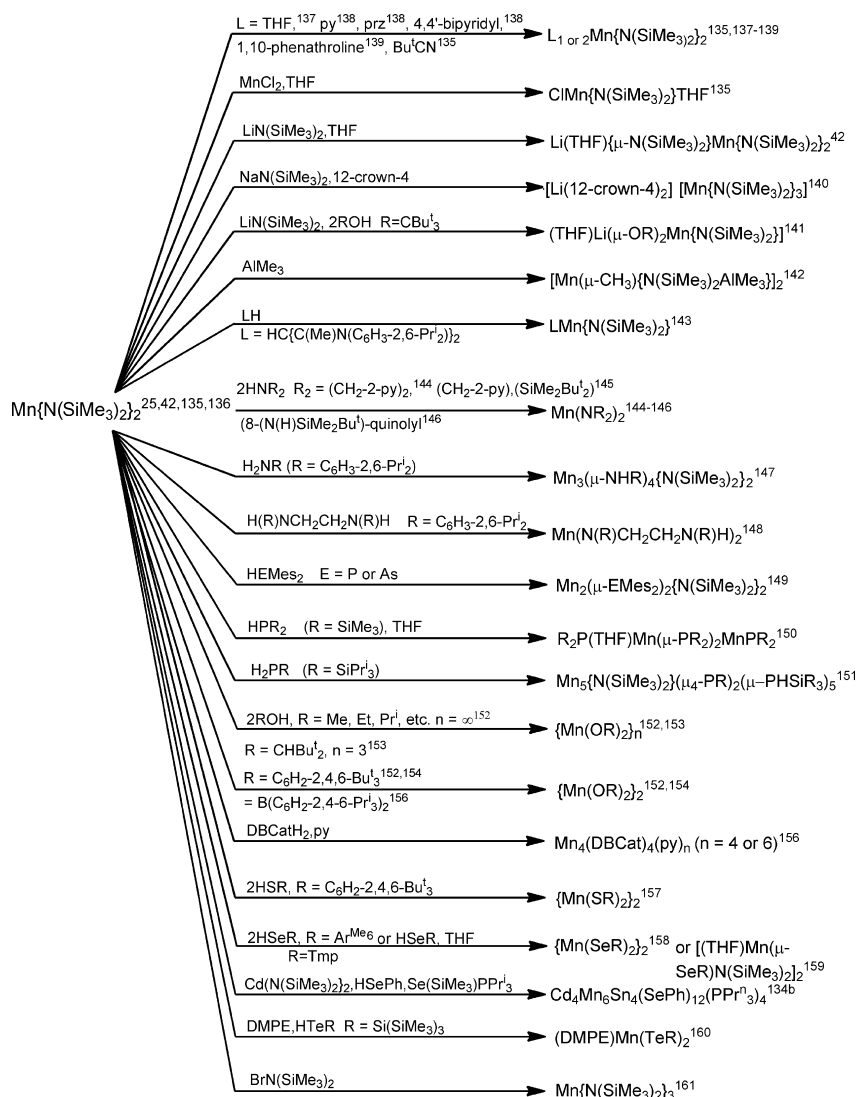
6.2. Manganese Complexes

The thermolysis of $\text{Mn}\{\text{N}(\text{SiMe}_3)_2\}_2$ vapor has been shown to lead to the deposition of manganese films on $\text{Si}\langle 100 \rangle$ surfaces.^{134a} When bistrimethylsilylamido manganese(II) together with $\text{Cd}\{\text{N}(\text{SiMe}_3)_2\}_2$ are reacted with PhSeH in the presence of PPr^n , and subsequently treated with either $\text{S}(\text{SiMe}_3)_2$ or $\text{Se}(\text{SiMe}_3)_2$, the ternary $\text{Cd}\text{-Mn}\text{-S/Se}$ cluster complexes $[\text{Cd}_4\text{Mn}_4\text{S}(\text{SePh})_{14}(\text{PPr}^n)_2]$ or $[\text{Cd}_4\text{Mn}_5\text{Se}_4(\text{SePh})_{12}(\text{PPr}^n)_4]$ were obtained. Thermolysis of the latter resulted in the formation of a mixture of a hexagonal phase $\text{Cd}_{1-x}\text{Mn}_x\text{Se}$ ($x = \text{ca. } 0.5$) and cubic phases $\text{Mn}_{1-x}\text{Cd}_x\text{Se}$ ($x < 0.05$).^{134b} Investigations of the chemistry of $\text{Mn}\{\text{N}(\text{SiMe}_3)_2\}_2$ have shown that it is a very useful substrate for the preparation of numerous other manganese compounds in a simple direct manner. A brief summary of its reaction chemistry is given in Scheme 3. These reactions underline the extreme reactivity of $\text{Mn}\{\text{N}(\text{SiMe}_3)_2\}_2$. It reacts readily with a variety of Lewis bases to afford either three- or four-coordinate complexes,^{135,136} and with 4,4'-bipyridyl it forms a two-dimensional polymeric structure.¹³⁸ It reacts with a further equivalent of $\text{LiN}(\text{SiMe}_3)_2$ to afford the THF solvated dimetal salt $(\text{THF})\text{Li}\{\mu\text{-N}(\text{SiMe}_3)_2\}_2\text{MnN}(\text{SiMe}_3)_2$.⁴² When this reaction is carried out with $\text{NaN}(\text{SiMe}_3)_2$ in the presence of 12-crown-4, the solvent separated ion pair salt $[\text{Na}(12\text{-crown-4})_2][\text{Mn}\{\text{N}(\text{SiMe}_3)_2\}_3]$ ¹⁴⁰ featuring a trigonal planar coordinated Mn^{2+} center in the $[\text{Mn}\{\text{N}(\text{SiMe}_3)_2\}_3]^-$ anion is obtained. It also reacts with a mixture of $\text{LiN}(\text{SiMe}_3)_2$ and Bu^t_3COH to give $\text{Li}(\text{Bu}^t_3\text{CO})_2\text{Mn}\{\text{N}(\text{SiMe}_3)_2\}$ and with AlMe_3 to give $[\text{Mn}(\mu\text{-Me})\{\text{N}(\text{SiMe}_3)_2\}_2\text{AlMe}_3]$.¹⁴²

The reactions with protic reagents underline the polarity of the $\text{Mn}\text{-N}$ bond.^{143–160} It reacts readily with a wide range of amines to eliminate either 1 or 2 equiv of $\text{HN}(\text{SiMe}_3)_2$. These reactions usually proceed smoothly under mild conditions and in high yield, and the products are easily purified because, due to its volatility, the eliminated $\text{HN}(\text{SiMe}_3)_2$ is easily separated. Scheme 3 provides several examples of such reactions with various amines,^{143–148} phosphines,^{149–151} arsines,¹⁴⁹ alcohols,^{152–156} thiols,¹⁵⁷ selenols,^{158,159} and a tellurool.¹⁶⁰ Also noteworthy is the reaction with $\text{BrN}(\text{SiMe}_3)_2$, which provides a rare example of a three-coordinate $\text{Mn}(\text{III})$ complex $\text{Mn}\{\text{N}(\text{SiMe}_3)_2\}_3$.¹⁶¹

The dialkyl $\text{Mn}\{\text{CH}(\text{SiMe}_3)_2\}_2$ has also been shown to undergo similar reactions with Lewis bases and protic species as shown in Scheme 4.¹⁶² In addition, $\text{Mn}\{\text{CH}(\text{SiMe}_3)_2\}_2$ acts as a useful transfer reagent for the $\text{-CH}(\text{SiMe}_3)_2$ group. For example, when it is treated with metal silyl amides, for example, of tin or lead, it affords the corresponding alkyls $\text{M}\{\text{CH}(\text{SiMe}_3)_2\}_2$ ($\text{M} = \text{Sn}$ or Pb) in good yields.¹⁶²

Treatment of the manganese diaryl $\text{Mn}(\text{Ar}^{\text{Pr}^i})_2$ with an excess of ammonia afforded the parent amido bridged dimeric

Scheme 3. Selected Reactions of $\text{Mn}\{\text{N}(\text{SiMe}_3)_2\}_2$ 

species $\{\text{Ar}^{\text{Pr}^i}_4(\text{H}_3\text{N})\text{Mn}(\mu\text{-NH}_2)\}_2$ with elimination of $\text{Ar}^{\text{Pr}^i}_4\text{H}$.

The less bulky dialkyl $\text{Mn}(\text{CH}_2\text{SiMe}_3)_2$, when treated with $\text{NaN}(\text{SiMe}_3)_2$ and $\text{HN}(\text{SiMe}_3)_2$ in the presence of trace amounts of oxygen, forms the inverted crown ether $\text{Na}_2\text{Mn}_2\{\text{N}(\text{SiMe}_3)_2\}_4\text{O}$ in which a central oxygen atom is planar coordinated by two sodium and two manganese ions in an alternating fashion.¹⁶⁴ These ions are μ_2 -bridged by the $-\text{N}(\text{SiMe}_3)_2$ groups. If the reaction is carried out with rigorous exclusion of oxygen, the dimetallic salt $\text{Na}\{\mu\text{-N}(\text{SiMe}_3)_2\}_2\text{MnCH}_2\text{SiMe}_3$, which crystallizes as a polymer in which the Na^+ ions bridge the amido and alkyl groups, is isolated.

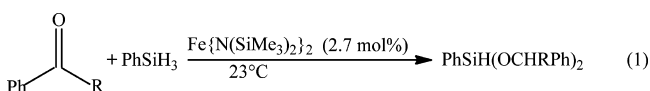
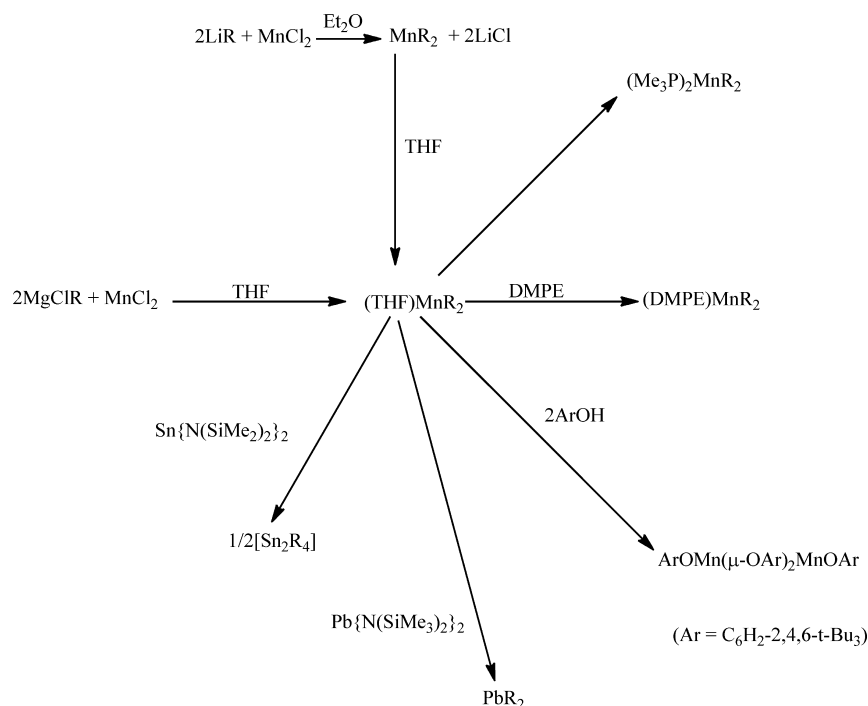
6.3. Iron Complexes

The largest portion of the investigations of the chemistry of two-coordinate iron complexes has been focused on $\text{Fe}\{\text{N}(\text{SiMe}_3)_2\}_2$, which is monomeric in the vapor⁴⁰ and solution⁴³ phases. The exploration of the behavior of this versatile species exceeds that of its neighboring analogues $\text{Mn}\{\text{N}(\text{SiMe}_3)_2\}_2$ or $\text{Co}\{\text{N}(\text{SiMe}_3)_2\}_2$. For example, $\text{Fe}\{\text{N}(\text{SiMe}_3)_2\}_2$ has been used to synthesize iron nanocubes arrayed in a superlattice via its reaction with H_2 in the presence of long-chain acids and

amines.^{165,166} Furthermore, $\text{Fe}\{\text{N}(\text{SiMe}_3)_2\}_2$, along with several other types of iron silylamides, have been employed as precursors to graft iron onto mesoporous silicon.¹⁶⁷ In addition, $\text{Fe}\{\text{N}(\text{SiMe}_3)_2\}_2$ has been used to synthesize siloxy derivatives of the type $\text{Fe}\{\text{OSi}(\text{O}^t\text{Bu})_3\}_2$ for grafting well-defined isolated species on the surface of mesoporous silica where the iron is immobilized with elimination of the silanol. Calcination affords Fe/SiO_2 materials whose catalytic properties could then be studied.¹⁶⁸

The two-coordinate iron diaryl monomer $\text{Fe}(\text{C}_6\text{H}_2\text{-2,4-6-Bu}^t_3)_2$ ^{85,96} and the related aryl dimer $\{\text{Fe}(\text{C}_6\text{H}_2\text{-2,4-6-Me}_3)_2\}_2$ ¹⁶⁹ were employed in a similar vein.¹⁷⁰ In these cases, the grafting was carried out by the immersion of a partially dehydroxylated silica disk in a hydrocarbon solution of the iron diaryl. Upon subsequent removal of the disk and drying it under reduced pressure, IR spectroscopy showed that the iron aryls had reacted with the silanol groups with formation of an $\text{Fe}-\text{O}-\text{Si}$ linkage and arene elimination.

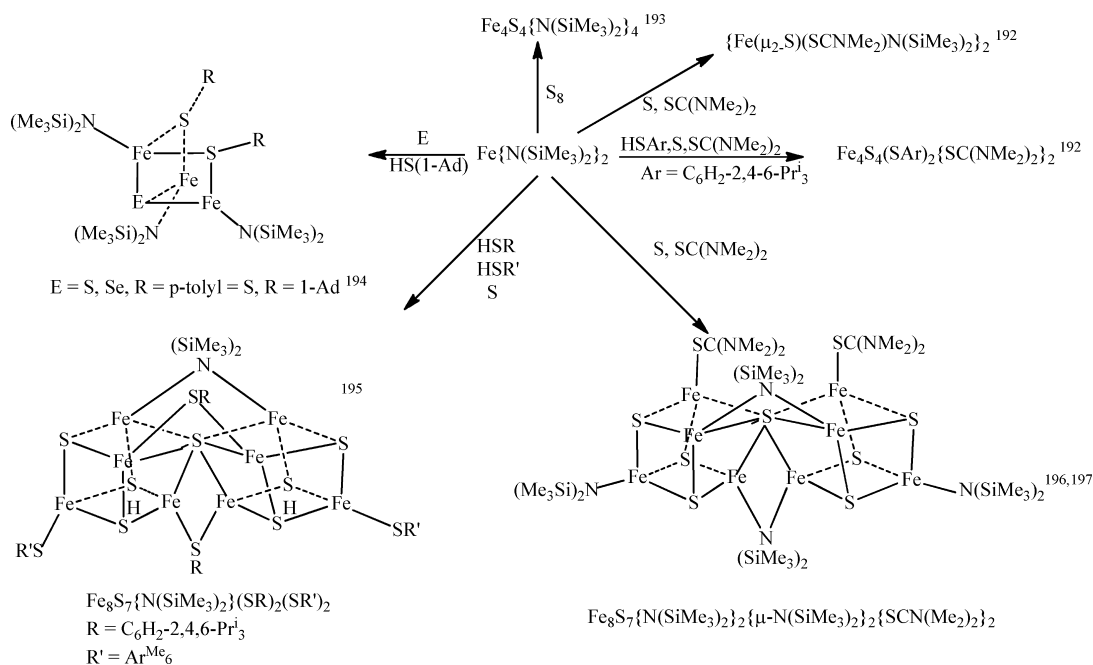
The molecule $\text{Fe}\{\text{N}(\text{SiMe}_3)_2\}_2$ has also found direct use as a hydrosilylation catalyst as shown in eq 1¹⁷¹ where either acetophenone or benzaldehyde underwent rapid hydrosilylation in the presence of 2.7 mol % of the metal amide. Several other ketones were tested and found to undergo analogous reactions,

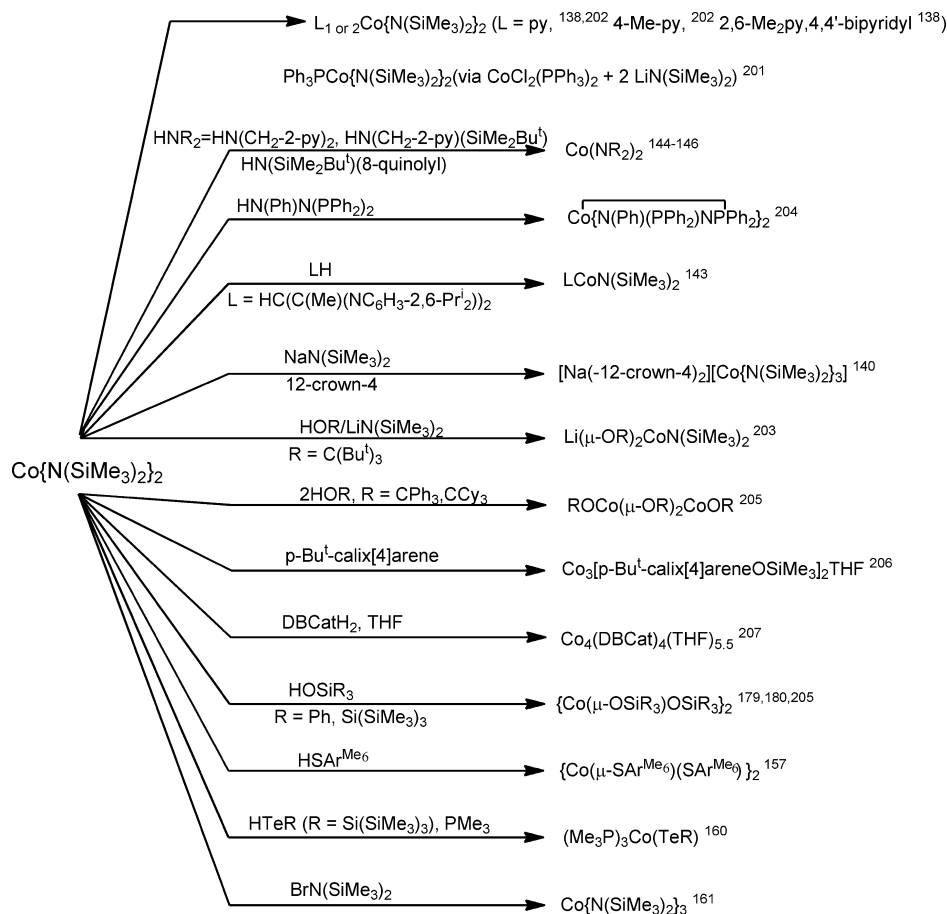
Scheme 4. Summary of the Reactions of MnR_2 ($\text{R} = -\text{CH}(\text{SiMe}_3)_2$)¹⁶²

but it was also found that very sterically crowded silanes were not hydrosilylated. The authors were originally led to these investigations of the amido iron species as a catalyst when the X-ray crystal structure of the complex between $\text{Fe}\{\text{N}(\text{SiMe}_3)_2\}_2$ and $\text{Me}(\text{H})\text{Si}(\text{8-quinolyl})$ displayed a δ -agostic $\text{Fe}\cdots\text{H}\cdots\text{Si}$ interaction. Further treatment with carbonyl complexes resulted in the dissociation of $\text{Me}(\text{H})\text{Si}(\text{8-quinolyl})_2$ as a free species in

solution. Heating of the reaction mixture produced the hydrosilylated product of 3-pentanone $\text{H}(\text{Et}_2\text{CHO})\text{Si}(\text{8-quinolyl})$.¹⁷²

The reactions of $\text{Fe}\{\text{N}(\text{SiMe}_3)_2\}_2$ with simple Lewis bases such as THF,⁴³ pyridine,¹³⁹ 4,4'-bipyridyl,¹³⁹ an *N*-heterocyclic carbene,^{173a} or phosphines,^{173b} resemble those of $\text{Mn}\{\text{N}(\text{SiMe}_3)_2\}_2$, which have already been illustrated in Scheme 3. Anionic complexes were formed with $\text{NaN}(\text{SiMe}_3)_2$ in the presence of 12-crown-4, which gave the solvent separated three-coordinate anion $[\text{Fe}\{\text{N}(\text{SiMe}_3)_2\}_3]^-$,¹⁴⁰ or with LiCl and THF to afford $(\text{THF})_3\text{Li}(\mu\text{-Cl})\text{Fe}\{\text{N}(\text{SiMe}_3)_2\}_2$.^{173c}

Scheme 5. Some Iron Sulfur Cluster Species Synthesized from $\text{Fe}\{\text{N}(\text{SiMe}_3)_2\}_2$ as the Iron Source

Scheme 6. Some Reactions of $\text{Co}\{\text{N}(\text{SiMe}_3)_2\}_2$ 

The reaction of $\text{Fe}\{\text{N}(\text{SiMe}_3)_2\}_2$ with various amine bases can readily displace one or both silylamido ligands and is generally facile. Numerous derivatives have been synthesized in this way from reactions of $\text{Fe}\{\text{N}(\text{SiMe}_3)_2\}_2$ with β -diketiminates, ¹⁴³ $\text{HN}(\text{CH}_2\text{-2-py})_2$, ¹⁴⁴ $\text{HN}(\text{CH}_2\text{-2-py})(\text{SiMe}_2\text{Bu}^t)$, ¹⁴⁵ (8-N(H)SiMe₂Bu^t)quinolyl, ¹⁴⁶ hexahydropyrimidopyridine, $\text{HNC}(\text{NEt}_2)_2$, and $\text{H}_2\text{NAr}^{\text{Me}_6,11}$ and $\text{H}_2\text{NAr}^{\text{Pr}_6,11}$ as well as the related (bisphosphinimino)methanes $\text{HC}\{\text{PPh}_2\text{N}(\text{Ar})\}\text{H}$ (Ar = $\text{C}_6\text{H}_2\text{-2,4-6-Me}_3$ or $\text{C}_6\text{H}_3\text{-2,6-Pr}^i_2$).¹⁷⁷ The reaction with HPMe_2 afforded the phosphido-bridged dimer $[\text{Fe}\{\mu\text{-PMe}_2\}\text{N}(\text{SiMe}_3)_2]_2$ ¹⁴⁹ in a similar manner to $\text{Mn}\{\text{N}(\text{SiMe}_3)_2\}_2$. $\text{Fe}\{\text{N}(\text{SiMe}_3)_2\}_2$ also reacts readily with a diverse array of alcohols, ^{104,154,178} catechols, ¹⁵⁶ phenols, ¹⁵⁴ diarylboronous acids, ¹⁵⁵ siloxides, ¹⁷⁹⁻¹⁸¹ germyloxides, ¹⁸⁰ thiols, ^{73,101-103,182-185} silthianes, ^{185,186} selenols, ^{185,187} or the tellurol $\text{HTe}\{\text{Si}(\text{SiMe}_3)_3\}$ ¹⁶⁰ to eliminate 1 or 2 equiv of hexamethyldisilazane to yield products that often have dimeric structures with bridging chalcogenolato ligands, which may also form further adducts with a range of Lewis bases.^{160,186} More complex structures can also be generated. For example, the treatment of $\text{RSi}(\text{OH})_3$ (R = $-\text{N}(\text{SiMe}_3)(\text{C}_6\text{H}_3\text{-2,6-Pr}^i_2)$) with $\text{Fe}\{\text{N}(\text{SiMe}_3)_2\}_2$ affords the unusual cluster species $[(\text{RSiO}_3)_2(\text{RSi}(\text{OH})\text{O}_2)_4(\mu\text{-OH})_2\text{Fe}_8(\text{THF})_4]$.¹⁸¹ Further reactions of the iron chalcogenolato products can lead to unusual structures. Thus, the reaction of $\text{Fe}\{\text{N}(\text{SiMe}_3)_2\}_2$ with the thiol MesSH in the presence of THF affords the simple thiolato bridged dimer $[\text{Fe}(\text{THF})\{\text{N}(\text{SiMe}_3)_2\}(\mu\text{-SMes})]_2$.^{188,189} However, treatment of this species with the 1,2-diarylhydrazines $\text{H}(\text{Ar})\text{NN}(\text{Ar})\text{H}$ (Ar = Ph, $\text{C}_6\text{H}_4\text{-4-Me}$ (*p*-tolyl), or Mes)

afforded the Fe_4N_4 Fe(III), imido-cubane $\text{Fe}_4(\text{NPh})_4(\text{SMes})_4$ and $\text{Fe}_4\{\text{N}(\text{p-tolyl})\}_4(\text{SMes})_4$.¹⁸⁹ A site-differentiated mono-anionic cubane species of formula $[\text{Fe}_4\{\text{N}(\text{p-tolyl})\}_4(\text{SC}_6\text{H}_3\text{-2,6-Me}_2)_3\{\text{N}(\text{SiMe}_3)_2\}_2][\text{Fe}(\text{THF})_6]$ could also be synthesized by variation of reactant stoichiometry in the above reaction. Although full mechanistic details are unavailable, the reaction is clearly a complex one that proceeds by hydrazine reduction, but there is evidence for disproportionation and N–C bond cleavage for reactions with 1,2-dialkylhydrazine.¹⁸⁹

The use of $\text{Fe}\{\text{N}(\text{SiMe}_3)_2\}_2$ has also led to important breakthroughs in the synthesis of biologically relevant^{190,191} iron–sulfur clusters. In essence, hydrocarbon solutions of $\text{Fe}\{\text{N}(\text{SiMe}_3)_2\}_2$ when treated with a thiol, tetramethylthiourea, or elemental sulfur, in various proportions, yield a variety of species with various structures as shown in Scheme 5.¹⁹²⁻¹⁹⁸

These include the remarkable Fe_8S_7 P-type clusters in which the Fe_4S_4 cubanes share a common sulfur vertex and two or three of the irons from each cubane are bridged to each other by thiolato and amido ligands.¹⁹⁵⁻¹⁹⁷ The bulky iron dithiolate $\{\text{Fe}(\text{STrip})(\mu\text{-S Ar}^{\text{Me}_4})\}_2$ was also shown to generate the 8Fe–7S cluster $[\{(\text{Ar}^{\text{Me}_4}\text{S})\text{Fe}_4\text{S}_2\}_2(\mu\text{-S Ar}^{\text{Me}_4})(\mu\text{-STrip})(\mu_6\text{-S})]$ upon reaction with sulfur.^{195a} In addition, $\text{Fe}\{\text{N}(\text{SiMe}_3)_2\}_2$, in the presence of various thiols, reacted with oxygen to afford various μ -oxo iron imido/thiolate clusters.^{195b} The cluster $\text{Fe}_8\text{S}_7\{\text{N}(\text{SiMe}_3)_2\}_2\{\mu\text{-N}(\text{SiMe}_3)_2\}_2\{\text{SC}(\text{NMe}_2)_2\}_2$ ¹⁹⁷ has been shown to C–H activate one of the methyl groups of $\text{Co}(\eta^5\text{-C}_5\text{Me}_5)_2$.¹⁹⁸ A selection of iron sulfur clusters of formula $[\text{Fe}_4\text{S}_4\{\text{N}(\text{SiMe}_3)_2\}_4]^{0,1-2-}$ is available by reaction of the

iron(III) starting material $\text{Fe}\{\text{N}(\text{SiMe}_3)_2\}_2\text{Cl}(\text{THF})$ with NaSH and subsequent reduction with sodium.¹⁹⁸

Iron diaryls have also been shown to undergo some unusual reactions that are useful for the synthesis of other derivatives. For example, the reaction of $\text{Fe}(\text{Ar}^{\text{Pr}^i})_2$ with O_2 afforded the first linear coordinated monomeric, divalent aryloxo $\text{Fe}(\text{OAr}^{\text{Pr}^i})_2$. This compound is resistant to oxidation and does not react further with oxygen.⁹⁹ $\text{Fe}(\text{Ar}^{\text{Pr}^i})_2$ also reacts with 4 equiv of CO to give the acyl/carbonyl derivative $\text{Fe}(\text{CO})_2\{\text{C}(\text{O})\text{Ar}^{\text{Pr}^i}\}_2$.⁹⁹ Treatment of $\text{Fe}(\text{Ar}^{\text{Pr}^i})_2$ with ammonia resulted in $\text{Ar}^{\text{Pr}^i}\text{H}$ elimination and formation of the parent dimeric amido complex $\{\text{Fe}(\text{Ar}^{\text{Pr}^i})(\mu\text{-NH}_2)\}_2$.¹⁶³ In addition, the monomeric diaryl $\text{Fe}(\text{Ar}^{\text{Me}_e})_2$ reacts with an ethylenediamine solution of K_4Ge in the presence 2,2,2-crypt to give $[\text{K}(2,2,2\text{-crypt})]_2[\text{Fe}@_{\text{Ge}_{10}}]\cdot 2\text{ethylenediamine}$.¹⁹⁹ The anion features iron at the center of a pentagonal prismatic array of 10 germanium atoms. Three equivalents of the iron diaryl FeMe_2 , which is dimerized in the solid state, reacts with the multidentate ligand $\text{C}_6\text{H}_6\text{-1,3,5-}[\text{N}(\text{H})\text{C}_6\text{H}_4\text{-2}\{\text{N}(\text{H})\text{-SiMe}_2\text{Bu}^t\}]$ to eliminate mesitylene to form a complex with a hexadentate amido ligand that includes three irons. Further reaction with an azido salt forms a nitride derivative with N₂ elimination.²⁰⁰

6.4. Cobalt Complexes

The reactions of $\text{Co}\{\text{N}(\text{SiMe}_3)_2\}_2$ (Scheme 6) resemble those of $\text{Mn}\{\text{N}(\text{SiMe}_3)_2\}_2$ and $\text{Fe}\{\text{N}(\text{SiMe}_3)_2\}_2$. Nonetheless, its reactions have not been as extensively studied as its manganese or iron congeners. The first well-characterized Lewis base complex of $\text{Co}\{\text{N}(\text{SiMe}_3)_2\}_2$ was $\text{Co}\{\text{N}(\text{SiMe}_3)_2\}_2\text{PPh}_3$. However, it was obtained not from $\text{Co}\{\text{N}(\text{SiMe}_3)_2\}_2$ but from the reaction of $\text{CoCl}_2(\text{PPh}_3)_2$ and 2 equiv of $\text{LiN}(\text{SiMe}_3)_2$. Lewis base complexes may also be obtained by the direct reaction of $\text{Co}\{\text{N}(\text{SiMe}_3)_2\}_2$ with pyridine to afford the bispyridine adduct $\text{Co}\{\text{N}(\text{SiMe}_3)_2\}_2(\text{py})_2$,²⁰² which has a very distorted tetrahedral coordination due to the differences in size between the $\text{-N}(\text{SiMe}_3)_2$ and pyridine ligands. Sublimation of this species afforded the mono pyridine adduct^{138,202} in which cobalt has a distorted three-coordinate planar environment. A three coordinate cobalt is also observed in $\text{Li}(\mu\text{-OR})_2\text{Co}\{\text{N}(\text{SiMe}_3)_2\}$ ($\text{R} = \text{C}_6\text{H}_5$, which was synthesized from $\text{Co}\{\text{N}(\text{SiMe}_3)_2\}_2$, HOR and $\text{LiN}(\text{SiMe}_3)_2$).²⁰³ Reaction of $\text{Co}\{\text{N}(\text{SiMe}_3)_2\}_2$ with 4,4'-bipyridyl yielded $\text{Co}\{\text{N}(\text{SiMe}_3)_2\}_2(4,4'\text{-bipyridyl})$, which has a chain structure in which four-coordinate cobalt atoms are connected by bridging 4,4'-bipyridyls. Magnetic measurements showed that each cobalt is for the most part magnetically independent. Addition of $\text{NaN}(\text{SiMe}_3)_2$ to $\text{Co}\{\text{N}(\text{SiMe}_3)_2\}_2$ in the presence of 12-crown-4 afforded the ion pair $[\text{Na}(12\text{-crown-4})]_2[\text{Co}\{\text{N}(\text{SiMe}_3)_2\}_3]^{140}$ featuring the three-coordinate planar coordinated anion $[\text{Co}\{\text{N}(\text{SiMe}_3)_2\}_3]^-$.

Like the metal–nitrogen bonds in its manganese and iron counterparts, the Co–N bond in $\text{Co}\{\text{N}(\text{SiMe}_3)_2\}_2$ is readily cleaved by protic reagents. The treatment of $\text{Co}\{\text{N}(\text{SiMe}_3)_2\}_2$ with $\text{HNR}_2 = \text{HN}(\text{CH}_2\text{-2-py})$, $\text{HN}(\text{CH}_2\text{-2-py})(\text{SiMe}_2\text{Bu}^t)$, or $\text{HN}\{(\text{SiMe}_2)\text{Bu}^t\}(8\text{-quinolyl})$ results in the displacement of both $\text{N}(\text{SiMe}_3)_2$ ligands to afford the corresponding $\text{Co}(\text{NR}_2)_2$ products.^{144–146} Similarly, the reaction with the β -diketimine $\text{LH} = \text{HC}\{\text{C}(\text{Me})\text{N}(\text{Dipp})\}_2\text{H}$ affords the three-coordinate product $\text{LCoN}(\text{SiMe}_3)_2$.¹⁴³ Reaction of the hydrazine $\text{HN}(\text{Ph})\text{N}(\text{PPh}_2)_2$ with $\text{Co}\{\text{N}(\text{SiMe}_3)_2\}_2$ afforded unusual product in which the initially generated $\text{Co}\{\text{N}(\text{Ph})\text{N}(\text{PPh}_2)_2\}_2$

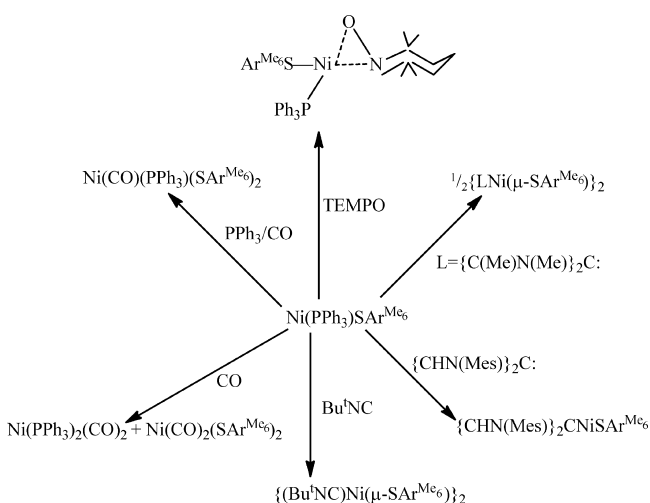
rearranged to yield $\text{Co}\{\text{N}(\text{Ph})\text{P}(\text{Ph})_2=\text{N}-\text{PPh}_2\}_2$, which has cobalt coordinated by two amide groups and by two -PPh_2 groups from the rearranged ligand.^{204a,b} Several other phosphine substituted hydrazines including $\text{HN}(\text{Ph})\text{N}(\text{Ph})\text{-}(\text{PPr}^i)_2$,^{204c} and $\text{HN}(\text{Ph})\text{N}(\text{Ph})\{\text{P}(\text{OR})_2\}$ ($\text{P}(\text{OR})_2 = \text{CH}_2(\text{Bu}^t\text{MeC}_6\text{H}_2\text{O})_2\text{P}$)^{204d} have been reacted with $\text{Co}\{\text{N}(\text{SiMe}_3)_2\}_2$ to produce products with similar structures.

Reaction with the alcohols HOCPh_3 or HOCCy_3 yielded the alkoxy bridged dimers $\text{ROCo}(\mu\text{-OR})_2\text{CoOR}$ ($\text{R} = \text{CPh}_3$ or CCy_3) featuring three-coordinate cobalt atoms.²⁰⁵ The reaction of $\text{Co}\{\text{N}(\text{SiMe}_3)_2\}_2$ with the calixarene $p\text{-Bu}^t\text{calix}[4]\text{arene}$ gave the trimetallic species $\text{Co}_3(p\text{-Bu}^t\text{calix}[4]\text{areneOSiMe}_3)_2(\text{THF})$ in which the three coordinated cobalt atoms are bridged by the two calixarenes in which one of the four oxygens from each ligand has been silylated with an SiMe_3 group. This complex along with related iron and titanium species were the first transition metal derivatives of calixarene ligands.²⁰⁶ The reaction with 3,5-ditert-butyl-catechol (DBCatH_2) in the presence of THF afforded the Co_4O_4 cubane species $\text{Co}_4(\text{DBCat})_4(\text{THF})_{55}$.²⁰⁷ The reaction $\text{Co}\{\text{N}(\text{SiMe}_3)_2\}_2$ with HOSiPh_2 in the presence of THF yielded the four-coordinate adduct $\text{Co}(\text{OSiPh}_2)_2(\text{THF})_2$,²⁰⁵ whereas the reaction with $\text{HOSi}(\text{SiMe}_3)_3$ gave the siloxy bridge dimer $(\text{Me}_3\text{Si})_3\text{SiOCo}\{\mu\text{-OSi}(\text{SiMe}_3)_3\}_2\text{CoOSi}(\text{SiMe}_3)_3$ featuring three-coordinate cobalt atoms. Several adducts of $\text{Co}\{\text{OSi}(\text{SiMe}_3)_3\}_2$ including examples with one or two THF molecules, DME, two acetonitriles, or benzonitriles or 2,2'-dipyridyl were also isolated and characterized by elemental analysis and magnetic measurements.¹⁷⁹ The cobalt(II) trisopropylsiloxy yielded $\text{Co}\{\text{OSiPr}^i\}_2$ as a purple oil, which was characterized by elemental analysis and IR spectroscopy. The addition of 2 equiv of the thiol $\text{HSAr}^{\text{Me}_e}$ to $\text{Co}\{\text{N}(\text{SiMe}_3)_2\}_2$ afforded the bithiolato species $\{\text{Co}(\text{SAr}^{\text{Me}_e})_2\}_2$, which has a bridged dimeric structure.¹⁵⁷ Reaction with the tellurol $\text{HTeSi}(\text{SiMe}_3)_3$ in the presence of trimethylphosphine yielded the Co(I) tellurolato phosphine complex $\text{Co}\{\text{Te}(\text{SiMe}_3)_3\}(\text{PMe}_3)_4$.¹⁶⁰

6.5. Nickel Complexes

The reaction chemistry of two-coordinate nickel complexes is not as developed as their iron, manganese, or cobalt analogues. However, the chemistry explored so far has displayed features that are almost unique to this element particularly in relation to their ability to exhibit two-coordination in two different oxidation states, that is, Ni(I) and Ni(II). The main restrictions on the chemistry derive from the absence of a convenient synthon with low-coordination and high hydrocarbon solubility such as $\text{Ni}\{\text{N}(\text{SiMe}_3)_2\}_2$, which, as stated above, is unstable. It is believed, however, that $\text{Ni}\{\text{N}(\text{SiMe}_3)_2\}_2$ is formed in the reaction of the Ni(I) species $\text{Ni}(\text{PPh}_3)_2\{\text{N}(\text{SiMe}_3)_2\}$ with $\text{HN}(\text{Ph})\text{N}(\text{PPh}_2)_2$.²⁰⁴ This affords $\text{Ni}\{\text{N}(\text{Ph})\text{PPh}_2\text{NPPh}_3\}\text{N}(\text{SiMe}_3)_2$ and, via the disproportionation of $\text{Ni}(\text{PPh}_3)\{\text{N}(\text{SiMe}_3)_2\}$ into $\text{Ni}\{\text{N}(\text{SiMe}_3)_2\}_2$ and $\text{Ni}(\text{PPh}_3)_2$, gives $\text{Ni}\{\text{N}(\text{Ph})\text{PPh}_2\text{NPPh}_3\}$. The stable amide $\{\text{Ni}(\text{NPh}_2)_2\}_2$, which has an amido bridged dimeric structure, reacts with HSSiPh_3 in the presence of TMEDA to form $\text{Ni}(\text{SSiPh}_3)_2(\text{TMEDA})$ ¹⁸⁶ as yellow crystals, which were characterized by elemental analysis and NMR spectroscopy.¹⁸⁶ The Ni(I) thiolato derivative $\text{Ni}(\text{PPh}_3)\text{SAr}^{\text{Me}_e}$ was also shown to display high reactivity toward various Lewis bases as shown in Scheme 7.

The redox reactions of the chemistry of two-coordinated Ni(I) species have also been investigated. The treatment of $[\{\text{CHN}(\text{Dipp})\}_2\text{C}]\text{Ni}\{\text{N}(\text{SiMe}_3)_2\}_2$ with $[\text{FeCp}_2][\text{BAR}^{\text{F}}_4]$ (Ar^{F}

Scheme 7. Some Reactions of Ni(PPh₃)SAr^{Me₆} with Lewis Bases¹¹¹

= C₆H₃-3,5-(CF₃)₂) afforded [{CHN(Dipp)}₂C]Ni(Me){N-(SiMe₃)SiMe₂(THF)}][BAR^F₄]. The cation of this salt features Ni(II) bound to the carbene, a methyl group, and the neutral silaimine ligand Me₃Si-N=SiMe₂(THF), which is η¹ coordinated through its nitrogen¹⁰⁹ to afford a rare T-shaped coordination at nickel(II). This remarkable result apparently arises from β-Me elimination from SiMe₃. Oxidation of {CHN(Dipp)}₂CNi{N(H)Dipp} in the same manner afforded cationic [{CHN(Dipp)}₂CNi{η³-NH(Dipp)}]⁺ in which the amide ligand is bound to Ni(II) through the nitrogen as well as ipso and ortho carbons of the Dipp ring. Removal of THF results in dimerization in which the two bridges are formed by nitrogen donor bonding to one nickel and by meta and para carbons interactions with the other.

The unique, two-coordinate Ni(II) imide LNiNAr^{Me₆} (L = {CHNC₆H₂-2,6(C₆H₂-2,6(CHPh₂)₂-4-Me)}₂C:) reacts with ethylene to give H₂C=C(H){N(H)Ar^{Me₆}} and LNi(η²-C₂H₄). The azametallocyclobutane complex LNiN(Ar^{Me₆})-CH₂CH₂ was identified spectroscopically as the intermediate in the cycloaddition of ethylene.¹¹⁰

7. CONCLUSIONS

At present, 80 two-coordinate, open-shell transition metal complexes have been isolated and characterized under ambient conditions. For the most part, they have been made accessible through the use of bulky ligands. However, only in the case of extreme crowding is strictly linear metal coordination observed. Despite the steric hindrance provided by the ligands employed, they have been shown to have an extensive coordination chemistry. In particular, the silylamido derivatives have proven to be extremely useful hydrocarbon soluble synthons for numerous other complexes. In addition to σ-bonding involving a wide variety of uninegative and neutral ligands, multiple bonding to ligands and to other metals has been demonstrated. Their magnetic properties have also attracted attention because linear coordination can lead to generally enhanced in-state and out-of-state spin orbit coupling as well as high magnetic anisotropy. This may afford high axial zero field splitting and high barriers to spin reversal, as a result of which they are of interest as possible single molecule magnets. Nonetheless, the field of open-shell, two-coordinate transition metal complexes

remains very underdeveloped. Currently, well-characterized derivatives are known only for five of the transition metals, all of which are from the first row. It seems probable that two coordination can be extended to divalent derivatives of the remaining first row elements scandium, titanium, vanadium, and copper with use of suitably large ligands and preparative routes. Stable two-coordinate, open-shell derivatives of the second and third row elements remain unknown, but the synthesis of these, which will open new chemical horizons, may also be anticipated.

AUTHOR INFORMATION

Corresponding Author

*E-mail: pppower@ucdavis.edu.

Notes

The authors declare no competing financial interest.

Biography



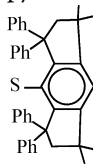
Philip Power received a B.A. from Trinity College Dublin in 1974 and a D. Phil. under M. F. Lappert from the University of Sussex in 1977. After postdoctoral studies with R. H. Holm at Stanford University, he joined the faculty at the Department of Chemistry at the University of California at Davis in 1981, where he is a Distinguished Professor of Chemistry. His main interests lie in the exploratory synthesis of new main group and transition metal complexes. A major theme of his work has been the use of sterically crowded ligands to stabilize species with new type of bonding, low coordination numbers, and high reactivity. He has been the recipient of several awards including the A. P. Sloan Foundation Fellow (1985), Alexander von Humboldt Fellowship for Senior U.S. Scientists (1992), Ludwig Mond Medal of the Royal Society of Chemistry (2005), F. A. Cotton Award in Synthetic Inorganic Chemistry (2005) and the Award in Organometallic Chemistry (2012) of the American Chemical Society, and was elected Fellow of the Royal Society of London (2005).

ACKNOWLEDGMENTS

I thank Jessica Boynton, Aimee Bryan, Chun-Yi Lin, and Dr. Christine Caputo for technical assistance and useful discussions, as well as Profs W. Reiff and G. Long for fruitful collaborations. Much of the work in this area was supported by the National Science Foundation.

LIST OF ABBREVIATIONS

1-Ad	1-adamantanyl
Ar	aryl
Ar ^{Ad₂} Me	C ₆ H ₃ -2,6(1-Ad) ₂ -4-Me

Ar ^{Ad} Pr ⁱ	C ₆ H ₂ -2,6(1-Ad) ₂ -4-Pr ⁱ
Ar ^F	C ₆ H ₃ -3,5-(CF ₃) ₂
Ar ^{Me₄}	C ₆ H ₃ -2,6(C ₆ H ₃ -2,6-Me ₂) ₂
Ar ^{Me₆}	C ₆ H ₃ -2,6(C ₆ H ₂ -2,4,6-Me ₃) ₂
Ar ^{Prⁱ}	C ₆ H ₃ -2,6(C ₆ H ₃ -2,6-Pr ⁱ) ₂
Ar ^{Prⁱ} -4-X	C ₆ H ₃ -2,6(C ₆ H ₃ -2,6-Pr ⁱ) ₂ -4-X (X = SiMe ₃ , OMe, or F)
Ar ^{Prⁱ} ₆	C ₆ H ₃ -2,6(C ₆ H ₂ -2,4,6-Pr ⁱ) ₂
Ar ^{Prⁱ} ₃	C ₆ H ₃ -2,6(C ₆ H ₂ -2,4,6-Pr ⁱ) ₂ -3,5-Pr ⁱ
Bz	benzyl
Cp	cyclopentadienyl
Cy	cyclohexyl (c-C ₆ H ₁₁)
Dipp	C ₆ H ₃ -2,6-Pr ⁱ ₂
DME	1,2-dimethoxyethane
ged	gas electron diffraction
Mes	C ₆ H ₂ -2,4,6-Me ₃
Mes [*]	C ₆ H ₂ -2,4,6-Bu ^t ₃
Ph	phenyl, C ₆ H ₅
py	pyridine
prz	pyrazine
SMPPhInd	
TEMPO	2,2,6,6-tetramethylpiperidine oxide
THF	tetrahydrofuran
TMEDA	N,N,N',N'-tetramethylethylenediamine
Trip	C ₆ H ₂ -2,4,6-Pr ⁱ ₃

REFERENCES

- Power, P. P. *Comments Inorg. Chem.* **1989**, *8*, 177.
- Power, P. P. *Chemtracts: Inorg. Chem.* **1994**, *6*, 181.
- Kays, D. L. *Dalton Trans.* **2011**, *40*, 769.
- Hargittai, M. *Coord. Chem. Rev.* **1988**, *91*, 35.
- Andrews, L. *Chem. Soc. Rev.* **2004**, *33*, 123.
- Power, P. P. *J. Organomet. Chem.* **2004**, *689*, 3904.
- For example, the ligand precursors HN(SiMe₃)₂, HN(SiMe₂Ph)₂, HN(SiMePh₂)₂, and HC(SiMe₃)₃, which are convertible to their lithium salt-transfer agents in one step, can be purchased from various chemical suppliers.
- Ni, C.; Power, P. P. *Struct. Bonding (Berlin)* **2010**, *136*, 59.
- Reiff, W. M.; LaPointe, A. M.; Witten, E. H. *J. Am. Chem. Soc.* **2004**, *126*, 10206.
- Reiff, W. M.; Schulz, C. E.; Whangbo, M. H.; Seo, J. I.; Lee, Y. S.; Potratz, G. R.; Spicer, C. W.; Girolami, G. S. *J. Am. Chem. Soc.* **2009**, *131*, 404.
- Merrill, W. A.; Stich, T. A.; Brynda, M.; Yeagle, G. J.; De Hont, R.; Fettinger, J. C.; Reiff, W. M.; Power, P. P. *J. Am. Chem. Soc.* **2009**, *131*, 12693.
- Drago, R. S. *Physical Methods in Chemistry*; Saunders: Philadelphia, PA, 1977; p 478.
- Nowitzki, B.; Hoppe, R. *Croat. Chem. Acta* **1964**, *57*, 537.
- Werner, A. Z. *Anorg. Chem.* **1893**, *3*, 267.
- Bethe, H. *Ann. Phys.* **1929**, *3*, 135.
- Mulliken, R. S. *Phys. Rev.* **1932**, *40*, 55.
- Van Vleck, J. H. *Chem. Phys.* **1935**, *3*, 803.
- Pauling, L. *The Nature of the Chemical Bond*; Cornell University Press: Ithaca, NY, 1940.
- Ballhausen, C. *Introduction to Ligand Field Theory*; McGraw-Hill: New York, 1962.
- Moffitt, W.; Ballhausen, C. *Annu. Rev. Phys. Chem.* **1956**, *7*, 107.
- Jorgensen, C. K. *Modern Aspects of Ligand Field Theory*; Elsevier: New York, 1971.
- For a review of earlier work with alkoxide ligands, see Chapter 1 in: Bradley, D. C.; Mehrotra, R. C.; Gaur, D. P. *Metal Alkoxides*; Academic Press: London, 1978.
- Bradley, D. C. *Adv. Inorg. Chem. Radiochem.* **1972**, *15*, 259.
- (a) Lappert, M. F.; Power, P. P.; Sanger, A. R.; Srivastava, R. C. *Metal and Metalloid Amides*; Ellis-Horwood: Chichester, 1980. (b) Lappert, M. F.; Power, P. P.; Protchenko, A.; Seeber, A. *Metal Amide Chemistry*; Wiley: Chichester, 2008.
- Bürger, H.; Wannagat, U. *Monatsh.* **1964**, *95*, 1099.
- Bürger, H.; Wannagat, U. *Monatsh.* **1963**, *94*, 1007.
- Bradley, D. C.; Hursthouse, M. B.; Rodesiler, P. F. *Chem. Commun.* **1969**, 14.
- Alyea, E. C.; Basi, J. S.; Bradley, D. C.; Chisholm, M. H. *Chem. Commun.* **1968**, 495.
- Bradley, D. C.; Hursthouse, M. B.; Newing, C. W. *Chem. Commun.* **1971**, 411.
- Bradley, D. C.; Fisher, K. J. *J. Am. Chem. Soc.* **1971**, *93*, 2058.
- Bradley, D. C. *Chem. Br.* **1975**, 393.
- Eller, P. G.; Bradley, D. C.; Hursthouse, M. B.; Meek, D. W. *Coord. Chem. Rev.* **1977**, *24*, 1.
- Alvarez, S. *Coord. Chem. Rev.* **1999**, *193–195*, 13.
- Cummins, C. C. *Prog. Inorg. Chem.* **1998**, *47*, 885.
- (a) Barker, G. K.; Lappert, M. F. *J. Organomet. Chem.* **1974**, *76*, C45. (b) Hitchcock, P. B.; Lappert, M. F.; Smith, R. G.; Bartlett, R. A.; Power, P. P. *J. Chem. Soc., Chem. Commun.* **1988**, 1007.
- Cummins, C. C. *Chem. Commun.* **1998**, 1777.
- Buttrus, N. H.; Eaborn, C.; Hitchcock, P. B.; Sullivan, A. C. *J. Chem. Soc., Chem. Commun.* **1985**, 1380.
- Andersen, R. A.; Haaland, A.; Rypdal, K.; Volden, H. V. *J. Chem. Soc., Chem. Commun.* **1985**, 1807.
- Bartlett, R. A.; Power, P. P. *J. Am. Chem. Soc.* **1987**, *109*, 7563.
- Andersen, R. A.; Faegri, K.; Green, J. C.; Haaland, A.; Lappert, M. F.; Leung, W. P.; Rypdal, K. *Inorg. Chem.* **1988**, *27*, 1782.
- Bradley, D. C.; Hursthouse, M. B.; Malik, K. M. A.; Moseler, R. *Trans. Met. Chem.* **1978**, *3*, 253.
- Murray, B. D.; Power, P. P. *Inorg. Chem.* **1984**, *23*, 4584.
- Olmstead, M. M.; Power, P. P.; Shoner, S. C. *Inorg. Chem.* **1991**, *30*, 2547.
- Andersen, R. A.; Berg, D. J.; Fernholt, L.; Faegri, K.; Green, J. L.; Haaland, A.; Lappert, M. F.; Leung, W.-P.; Rypdal, K. *Acta Chem. Scand.* **1988**, *A42*, 554.
- Companion, A. L.; Komarynsky, M. A. *J. Chem. Educ.* **1964**, *41*, 257.
- Krishnamurthy, R.; Schaap, W. B. *J. Chem. Educ.* **1969**, *46*, 799.
- Demuyneck, J.; Schaefer, H. F. *J. Chem. Phys.* **1980**, *72*, 311.
- Siegbahn, P. E. M.; Blomberg, M. R. A.; Bauschlicher, C. W. *J. Chem. Phys.* **1984**, *81*, 1373.
- (a) Balasubramanian, K. *Int. J. Quantum Chem.* **1988**, *22*, 465. (b) Fujii, T. S.; Iwata, S. *Chem. Phys. Lett.* **1996**, *251*, 150.
- Ma, B.; Collins, C. L.; Schaefer, H. F. *J. Am. Chem. Soc.* **1996**, *118*, 870.
- Platts, J. A. *J. Mol. Struct. (THEOCHEM)* **2001**, *541*, 111.
- (a) Wang, X.; Chertihin, G. V.; Andrews, L. *J. Phys. Chem. A* **2002**, *106*, 9213. (b) Xiao, Z. L.; Hauge, R. M.; Margrave, J. L. *J. Phys. Chem.* **1991**, *95*, 2696. (c) Wang, X.; Andrews, L. *J. Phys. Chem. A* **2003**, *107*, 570. (d) Wang, X.; Andrews, L. *J. Phys. Chem. A* **2003**, *107*, 4081. (e) Chertihin, G. V.; Andrews, L. *J. Phys. Chem. A* **1995**, *99*, 1214. (f) Billups, W. E.; Chang, S. C.; Hauge, B. H.; Margrave, J. L. *J. Am. Chem. Soc.* **1995**, *117*, 1387. (g) Li, S.; Van Zee, R. J.; Weltner, W.; Cory, M. G.; Zerner, M. C. *J. Phys. Chem.* **1997**, *106*, 2055.
- (a) Tanaka, K.; Nobusada, K. *Chem. Phys. Lett.* **2004**, *388*, 389. (b) Martini, H.; Marian, C. M.; Perić, M. *Mol. Phys.* **1998**, *95*, 27.
- Deleuw, B. J.; Yamaguchi, Y.; Schaefer, H. F. *Mol. Phys.* **1995**, *84*, 1109.
- Moore, C. E. *Atomic Energy Levels*; U.S. Natl. Bur. Stand. Circ. No. 467 (Washington, DC, 1949).
- Van Zee, R. J.; Li, S.; Hamrick, M.; Weltner, W. *J. Chem. Phys.* **1992**, *97*, 8123.

- (57) Van Zee, R. J.; Li, S.; Weltner, W. J. *Chem. Phys.* **1995**, *102*, 4367.
- (58) Rosi, M.; Bauschlicher, C. W.; Langhoff, S. R.; Partridge, H. J. *Chem. Phys.* **1990**, *94*, 8656.
- (59) Hargittai, M.; Subbotina, N. Y.; Kolonits, M.; Gershikov, A. G. J. *Chem. Phys.* **1991**, *94*, 7278.
- (60) (a) Varga, Z.; Vest, B.; Schwerdtfeger, P.; Hargittai, P. *Inorg. Chem.* **2010**, *49*, 2816. (b) Vogal, M.; Wenzel, W. J. *Chem. Phys.* **2005**, *125*, 194110.
- (61) Vest, B.; Varga, Z.; Hargittai, M.; Hermann, A.; Schwerdtfeger, P. *Chem.-Eur. J.* **2008**, *14*, 5130.
- (62) Varga, Z.; Kulonits, M.; Hargittai, M. *Struct. Chem.* **2011**, *22*, 327.
- (63) Nielsen, I. M. B.; Allendorf, M. D. *J. Phys. Chem. A* **2005**, *109*, 928.
- (64) Bridgeman, A. J.; Bridgeman, C. H. *Chem. Phys. Lett.* **1997**, *272*, 173.
- (65) Wang, S. G.; Schwarz, W. H. E. *J. Chem. Phys.* **1998**, *109*, 7252.
- (66) Chen, H.; Bartlett, R. A.; Olmstead, M. M.; Power, P. P.; Shoner, S. C. *J. Am. Chem. Soc.* **1990**, *112*, 1048.
- (67) Bartlett, R. A.; Chen, H.; Power, P. P. *Angew. Chem., Int. Ed. Engl.* **1989**, *28*, 316.
- (68) Betz, P.; Jolly, P. W.; Kreuger, C.; Zakrewski, U. *Organometallics* **1991**, *10*, 3520.
- (69) Boynton, J. N.; Merrill, W. A.; Fettingner, J. C.; Reiff, W. M.; Power, P. P. *Inorg. Chem.* **2012**, *51*, 3212.
- (70) Gavenonis, J.; Tilley, T. D. *Organometallics* **2002**, *21*, 5549.
- (71) Ditri, T. B.; Fox, B. J.; Moore, C. E.; Rheingold, A. L.; Figueroa, J. S. *Inorg. Chem.* **2009**, *48*, 8362.
- (72) Twamley, B.; Hwang, C.-S.; Hardman, N. J.; Power, P. P. *J. Organomet. Chem.* **2000**, *609*, 152.
- (73) Nguyen, T.; Panda, A.; Olmstead, M. M.; Richards, A. F.; Stender, M.; Brynda, M.; Power, P. P. *J. Am. Chem. Soc.* **2005**, *127*, 8545.
- (74) Nguyen, T.; Sutton, A. D.; Brynda, M.; Fettingner, J. C.; Long, G. J.; Power, P. P. *Science* **2005**, *310*, 844.
- (75) Wolf, R.; Ni, C.; Nguyen, T.; Brynda, M.; Long, G. J.; Sutton, A. D.; Fischer, R. C.; Fettingner, J. C.; Hellman, M.; Pu, L.; Power, P. P. *Inorg. Chem.* **2007**, *46*, 11277.
- (76) (a) Weinhold, F.; Landis, C. *Valency and Bonding*; Cambridge University Press: Cambridge, 2005; p 557. (b) Orgel, L. E. *Introduction to Transition Metal Chemistry*; Wiley: New York, 1960; p 68.
- (77) (a) Brynda, M.; Gagliardi, L.; Widmark, P.; Power, P. P.; Roos, B. *Angew. Chem., Int. Ed.* **2006**, *45*, 3804. (b) LaMaccia, G.; Gagliardi, L.; Power, P. P.; Brynda, M. *J. Am. Chem. Soc.* **2008**, *130*, 5104.
- (78) (a) Noor, A.; Kempe, R. *Chem. Rec.* **2010**, *10*, 413. (b) Tsai, Y.-C.; Chang, C.-C. *Chem. Lett.* **2009**, *38*, 1122. (c) Kreisel, K. A.; Yap, G. P. A.; Dmitrenko, O.; Landis, C.; Theopold, K. H. *J. Am. Chem. Soc.* **2007**, *129*, 14162.
- (79) LaMacchia, G.; Li Manni, G.; Todorova, T. K.; Brynda, M.; Aquilante, F.; Roos, B.; Gagliardi, L. *Inorg. Chem.* **2010**, *49*, 5216.
- (80) Wolf, R.; Brynda, M.; Ni, C.; Long, G. J.; Power, P. P. *J. Am. Chem. Soc.* **2007**, *129*, 6076.
- (81) Lei, H.; Guo, J.-D.; Fettingner, J. C.; Nagase, S.; Power, P. P. *J. Am. Chem. Soc.* **2010**, *132*, 17399.
- (82) Plotkin, J. S.; Shore, S. G. *Inorg. Chem.* **1981**, *20*, 284.
- (83) (a) Andersen, R. A.; Carmona-Guzman, E.; Gibson, J. F.; Wilkinson, G. J. *Chem. Soc., Dalton Trans.* **1976**, 2204. (b) Alberoli, A.; Blair, V. L.; Carrella, L. M.; Clegg, W.; Kennedy, A. R.; Klett, J.; Mulvey, R. E.; Newton, S.; Rentschler, E.; Russo, L. *Organometallics* **2009**, *28*, 2112.
- (84) Power, P. P.; Wehmschulte, R. J. *Organometallics* **1995**, *14*, 3264.
- (85) Kays, D. L.; Cowley, A. R. *Chem. Commun.* **2007**, 1053.
- (86) Ni, C.; Fettingner, J. C.; Long, G. J.; Power, P. P. *Dalton Trans.* **2010**, *39*, 10659.
- (87) Ni, C.; Fettingner, J. C.; Long, G. J.; Power, P. P. *Inorg. Chem.* **2009**, *48*, 2443.
- (88) Sutton, A. D.; Nguyen, T.; Fettingner, J. C.; Olmstead, M. M.; Long, G. J.; Power, P. P. *Inorg. Chem.* **2007**, *46*, 4809.
- (89) Ni, C.; Rekken, B.; Fettingner, J. C.; Long, G. J.; Power, P. P. *Dalton Trans.* **2009**, 8349.
- (90) Chen, H.; Bartlett, R. A.; Dias, H. V. R.; Olmstead, M. M.; Power, P. P. *J. Am. Chem. Soc.* **1989**, *111*, 4338.
- (91) Bartlett, R. A.; Feng, X.; Olmstead, M. M.; Power, P. P.; Weese, K. J. *J. Am. Chem. Soc.* **1987**, *109*, 4851.
- (92) Ashley, A. F.; Cowley, A. R.; Green, J. L.; Johnston, D. R.; Watkin, D. J.; Kays, D. L. *Eur. J. Inorg. Chem.* **2009**, 2547.
- (93) Ellison, J. J.; Ruhlandt-Senge, K.; Hope, H. H.; Power, P. P. *Inorg. Chem.* **1995**, *34*, 49.
- (94) An-Yeung, H. Y.; Lam, C. H.; Lam, C.-K.; Wang, W.-Y.; Lee, H. K. *Inorg. Chem.* **2007**, *46*, 7695.
- (95) Lin, C.-Y.; Fettingner, J. C.; Power, P. P., unpublished work.
- (96) Müller, H.; Seidel, W.; Görls, H. *Angew. Chem., Int. Ed. Engl.* **1995**, *34*, 325.
- (97) Viehhaus, T.; Schwartz, W.; Hübler, K.; Locke, K.; Weidlein, J. Z. *Anorg. Allg. Chem.* **2001**, *627*, 715.
- (98) LaPointe, A. M. *Inorg. Chim. Acta* **2003**, *345*, 359.
- (99) Ni, C.; Power, P. P. *Chem. Commun.* **2009**, *37*, 5543.
- (100) Ni, C.; Fettingner, J. C.; Long, G. J.; Power, P. P. *Chem. Commun.* **2008**, *45*, 6045.
- (101) Ellison, J. J.; Ruhlandt-Senge, K.; Power, P. P. *Angew. Chem., Int. Ed. Engl.* **1994**, *33*, 1178.
- (102) Ohta, S.; Ohki, Y.; Ikagawa, Y.; Suizu, R.; Tatsumi, K. *J. Organomet. Chem.* **2007**, *692*, 4792.
- (103) Kobayashi, Y.; Matsuo, T.; Ito, M.; Watanabe, L.; Ishi, Y.; Tamao, K. *KURRI-KR* **2010**, *152*, 54.
- (104) (a) Bryan, A. M.; Fettingner, J. C., unpublished results. (b) Hatanaka, T.; Miyake, R.; Ishida, Y.; Kawaguchi, H. *J. Organomet. Chem.* **2011**, *696*, 4046.
- (105) Bryan, A. M.; Merrill, W. A.; Fettingner, J. C.; Reiff, W. M.; Power, P. P. *Inorg. Chem.* **2012**, *51*, 3366.
- (106) Ni, C.; Stich, T. A.; Long, G. J.; Power, P. P. *Chem. Commun.* **2010**, 4466.
- (107) However, some nickel diorganoamido derivatives such as the dimer $\{Ni(NPh_2)_2\}_2$ were shown to be stable, see: Hope, H.; Olmstead, M. M.; Murray, B. D.; Power, P. P. *J. Am. Chem. Soc.* **1985**, *107*, 712.
- (108) Li, J.; Song, H.; Cui, C.; Cheng, J. P. *Inorg. Chem.* **2008**, *47*, 3468.
- (109) Laskowski, C. A.; Hillhouse, G. L. *J. Am. Chem. Soc.* **2008**, *130*, 13486.
- (110) Laskowski, C. A.; Miller, A. J. M.; Hillhouse, G. L.; Cundari, T. R. *J. Am. Chem. Soc.* **2011**, *133*, 771.
- (111) Ito, M.; Matsumoto, K.; Tatsumi, K. *Inorg. Chem.* **2009**, *48*, 2215.
- (112) Bersuker, I. B. *Chem. Rev.* **2001**, *101*, 1067.
- (113) (a) Shannon, R. D. *Acta Crystallogr.* **1976**, *A32*, 751. (b) Pyykkö, P.; Atsumi, M. *Chem.-Eur. J.* **2009**, *15*, 186.
- (114) Edema, J. J. H.; Gambarotta, S. *Inorg. Chem.* **1989**, *28*, 812.
- (115) Edema, J. J. H.; Gambarotta, S.; Meetsma, A.; Spek, A. L.; Smeets, W. J. J.; Chiang, M. Y. *J. Chem. Soc., Dalton Trans.* **1993**, 789.
- (116) Evans, D. J.; Hughes, D. L.; Silver, J. *Inorg. Chem.* **1997**, *36*, 747.
- (117) (a) Dai, D.; Whangbo, M.-H. *Inorg. Chem.* **2005**, *44*, 4407. (b) Kuzmann, E.; Szalay, R.; Vértés, A.; Hommanay, Z.; Pápai, I.; de Châtel, P.; Klencsár, Z.; Szepes, L. *Struct. Chem.* **2009**, *20*, 453.
- (118) Berg, R. A.; Sinanoglu, O. *J. Chem. Phys.* **1960**, *32*, 1082.
- (119) Hougen, J. T.; Leroi, G. E.; James, T. C. *J. Chem. Phys.* **1961**, *34*, 1670.
- (120) DeKock, C. W.; Gruen, D. M. *J. Chem. Phys.* **1966**, *44*, 4387.
- (121) Holloway, C. E.; Mabbs, F. E.; Small, W. R. *J. Chem. Soc. A* **1968**, 2980.
- (122) Alyea, E. C.; Bradley, D. C. *J. Chem. Soc. A* **1969**, 2330.
- (123) Evans, D. F. *J. Chem. Soc.* **1959**, 2003.
- (124) Buschow, K. H. J.; DeBoer, F. R. *Physics of Magnetism and Magnetic Materials*; Kluwer: Dordrecht, 2003; Chapter 2.

- (125) Caneschi, A.; Gatteschi, D.; Sessoli, R.; Barra, A.-L.; Brunel, L. C.; Guillot, M. *J. Am. Chem. Soc.* **1991**, *113*, 5873.
- (126) Christou, G.; Gatteschi, D.; Hendrickson, D. N.; Sessoli, R. *MRS Bull.* **2000**, 66.
- (127) Boča, R. *Coord. Chem. Rev.* **2004**, *248*, 757.
- (128) Figgis, B. N. *Introduction to Ligand Fields*; Wiley: New York, 1966; p 261.
- (129) Ruppa, K. B. P.; Feghali, K.; Kovacs, I.; Aparna, L.; Gambarotta, S.; Yap, G. P. A.; Bensimon, C. *J. Chem. Soc., Dalton Trans.* **1998**, 1595.
- (130) Schulzke, C.; Enright, D.; Sigiyama, H.; LeBlanc, G.; Gambarotta, S.; Yap, G. P. A.; Thompson, L. K.; Wilson, D. R.; Duchateau, R. *Organometallics* **2002**, *21*, 3810.
- (131) Ni, C.; Ellis, B. D.; Long, G. J.; Power, P. P. *Chem. Commun.* **2009**, 2332.
- (132) La Maccia, G.; Gagliardi, L.; Power, P. P.; Brynda, M. A. *J. Am. Chem. Soc.* **2008**, *130*, 5104.
- (133) Nguyen, T.; Merrill, W. A.; Ni, C.; Lei, H.; Fettinger, J. C.; Ellis, B. D.; Long, G. J.; Brynda, M.; Power, P. P. *Angew. Chem., Int. Ed.* **2008**, *47*, 9115.
- (134) (a) Baxter, D. P.; Chisholm, M. H.; Gama, G. J.; Hector, A. L.; Parkin, I. P. *Chem. Vap. Deposition* **1995**, *1*, 49. (b) Eichöfer, A.; Hampe, O.; Lebedkin, S.; Weigand, F. *Inorg. Chem.* **2010**, *49*, 7331.
- (135) Horvath, B.; Mösel, R.; Horvath, E. G. *Z. Anorg. Allg. Chem.* **1979**, *450*, 165.
- (136) Bradley, D. C.; Hursthouse, M. B.; Abdul Malik, K. M.; Mösel, R. *Transition Met. Chem.* **1978**, *3*, 253.
- (137) Bradley, D. C.; Hursthouse, M. B.; Ibrahim, A. A.; Abdul Malik, K. M.; Motevalli, M.; Mösel, R.; Powell, H.; Runnacles, J. D.; Sullivan, A. C. *Polyhedron* **1990**, *9*, 2959.
- (138) Panda, A.; Stender, M.; Olmstead, M. M.; Klavins, P.; Power, P. P. *Polyhedron* **2003**, *22*, 67.
- (139) Andruh, M.; Roesky, H. W.; Noltemeyer, M.; Schmidt, H. G. *Z. Naturforsch., B* **1994**, *49*, 31.
- (140) Putzer, M. A.; Neumüller, B.; Dehnicke, K.; Magull, J. *Chem. Ber.* **1996**, *129*, 715.
- (141) Murray, B. D.; Power, P. P. *J. Am. Chem. Soc.* **1984**, *106*, 7011.
- (142) Niemeyer, M.; Power, P. P. *Chem. Commun.* **1996**, 1573.
- (143) Panda, A.; Stender, M.; Wright, R. J.; Olmstead, M. M.; Klavins, P.; Power, P. P. *Inorg. Chem.* **2002**, *41*, 3909.
- (144) Malassa, A.; Agthe, C.; Görls, H.; Friedrich, M.; Westerhausen, M. J. *Organomet. Chem.* **2010**, *695*, 1641.
- (145) Koch, C.; Malassa, A.; Agthe, C.; Görls, H.; Biedermann, R.; Krautscheid, H.; Westerhausen, M. Z. *Anorg. Allg. Chem.* **2007**, *633*, 375.
- (146) Malassa, A.; Agthe, C.; Görls, H.; Podewitz, M.; Yu, L.; Herrmann, C.; Reiken, M.; Westerhausen, M. *Eur. J. Inorg. Chem.* **2010**, 1777.
- (147) Kennepohl, D. K.; Brooker, S.; Sheldrick, G. M.; Roesky, H. W. *Z. Naturforsch., B* **1992**, 479.
- (148) Chen, H.; Bartlett, R. A.; Diaz, H. V. R.; Olmstead, M. M.; Power, P. P. *Inorg. Chem.* **1991**, *30*, 2487.
- (149) Chen, H.; Olmstead, M. M.; Pestana, D. L.; Power, P. P. *Inorg. Chem.* **1991**, *30*, 1783.
- (150) Goel, S. C.; Chang, M. Y.; Rauscher, D. J.; Buhro, W. E. *J. Am. Chem. Soc.* **1993**, *115*, 160.
- (151) von Hänisch, C.; Weigend, F.; Clérac, R. *Inorg. Chem.* **2008**, *47*, 1460.
- (152) Horvath, B.; Mösel, R.; Horvath, E. G. *Z. Anorg. Allg. Chem.* **1979**, *441*, 41.
- (153) Murray, D. D.; Hope, H.; Power, P. P. *J. Am. Chem. Soc.* **1985**, *107*, 169.
- (154) Bartlett, R. A.; Ellison, J. J.; Power, P. P.; Shoner, S. C. *Inorg. Chem.* **1991**, *30*, 2888.
- (155) Chen, H.; Power, P. P.; Shoner, S. C. *Inorg. Chem.* **1991**, *30*, 2884.
- (156) Shoner, S. C.; Power, P. P. *Inorg. Chem.* **1992**, *31*, 1001.
- (157) Power, P. P.; Shoner, S. C. *Angew. Chem., Int. Ed. Engl.* **1991**, *30*, 330.
- (158) Ellison, J. J.; Ruhlandt-Senge, K.; Hope, H.; Power, P. P. *Inorg. Chem.* **1995**, *34*, 49.
- (159) Bochmann, M.; Powell, A. K.; Song, X. *Inorg. Chem.* **1994**, *33*, 400.
- (160) Gindelberger, D. E.; Arnold, J. L. *Inorg. Chem.* **1993**, *32*, 5813.
- (161) Ellison, J. J.; Power, P. P.; Shoner, S. C. *J. Am. Chem. Soc.* **1989**, *111*, 8044.
- (162) Hitchcock, P. P.; Lappert, M. F.; Leung, W.-P.; Buttrus, N. H. *J. Organomet. Chem.* **1990**, *394*, 57.
- (163) Ni, C.; Lei, H.; Power, P. P. *Organometallics* **2010**, *29*, 1988.
- (164) Kennedy, A. R.; Klett, J.; Mulvey, R. E.; Newton, S.; Wright, D. S. *Chem. Commun.* **2008**, 308.
- (165) Dumestre, F.; Chaudret, B.; Amiens, C.; Renard, P.; Fejes, P. *Science* **2004**, *303*, 821.
- (166) Lacroix, L.-M.; Lacharze, S.; Falqui, A.; Respaud, M.; Chaudret, B. *J. Am. Chem. Soc.* **2009**, *131*, 549.
- (167) Deschner, T.; Tornroos, K. W.; Anwander, R. *Inorg. Chem.* **2011**, *50*, 7217.
- (168) Holland, A. W.; Li, G.; Shakim, A.; Long, G. J.; Bell, A. T.; Tilley, T. D. *J. Catal.* **2005**, *235*, 150.
- (169) Mueller, H.; Seidel, H.; Görls, H. *J. Organomet. Chem.* **1993**, *445*, 133.
- (170) Roukoss, C.; Basset, J.-M.; Copéret, C.; Lucas, C.; Kuntz, E. C. *R. Chimie* **2008**, *11*, 620.
- (171) Yang, J.; Tilley, T. D. *Angew. Chem., Int. Ed.* **2010**, *49*, 10186.
- (172) Yang, J.; Fasulo, M.; Tilley, T. D. *New J. Chem.* **2010**, *34*, 2528.
- (173) (a) Layfield, R. A.; McDouall, J. J. W.; Scheer, M.; Schwarzmaler, C.; Tuna, F. *Chem. Commun.* **2011**, *47*, 10623. (b) Lin, P.-M.; Smythe, N. C.; Gorelsky, S. I.; Maguire, S.; Hanson, N. J.; Korobkov, I.; Scott, B. L.; Gordon, J. C.; Baker, R. T.; Murugesu, M. *J. Am. Chem. Soc.* **2011**, *133*, 15806. (c) Siemeling, U.; Vorfeld, U.; Neumann, B.; Stammler, H.-G. *Inorg. Chem.* **2000**, *39*, 5159.
- (174) Frazier, B. A.; Wolczanski, P. T.; Lobkovsky, E. B.; Cundari, T. *J. Am. Chem. Soc.* **2009**, *131*, 3428.
- (175) Sulway, S. A.; Collison, D.; McDouall, J. J.; Tuna, S.; Layfield, R. A. *Inorg. Chem.* **2011**, *50*, 2521.
- (176) Bunge, S. D.; Berthe, J. A.; Cleland, T. L. *Inorg. Chem.* **2009**, *48*, 8037.
- (177) Hill, M. S.; Hitchcock, P. B. *J. Organomet. Chem.* **2004**, *689*, 3163.
- (178) Herrmann, W. A.; Huber, N. W. *Chem. Ber.* **1994**, *127*, 821.
- (179) Chesnokova, T. A.; Zhezlova, E. V.; Kornev, A. N.; Fedotova, Y. V.; Zakharov, Z. V.; Fukin, G. K.; Kursky, Y. A.; Mushtina, T. G.; Domrachev, G. A. *J. Organomet. Chem.* **2002**, *642*, 20.
- (180) (a) Fedotova, Y. V.; Zhezlova, E. V.; Mushtina, T. G.; Kornev, A. N.; Chesnokova, T. A.; Fukin, G. K.; Zakharov, Z. V.; Domrachev, G. A. *Russ. Chem. Bull.* **2003**, *52*, 414. (b) Kornev, A. N.; Chesnokova, T. A.; Zhezlova, E. V.; Fukin, G. K.; Zakharov, L. L.; Domrachev, G. A. *Dokl. Akad. Nauk* **1999**, *369*, 203.
- (181) Nehete, U. N.; Roesky, H. W.; Zhu, H.; Nembenna, S.; Schmid, H. G.; Noltemeyer, M.; Bogdanov, D.; Samwer, K. *Inorg. Chem.* **2006**, *44*, 7243.
- (182) Ruhlandt-Senge, K.; Power, P. P. *Bull. Soc. Chim. Fr.* **1993**, *129*, 594.
- (183) MacDonnell, S. M.; Ruhlandt-Senge, K.; Ellison, J. J.; Holm, R. H.; Power, P. P. *Inorg. Chem.* **1995**, *34*, 1815.
- (184) Hauptmann, R.; Kliff, R.; Scheneider, J.; Henkel, G. Z. *Anorg. Allg. Chem.* **1998**, *624*, 1927.
- (185) Komuro, T.; Kawaguchi, H.; Tatsumi, K. *Inorg. Chem.* **2002**, *41*, 5083.
- (186) Sydora, O. L.; Wolczanski, P. T.; Lobkovsky, E. B. *Angew. Chem., Int. Ed.* **2003**, *42*, 2685.
- (187) Hauptmann, R.; Kliff, R.; Henkel, G. *Angew. Chem., Int. Ed.* **1999**, *38*, 377.
- (188) Verma, A. K.; Lee, S. C. *J. Am. Chem. Soc.* **1999**, *121*, 10838.
- (189) Zdilla, M. J.; Verma, A. K.; Lee, S. C. *Inorg. Chem.* **2011**, *50*, 1551.
- (190) Rao, C. V.; Holm, R. H. *Chem. Rev.* **2004**, *104*, 527.
- (191) Lee, S. C.; Holm, R. H. *Chem. Rev.* **2004**, *104*, 1135.

- (192) Ohki, Y.; Sunada, Y.; Honda, M.; Katada, M.; Masada, K.; Tatsumi, K. *J. Am. Chem. Soc.* **2003**, *125*, 4052.
- (193) Ohki, Y.; Sunada, Y.; Tatsumi, K. *Chem. Lett.* **2005**, *34*, 172.
- (194) Praydun, R.; Holm, R. H. *Inorg. Chem.* **2008**, *47*, 3366.
- (195) (a) Ohki, Y.; Ikagawa, Y.; Tatsumi, K. *J. Am. Chem. Soc.* **2007**, *129*, 10457. (b) Ohta, S.; Yokozawa, S.; Ohki, Y.; Tatsumi, K. *Inorg. Chem.* **2012**, *51*, 2645.
- (196) Ohki, Y.; Imada, M.; Murata, A.; Sunada, Y.; Ohta, S.; Honda, M.; Sasamori, T.; Tokitoh, N.; Katada, M.; Tatsumi, K. *J. Am. Chem. Soc.* **2009**, *131*, 13168.
- (197) Ohki, Y.; Murata, A.; Imada, M.; Tatsumi, K. *Inorg. Chem.* **2009**, *48*, 4271.
- (198) Sharp, C. R.; Duncan, J. S.; Lee, S. C. *Inorg. Chem.* **2010**, *49*, 6697.
- (199) Zhou, P.; Denning, M. S.; Kays, D. L.; Goicoechea, J. M. *J. Am. Chem. Soc.* **2009**, *131*, 2802.
- (200) Powers, T. M.; Fout, A. R.; Zhang, S.-L.; Betley, T. A. *J. Am. Chem. Soc.* **2011**, *133*, 3336.
- (201) Bradley, D. C.; Hursthouse, M. B.; Smallwood, R. J.; Welch, A. *J. Chem. Soc., Chem. Commun.* **1972**, 567.
- (202) Fischer, K. J. *Inorg. Nucl. Chem. Lett.* **1973**, *9*, 921.
- (203) Olmstead, M. M.; Power, P. P.; Sigel, G. A. *Inorg. Chem.* **1986**, *25*, 1027.
- (204) (a) Sushev, V. V.; Kornev, A. N.; Min'ko, Y. A.; Belina, N. V.; Kunsky, Y. A.; Kuznetsova, O. V.; Fuken, G. K.; Baranov, E. V.; Cherkasov, V. K.; Abakumov, G. A. *J. Organomet. Chem.* **2006**, *691*, 879. (b) Sushev, V. V.; Kornev, A. N.; Fedotova, Y. V.; Kursky, Y. A.; Mushtina, T. G.; Abakumov, G. A.; Zakharov, L. N.; Rheingold, A. L. *J. Organomet. Chem.* **2003**, *676*, 89. (c) Fedotova, Y. V.; Kornev, A. N.; Sushev, V. V.; Kursky, Y. A.; Mushtina, T. G.; Makarenko, N. P.; Fukin, G. K.; Abakumov, G. A.; Zakharov, L. N.; Rheingold, A. L. *J. Organomet. Chem.* **2004**, *689*, 3060. (d) Sushev, V. V.; Belina, N. V.; Fuken, G. K.; Kursky, Y. A.; Kornev, A. N.; Abakumov, G. A. *Inorg. Chem.* **2008**, *47*, 2608. (e) Kornev, A. N.; Sushev, V. V.; Fukin, G. K.; Baranov, E. V.; Abakumov, G. A. *J. Organomet. Chem.* **2010**, *695*, 637.
- (205) Sigel, G. A.; Bartlett, R. A.; Decker, D.; Olmstead, M. M.; Power, P. P. *Inorg. Chem.* **1987**, *26*, 1773.
- (206) Olmstead, M. M.; Sigel, G. A.; Hope, H.; Xu, X.; Power, P. P. *J. Am. Chem. Soc.* **1985**, *107*, 8087.
- (207) Olmstead, M. M.; Power, P. P.; Sigel, G. A. *Inorg. Chem.* **1988**, *27*, 580.

NOTE ADDED AFTER ASAP PUBLICATION

This paper was originally published to the Web on 4/5/2012 with various text and table errors. These were corrected in the version published on 5/10/2012.